NECK INJURY CRITERIA DEVELOPMENT FOR USE IN SYSTEM LEVEL EJECTION TESTING; CHARACTERIZATION OF ATD TO HUMAN RESPONSE CORRELATION UNDER GY ACCELERATIVE INPUT

THESIS

Stephen J. Satava II, Captain, USAF

AFIT-ENV-MS-17-M-221

DEPARTMENT OF THE AIR FORCE
AIR UNIVERSITY

AIR FORCE INSTITUTE OF TECHNOLOGY

Wright-Patterson Air Force Base, Ohio

AFIT-ENV-MS-17-M-221

NECK INJURY CRITERIA DEVELOPMENT FOR USE IN SYSTEM LEVEL EJECTION TESTING; CHARACTERIZATION OF ATD TO HUMAN RESPONSE CORRELATION UNDER GY ACCELERATIVE INPUT

THESIS

Presented to the Faculty

Department of Systems Engineering and Management

Graduate School of Engineering and Management

Air Force Institute of Technology

Air University

Air Education and Training Command

In Partial Fulfillment of the Requirements for the

Degree of Master of Science in Systems Engineering

Stephen J. Satava II, MS

Captain, USAF

March 2017

AFIT-ENV-MS-17-M-221

NECK INJURY CRITERIA DEVELOPMENT FOR USE IN SYSTEM LEVEL EJECTION TESTING; CHARACTERIZATION OF ATD TO HUMAN RESPONSE CORRELATION UNDER GY ACCELERATIVE INPUT

Stephen J. Satava II, MS
Captain, USAF

Committee Membership:

Jeffrey C. Parr, PhD, Lt Col, USAF
Chair

Michael E. Miller, PhD
Member

Chris Perry, PhD
Member

Abstract

Increased neck injury risk during ejection due to the increasing mass of modern Helmet Mounted Displays (HMDs) drove Parr et al. (2013, 2014, 2015) to define new neck injury criteria to reduce subjective interpretation of ejection system test results and provide early input to HMD and escape system design. Parr et al. provided a method for quantitative evaluation by applying the Multi-Axial Neck Injury Criteria (MANIC) to the primary axes of acceleration during ejection. This application provides clear guidance for assessment of MANIC responses with respect to the AFLCMC's requirement for ejection systems to maintain risk of Abbreviated Injury Scale (AIS) 2 injury below 5%. The latest revision of MIL-HDBK-516 includes MANIC interpretation, as described by Parr et al., to guide HMD and escape system evaluation.

This research developed a MANIC(Gy) transfer function to make MIL-HDBK-516 criteria applicable to cost effective Anthropometric Test Device (ATD) escape system testing in the Gy acceleration axis. Statistical analysis of the six primary neck loads for ATDs revealed Mx (side bending) response significance through the t-test ($p < 0.0001$). This result necessitated adjustment to the human MANIC(Gy) calculation developed by Parr et al. before applying it to ATDs. Multiple regression of ATD Six Factor (SF) MANIC(Gy) and human MANIC(Gy) produced models for quantifying differences in human and ATD responses across the applicable Gy acceleration range. The resulting deltas between the regression models at instantaneous peak-G values defined the transfer function between ATD and human responses. Parametric survival analysis for transformed ATD SF MANIC(Gy) responses produced ATD injury risk curves for AIS 2 ($s = 0.1132$, $\mu = 0.7563$) and AIS 3 ($s = 0.1704$, $\mu = 0.9691$) injury. This method reveals 5% risk of AIS 2 injury during Gy accelerations corresponds to a MANIC(Gy) of 0.473 (95% CI 0.28,0.67) for humans and 0.423 (95% CI 0.25, 0.359) for ATDs.

Acknowledgments

Thank you to my wife for her strength and support throughout my academic career.

I would also like to thank my advisor, Lt Col Parr, for his guidance and support during my AFIT in-residence experience.

Stephen J. Satava II

Table of Contents

List of Figures

Page

List of Tables

Page

Neck Injury Criteria Development for Use in System Level Ejection Testing; Characterization of ATD to Human Response Correlation Under Gy Accelerative Input

I. Introduction

Background

Modern Helmet Mounted Displays (HMD) equip pilots with night vision, weapons cuing, onboard systems management, and many other enhancements. These capabilities are essential in modern warfare, but increasing HMD capability often comes at the cost of increased helmet weight and shifts in helmet Center of Gravity (CG). These changes then increase loads and moments on a pilot's neck in accelerative environments (Gallagher, 2008; Perry et al., 2003; Manoogian et al., 2005; Bevan, 2010). Previous attempts to quantify limits for HMD weight and CG placement have been difficult due to limited human injury data during ejection and the qualitative nature of fatigue effects.

Parr and colleagues developed pilot-scale risk functions and an associated neck injury criteria known as the Multi-Axial Neck Injury Criteria (MANIC), which meet the Air Force Life Cycle Management Center's (AFLCMC) requirements for evaluating pilot neck injury risk (Parr, 2014; Parr et al., 2015; MIL-HDBK-516C). The MANIC combines the six primary neck loads to provide a comprehensive evaluation of neck injury accelerations and is defined in Equation 1 (Parr, 2014; Parr et al., 2015; Perry et al., 2003).

$$MANIC = \sqrt{\left(\frac{Fx}{Fxcrit}\right)^2 + \left(\frac{Fy}{Fycrit}\right)^2 + \left(\frac{Fz}{Fzcrit}\right)^2 + \left(\frac{Mx}{Mxcrit}\right)^2 + \left(\frac{My}{Mycrit}\right)^2 + \left(\frac{Mz}{Mzcrit}\right)^2} \quad (1)$$

In application, limitations in human and Post Mortem Human Subject (PMHS) data require modified MANIC structures, described in detail later in this work, be use for each axis of acceleration (Gx, Gy, Gz), denoted MANIC(Gx), MANIC(Gy), and MANIC(Gz). To define

acceleration-axis specific risk functions for moderate and serious neck injuries Parr et al. combined human and PMHS force, moment, and injury data into a single data set since human subject testing cannot be conducted in a representative ejection environment due to the potential for injury (Parr, 2014; Parr et al., 2014; Parr et al., 2015).

Significant expenses associated with PMHS testing further limit available data for evaluating neck injuries and drives researchers to employ Anthropomorphic Test Devices (ATD) for data collection at injurious levels of acceleration. Biofidelic differences that exist between ATDs and humans require ATD MANIC responses to be converted to an equivalent human response before they can be accurately associated with human injury probabilities (Watkins, 1992; Herbst, 1998; Seemann, 1986).

Problem Statement

Parr and colleagues developed the MANIC using human and PMHS neck injury data, but limits on testing for safety and cost considerations have left significant gaps in the data required to fully implement the MANIC (Parr, 2014; Parr et al., 2014; Parr et al., 2015). Therefore, a transfer function is required to convert ATD MANIC responses to an equivalent human response, making ATD data applicable to the human risk functions developed by Parr et al. (2014, 2015). Zink (2015) developed transfer functions for the ATD response under -Gx accelerative input for MANIC(Gx) implementation. This research seeks to expand on the efforts of Parr et al. (2015) and Zinck (2015) by developing ATD response correlations under Gy accelerative input for use with MANIC(Gy) implementation. In doing so, the following investigative questions will be addressed:

- Is side bending (Mx) a significant neck loading mechanism when evaluating ATD and/or human MANIC(Gy) responses?

- Is the MANIC(Gy) equation presented by Parr et al. (2015) appropriate when calculating ATD MANIC(Gy) responses?
- What is the difference in expected MANIC(Gy) between human/PMHS and ATDs over the range of Gy accelerative input observed from previous laboratory experiments?
- What is an appropriate transfer function for making human-based Gy risk functions, developed by Parr et al. (2015), and associated neck injury criterion more appropriate for ejection system testing with ATDs?

Justification

Previously, Air Force ejection seat weight ranges were adjusted to increase the available selection pool for Air Force pilot selection. This change was initiated to include a larger portion of the female population in the Air Force fighter pilot community (Zinck, 2015:15). Additionally, Generation III HMD designs add 2.60lbs to the helmet weight. The combination of lighter pilots with heavier helmets inherently increases the risk for neck injury, but the specific risk increase has not been adequately quantified.

The MANIC was generated to help quantify neck injury risk associated with varying pilot anthropometric factors (e.g. pilot weight) and increasing HMD mass. To complete neck injury risk evaluations using the MANIC, either additional human/PMHS testing need to be completed or transfer functions must be generated to associate ATD responses with human injury likelihood. Provided current budget constraints throughout the Department of Defense, additional testing is unlikely to be accomplished in the near term. Zinck (2015) provided a proof of concept for development of an ATD to human transfer function under -Gx accelerative input (frontal impact). The next logical step to ensuring applicability of the MANIC to testing with

ATDs is to develop an ATD to human transfer function under Gy accelerative input (side impact).

Assumptions/Limitations

ATD and human response is known to be different under accelerative input (Watkins, 1992; Herbst, 1998; Seemann, 1986). The Hybrid III ATD neck under investigation in this research has a higher resistance to rotation about the z-axis than that of a human (Watkins, 1992:32). However, this is an acceptable discrepancy because the technique utilized in this research independently calculates the neck MANIC(Gy) responses of ATDs and humans, then correlates the difference in responses. Independently calculating the MANIC responses allows for the difference in the rotational resistance about the z-axis to be accounted for.

Ethical and safety considerations prevent the use of human subjects at high levels of Gy accelerative input. To fill the data gaps PMHS are substituted at potentially hazardous accelerations. Similar to Parr et al (2013, 2014, 2015), the PMHS response will be assumed to be similar to that of a human and to provide representative neck responses to Gy accelerative input.

Cost and time requirements associated with human and PMHS testing make additional testing unfeasible within the timetable for this research. Therefore, this research will be limited to data collected during previous human/PMHS Gy testing for all human data analysis and investigative research. The available PMHS testing under Gy accelerative input that recorded neck loads at the occipital condyles (FAA 2011 Study) was conducted without any head supported mass (no helmet) and only with 50^{th} percentile male subjects. Human testing in the area of interest is always conducted with some type of helmet for safety considerations. These

data limitations cause complications when attempting to differentiate between helmet, gender, and PMHS effects on MANIC(Gy) responses.

Expected Contributions

The transfer function developed in this work and applied to the previously developed human MANIC(Gy) risk functions will provide a foundation for evaluating military escape system testing under Gy accelerative input. Additionally, statistical analysis will help further work done by Zinck (2015) to develop transfer functions in the Gx plane and will set the foundation for future research to analyze responses under Gz accelerative input. Collectively this research will be applicable to any domain where occupants experience high acceleration environments.

II. Literature Review

Introduction

HMDs provide pilots with a wide array of in-flight capabilities, but do so at the cost of higher helmet weights and shifted helmet mass properties that cause loading hazards on a pilot's neck (Gallagher, 2008; Perry et al., 2003; Manoogian et al., 2005; Bevan, 2010; Parr et al., 2014; Parr et al., 2015). Previous aerospace research has attempted to quantify limits for HMD weight and CG placement in accelerative environments, but this effort has proven difficult for numerous reasons, to include high expense associated with human/PMHS testing, limited human injury data during ejection, and the qualitative nature of fatigue effects (Eveland, 2008; Gallagher, 2008; Parr et al., 2014; Parr et al., 2015).

Human subjects exposed to high accelerations while wearing an HMD consistently experience higher neck loads as compared to subjects exposed to a similar environment who were not wearing an HMD (Parr, 2014:3 as referenced from Buhrman and Perry, 1994; Perry, 1998; Doczy et al., 2004). "Therefore, it is important that pilot neck response due to heavier HMDs is understood and characterized using a standard evaluation criterion while understanding the influence of pilot anthropometric and biomechanical characteristics on the likelihood of injury" (Parr, 2014:4) Additionally, clearly defined HMD limits will help reduce overall system cost through the inclusion of injury criteria during the HMD prototype phase, rather than waiting until final testing to discover potential hazards.

The primary motivation behind the research conducted by Parr was "the lack of comprehensive, multi-axial, aviation-specific neck injury criteria for accelerative environments that is satisfactory to the acquisition escape community requirements" (Parr, 2014:7). This research aims to further the development of accurate neck injury criteria for evaluating ejection

systems. This chapter summarizes and defines the applicable acceleration axes, anatomical coordinate planes, injury ratings, and survivability analysis necessary for understanding MANIC application. Additionally, this chapter briefly discusses historical neck injury criteria shortfalls that provided motivation for development and application of the MANIC to ejection environments.

Coordinate Planes

Acceleration Axes (Gx, Gy, Gz)

Accelerations experienced by a pilot during ejection occur in three primary axes designated Gx, Gy, and Gz. These axes represent the accelerations as measured in multiples of gravitation force (Gs) in the directions shown in Figure 1. Since human anatomy is assumed to be symmetrical about the sagittal plane, Gy is always expressed as positive unless specifically noted for test-setup purposes.

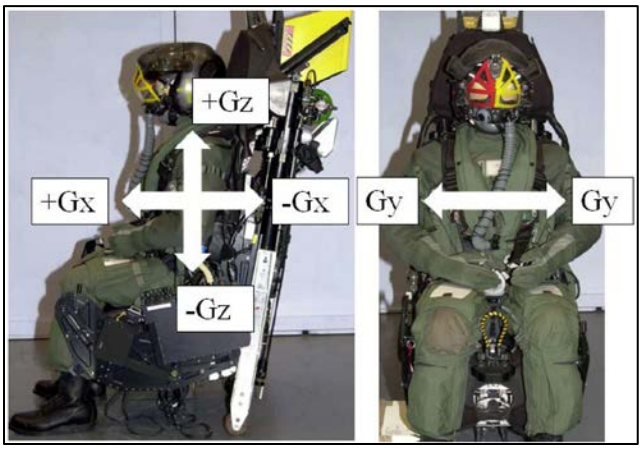

Figure 1. Three primary axes of acceleration (Parr, 2014:148)

Anatomical (Head, Fxyz, Mxyz)

The head attaches to the neck (cervical spine) at the occipital condyles. The occipital condyles provide the center of rotation for the head on the cervical spine and are widely used as a

point of measurement for upper neck moments and loads when investigating neck injuries (Chancey et al., 2007). The forces and moments in this research are all referenced from the occipital condyles either through direct measurement (the case the ATDs and PMHS) or calculation.

During ejection the neck can be subjected to axial loading (tension [+*Fz*] or compression [-*Fz*], frontal shear [*Fx*], side shear [*Fy*]), anterior/posterior bending (flexion [+*My*], extension [-*My*]), side bending (*Mx*), and twisting (*Mz*) (Parr, 2014:19). These forces and moments are referenced about the anatomical coordinate system shown in Figure 2.

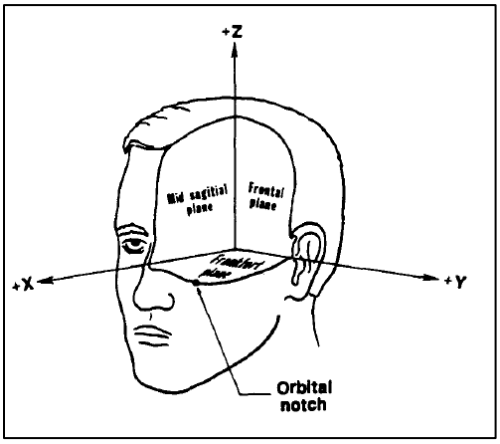

Figure 2. Anatomical Coordinate System (Rash, 1996)

Injury Classification

The Department of Defense Handbook, MIL-HDBK-516C, specifies that applied and inertial forces during escape do not exceed a 5% human incapacitating injury probability for speeds up to at least 350 knots equivalent air speed (KEAS) for legacy aircraft and 450 KEAS for aircraft in development (MIL-HDBK-516C, 2014:358). The AFLCMC escape system oversight office further specified that risk should be limited to no more than 5% chance of incurring Abbreviated Injury Scale (AIS) 2 injury during ejection (Parr et al., 2013; MIL-HDBK-516C).

The AIS is an internationally recognized anatomical scoring system first introduced in 1969 and is currently maintained by the Association for the Advancement of Automotive Medicine (AAM, 2017; Brohi, 2007). Injuries are classified on a six-point scale, shown in Table 1, to identify the associated threat to life of an injury (AAM, 2017; Brohi, 2007).

Table 1. Abbreviated Injury Scale (Brohi, 2007)

AIS Score	Injury
1	Minor
2	Moderate
3	Serious
4	Severe
5	Critical
6	Unsurvivable

Injury Probabilities

A statistical method known as Survival analysis (SA) has been used in previous research to generate risk functions from human and PMHS data (Parr, 2014; Parr et al., 2014; Parr et al., 2015; Bass et al., 2006). SA more appropriately models small data sets (n<100) and censored data than logistic regression (Parr et al., 2013). Utilizing injurious and non-injurious data points from human and PMHS testing, Parr used SA to develop risk curves that indicate probability of neck injury at various AIS levels (AIS 2+ is shown in Figure 3). Pass/fail criteria is interpolated from the risk curve based on the safety limits imposed by the practitioner; e.g. the curve shown in Figure 3 dictates that a MANIC(Gy) of ~0.5 corresponds to a 5% probability of AIS 2+ injury, thus if the requirement is no more than 5% risk of AIS 2 a MANIC(Gy) test result greater than 0.5 would be considered a fail (Parr et al, 2015). Additional details on SA methods and computation as associated with human MANIC(Gy) development can be found in Parr (2014) and Parr et al. (2015). SA methods and computations utilized in this research are detailed later in this work.

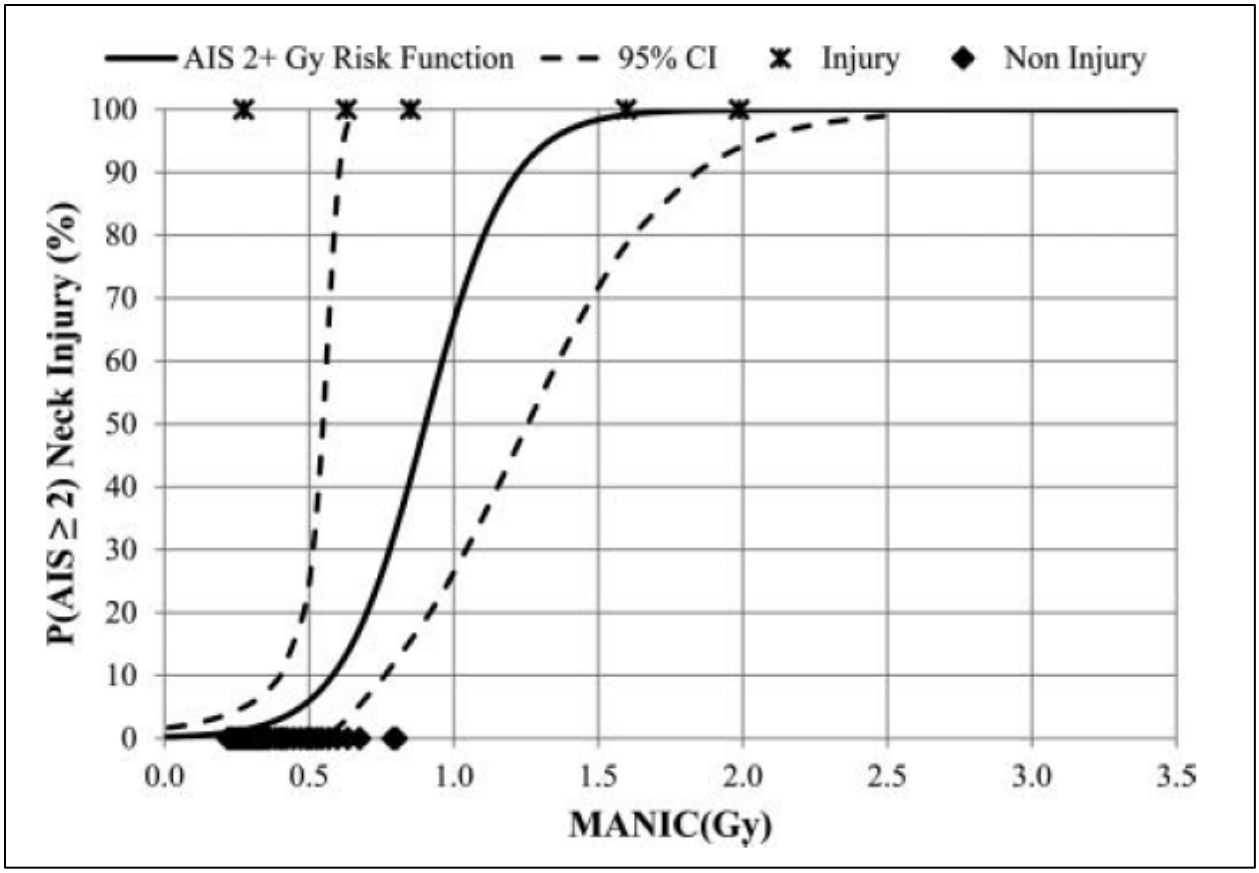

Figure 3. Probability of AIS 2 or greater MANIC (Gy) Risk Function (Parr et al., 2015)

Previous Neck Injury Criteria

Several criteria have been developed in an effort to characterize injury limits associated with human neck loading in ejection environments. Such criteria as the Knox Box, US Navy 12-part neck injury criteria known as the NIC, and the Federal Aviation Administration (FAA) 'neck injury criteria for side-facing aircraft seats' provide guidance for ejection seat and crew equipment development (Parr, 2014:9, Nichols, 2006, FAA, 2011). Both the Knox Box and NIC have extremely limited ability to quantify injury associated with HMDs (Parr, 2014).

The FAA criterion is most applicable to this research due to its focus on accelerations in the Gy axis and use of PMHS data. **Table 2** highlights the findings from the FAA's comparison of EuroSID-2 (ES-2) ATD measurements to PMHS injury results in the same accelerative

environment. There are two primary shortfalls when applying the FAA criteria to military aircraft escape systems: 1) the criteria is focused on AIS 3+ injury (AFLCMC requires AIS 2 or less), and 2) the FAA criteria development did not include data from human subjects. These issues do not completely negate applicability of the FAA criteria, but do require additional information to provide robust guidance to escape system and/or HMD development.

Table 2. FAA Neck Injury Criteria for Side Facing Aircraft Seats

Probability of AIS 3+	Injury Assessment Reference Value
50%	≤2300N Tension measured in ES-2 ATD
25%	≤1800N Tension measured in ES-2 ATD

Further discussion of neck injury criteria applicability and shortfalls when evaluating aircraft escape systems are discussed by Parr (Parr, 2014; Parr et al., 2013; Parr et al., 2014, Parr et al., 2015). The criterion under investigation in this research is the MANIC(Gy) as implemented by Parr et al. (2015).

Transfer Function

MANIC Definition

To properly compensate for pilot anthropometric factors (such as weight, neck size, etc) and maintain consistent criteria for risk function development, Perry et al proposed the mathematical expression referred to in this research as the MANIC (Perry et al., 2003). The MANIC was initially called the Neck Multi-axial Dynamic Response Criteria (NMDRC) and is shown in Equation 2 (Parr et al., 2014; Perry et al., 2003).

$$MANIC = \sqrt{\left(\frac{Fx}{Fxcrit}\right)^2 + \left(\frac{Fy}{Fycrit}\right)^2 + \left(\frac{Fz}{Fzcrit}\right)^2 + \left(\frac{Mx}{Mxcrit}\right)^2 + \left(\frac{My}{Mycrit}\right)^2 + \left(\frac{Mz}{Mzcrit}\right)^2} \quad (2)$$

The MANIC structure provides a unit-less, quantitative criteria for ejection system evaluation utilizing the six primary neck loads (Fx, Fy, Fz, Mx, My, and Mz) and critical values (Fxcrit, Fycrit, Fzcrit, Mxcrit, Mycrit, Mzcrit) to scale effects of a subject's anthropometric factors on their neck response. Parr's implementation of the MANIC specifically utilizes instantaneous peak MANIC responses from human and PMHS time history data to evaluate AIS 2 and AIS 3 injury probabilities in the Gx, Gy, and Gz axes (Parr, 2014; Parr et al., 2014; Parr et al., 2015). Limitations in available upper neck response and injury data forced truncation of the full MANIC equation in each axis. The final Gx, Gy, and Gz MANIC equations presented by Parr are shown in Table 3.

Table 3. MANIC Summary (Parr, 2014:189)

Acceleration Axis	Definition	Injury Limits
MANIC(-Gx)	$\left\|\frac{F_Z}{F_{Zcrit}}\right\| + \left\|\frac{M_Y}{M_{Ycrit}}\right\|$	Peak MANIC(-Gx) < 0.56 Less than 5% Risk of AIS 2+ Injury (<0.72 for AIS 3+)
MANIC(Gy)	$\sqrt{\left(\frac{Fx}{Fxcrit}\right)^2 + \left(\frac{Fy}{Fycrit}\right)^2 + \left(\frac{Fz}{Fzcrit}\right)^2 + \left(\frac{My}{Mycrit}\right)^2 + \left(\frac{Mz}{Mzcrit}\right)^2}$	Peak MANIC(Gy) < 0.48 Less than 5% Risk of AIS 2+ Injury (<0.53 for AIS 3+)
MANIC(-Gz)	$+F_Z$	Peak MANIC(-Gz) < 922 N/207 lb Less than 5% Risk of AIS 2+ Injury (<1136 N/256 lb for AIS 3+)

The latest USAF revision of MIL-HDBK-516, Airworthiness Certification Criteria, implements Parr's MANIC(Gy), supplemented by the Neck Moment Index about the x axis (or NMIx), as a new escape system safety compatibility criteria. The NMIx utilizes Mx (side bending) responses with an anthropometric compensating critical value to evaluate Mx neck injury risk. Together, the MANIC(Gy) and NMIx provide quantitative criteria for the

development and testing of escape systems. Additional details on implementation of the NMIx can be found in Crew Systems Bulletin EZFC-CSB-16-001 (2016).

Since a majority of ejection system testing is performed with ATDs for cost and safety considerations, Parr suggested that future work should develop a human to Hybrid III ATD neck transfer function that would make ATD test data more appropriately applicable to the human-based injury risk functions and associated criteria (Parr, 2014:13; Parr et al., 2013). Such transfer functions would improve the robustness of the current injury probability calculations and provide a basis for system evaluation during early developmental testing utilizing ATDs. For purposes of this research, two versions of the MANIC were utilized to interpret Human and ATD neck responses under Gy acceleration; the five factor equation posed by Parr et al (2015) will be referred to as MANIC(Gy); and an alternate form utilizing all six primary loads will be referred to as the Six-Factor MANIC(Gy), or SF-MANIC(Gy).

MANIC(-Gx) Transfer Function

Zinck furthered Parr's research by developing a transfer function that converts ATD MANIC(-Gx), i.e. frontal impact, responses to equivalent human MANIC(-Gx) responses (Zinck, 2015). To develop the -Gx transfer function Zinck calculated peak MANIC(-Gx) responses, using the equation from Table 3, for ATDs under -Gx accelerative input; developed a representative model of ATD MANIC(-Gx) responses using linear regression; then compared the ATD linear regression model to a human/PMHS linear regression model (Zinck, 2015). The delta between the models is used to transform an ATD MANIC(-Gx) response into a human MANIC(-Gx) response at the corresponding -Gx accelerative input. The resulting transformed response could then be evaluated using the risk functions developed by Parr et al. to determine the probability of human neck injury for an ATD response at a specific –Gx accelerative input.

The MANIC(-Gx) linear regression model equations developed by Zinck (2015) are shown in Equations 3 and 4, and Figure 4 contains a plot of the two models, with the human MANIC(-Gx) utilizing Regression Through the Origin (RTO).

$$\text{Human MANIC}(-\text{Gx}) = 0.0400669 * \text{PeakG} \quad (3)$$

$$\text{ATD MANIC}(-\text{Gx}) = 0.0177993 * \text{PeakG} + 0.0438443 \quad (4)$$

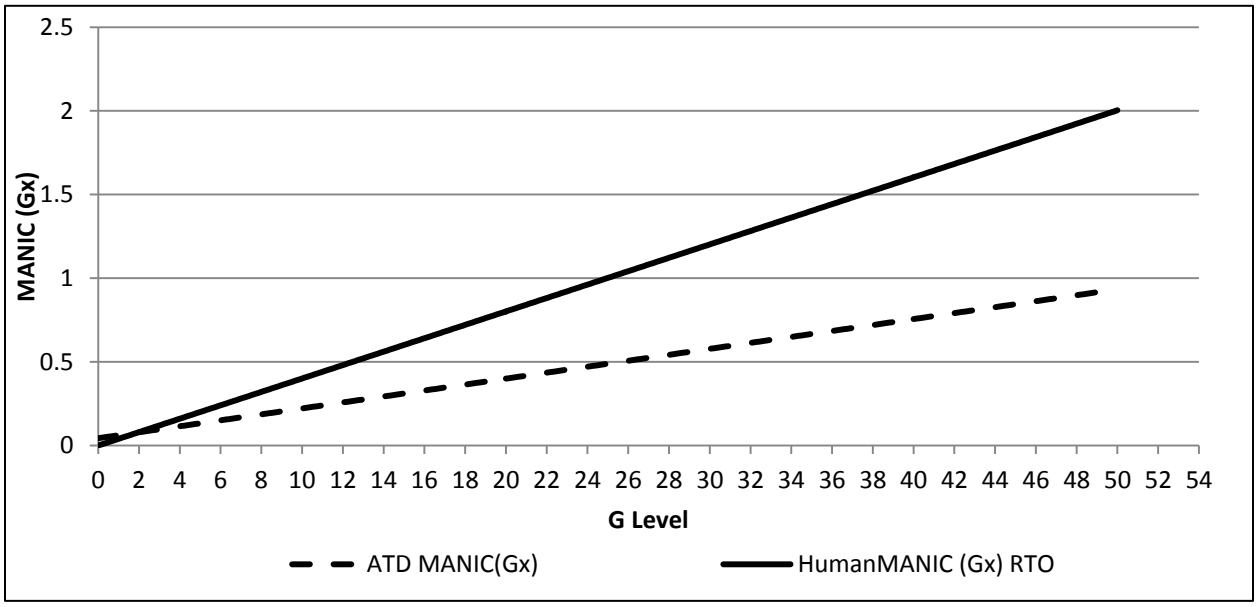

Figure 4. ATD and Human MANIC(-Gx) Linear Regression Models (Zinck, 2015:53)

Gy (lateral impact) Introduction

Similar to the research conducted by Zinck, this research seeks to further Parr's implementation of the MANIC and aid in HMD and ejection system development. Specifically, this research seeks to develop an ATD to human transfer function for Gy accelerative inputs. The method for developing the MANIC(Gy) transfer function is detailed in the next chapter of this work.

III. Methods

Introduction

This chapter describes the methods used to develop an ATD MANIC(Gy) to human MANIC(Gy) transfer function and evaluate the resulting response using the human Gy risk functions developed by Parr et al (2015). Linear regression was selected to construct models that would accurately reflect MANIC(Gy) response differences between the two subject types at varying peak Gy accelerations. A transfer function was then defined using the delta in MANIC(Gy) response at a specified G between the human and ATD models.

Data Selection and Screening

The Air Force Biodynamics Data Bank (BIODYN) on the Collaborative Biomechanics Data Network (CBDN) served as the primary data source for this research. The BIODYN data naming convention is by year and calendar test number iteration, e.g. the 10^{th} study conducted in 2016 is annotated as '201610'. The naming convention for each test run within a study is by facility and iteration number, e.g. Horizontal Impulse Accelerator (HIA) test 6557 is annotated as HIA6557. To implement human Gy risk functions, Parr et al (2015) utilized human Gy test results from the BIODYN 199805 study and PMHS injury data from the FAA 2011 side impact study (Parr 2014:109-110, Parr et al, 2015, FAA, 2011). This data was selected because it provided the highest human Gy exposure of any test conducted at the AFRL HIA to date (Parr et al, 2015). Additional details on Parr's data selection and rationale can be found in Parr (2014) and Parr et al. (2015).

To ensure applicability of the human Gy risk function developed by Parr et al. (2015) to this research, BIODYN data for Gy acceleration of Hybrid III ATD testing was investigated. A summary of the Gy data reviewed for applicability is shown in Figure 5. Other lateral impact

studies were investigated for potential data applicability, but complications arose in finding data sets that recorded neck loading at the occipital condyles in a Gy accelerative environment.

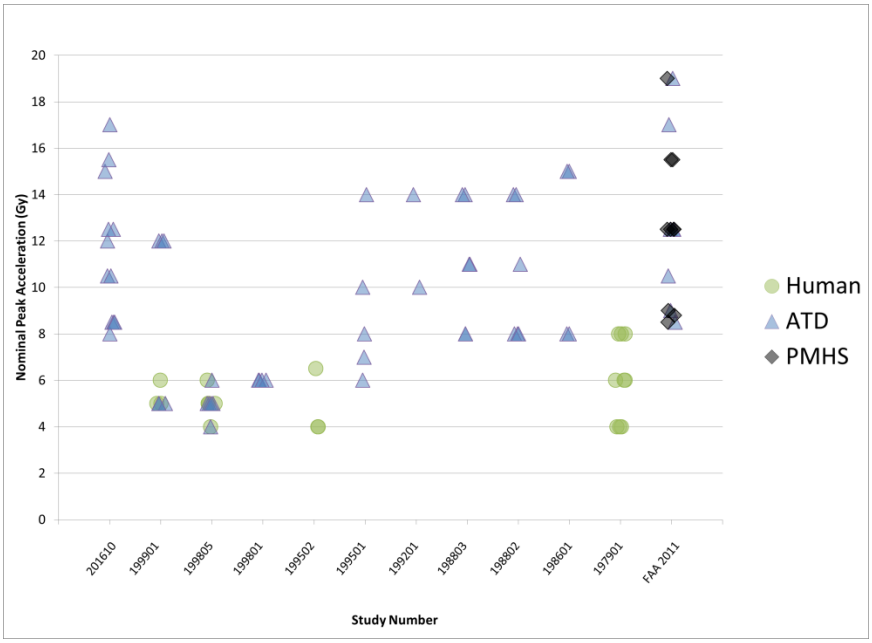

Figure 5. Gy Study vs Nominal Acceleration by Subject Type

All BIODYN Gy testing was conducted on the Air Force Research Laboratory (AFRL) HIA at Wright-Patterson Air Force Base (AFB), OH. The studies selected for this research were 201610, 199101, 199805, 199801, and 199501 for three reasons: 1) sufficient distribution of subjects to span upper neck critical values (discussed later in this chapter); 2) sufficient span of nominal G accelerations; 3) use of the Hybrid III ATD neck to ensure comparability to research conducted by Parr and Zinck (Parr, 2014, Parr et al., 2015, Zinck, 2015). The ATDs used in the selected studies were the large Advanced Dynamic Anthropomorphic Manikin (ADAM), Lightest Occupant In Service (LOIS), small and large Joint Primary Air Training System (JPATS) manikins, Hybrid III (HB-3) 50th percentile male manikin, and the Aerospace Hybrid III 50th percentile male (AERO50) manikin. The EuroSID-2 (ES-2) manikin used during the

FAA2011 testing was not incorporated into results for this study since the ES-2 does not use a Hybrid III neck (FAA, 2011).

PMHS data collected at Wayne State University and the Medical College of Wisconsin for the FAA 2011 study was used by Parr et al. (2015) to define the human Gy risk functions and is the only PMHS Gy data known to meet the data requirements for this study (Parr et al, 2015, FAA, 2011). Due to the aforementioned considerations, the FAA 2011 PMHS injury data was required to supplement the human test data from study 199805 to recreate the risk curves presented by Parr et al. (2015), and to evaluate ATD MANIC(Gy) risk probability.

Table 4 contains a summary of the applicable tests, the original rationale for conducting each test, and subjects involved. A summary of the test conditions for each study is included in Appendix A; full details of each test run and associated setup can be found on the BIODYN database.

Table 4. Summary of Applicable Gy Studies

Study	Subjects	Nominal G Levels	Facility	Test Purpose
201610	AERO50	8, 8.5, 10.5, 12.5, 15, 15.5, 17	HIA, Wright-Patt AFB	Investigation of AERO50 Head and Neck Response under Gy accelerative input as compared to FAA 2011Study ES-2 and PMHS Results
199901	HB-3 Humans	5, 12	HIA, Wright-Patt AFB	Race Helmet Instrumentation Study
199805	ADAM-L Humans	4, 5, 6	HIA, Wright-Patt AFB	Investigation of Human Head and Neck Response to +Gy Impact Acceleration
199801	LOIS ADAM-L	6	HIA, Wright-Patt AFB	Investigation of Occupant Restraint Improvements to the UPCo SIIIS-3 AV-8B Ejection seat
199501	JPATS-S/L ADAM-L	6, 7, 8, 10, 14	HIA, Wright-Patt AFB	Impact Testing of the JPATS Manikins
FAA 2011	ES-2 PMHS	8.5, 9, 12.5, 15.5, 19	Wayne State University Medical College of WI	FAA Neck Injury Criteria for Side-Facing Aircraft Seats

Study 201610 was conducted specifically in support of this research. For direct comparability to the FAA 2011 results, testing was performed on the HIA at equivalent G levels to quantify potential differences in responses between Hybrid III manikins, ES-2, and PMHS. This also provided Gy accelerations in the upper limits of the Gy range (15-17Gs) to complete the ATD data set. Due to physical limitation of the available seat configuration, testing for study 201610 was limited to 17Gs. Testing setup and procedures were in accordance with standard HIA process. Additional details about test setup and procedures can be found in the test plan (Appendix B)

Once the data sets were chosen, each study was screened for anomalous data. Responses of the six primary neck loads (Fx, Fy, Fz, Mx, My, Mz) and the sled accelerations (Gx, Gy, Gz) were plotted to ensure a nominal response during each test run. For screening purposes, a nominal response was qualitatively evaluated from the following criteria: steady rise and fall of Gy sled input acceleration (recorded as 'SLED X ACCEL due to seat configuration), sled Gx and Gz accelerations less than 1.5Gs (recorded as 'SLED Y ACCEL' and 'SLED Z ACCEL' respectively), and peak response of neck loads within 50-100ms of the peak Gy sled input acceleration. Screening criteria were approximated from evaluation of five studies and 106 test runs. Figure 6 contains examples of nominal human and ATD responses. Of the 108 available ATD test runs in the five selected studies, two were missing time history data (199501 HIA5223 and HIA5256) and were omitted from this study. Of the remaining 106 ATD test runs, two required censoring (199801 HIA6534 and 201610 HIA9221) of recorded input spikes after the test was over. All human data was required to be censored past 215ms due to recorded input spikes after the test was over. The same approach to censoring the human data was also taken by Parr et al during human Gy risk function development (Parr et al, 2015).

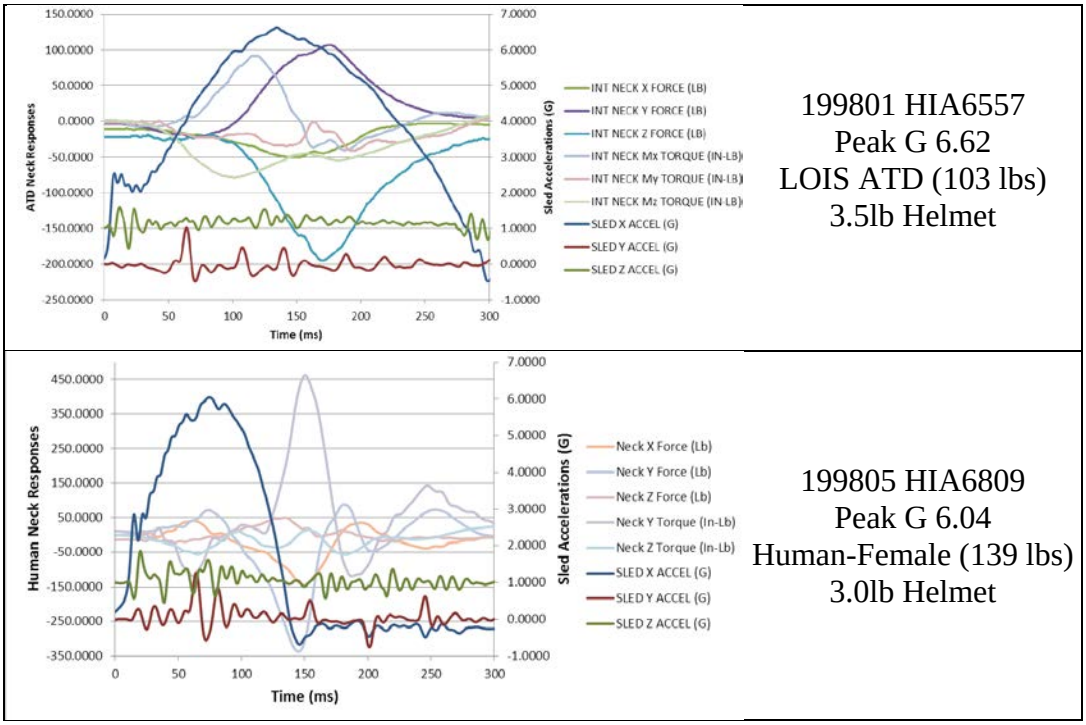

Figure 6. Nominal ATD and Human Neck Load Data

MANIC Calculations

The ideal MANIC as defied by Perry et. al. is shown in Equation 5 (Perry et al., 2003; Parr et al., 2015).

$$MANIC = \sqrt{\left(\frac{Fx}{Fxcrit}\right)^2 + \left(\frac{Fy}{Fycrit}\right)^2 + \left(\frac{Fz}{Fzcrit}\right)^2 + \left(\frac{Mx}{Mxcrit}\right)^2 + \left(\frac{My}{Mycrit}\right)^2 + \left(\frac{Mz}{Mzcrit}\right)^2} \quad (5)$$

Where

Fx = observed x direction shear loading

Fxcrit = critical intercept value for x direction shear loading

Fy = observed y direction shear loading

Fycrit = critical intercept value for y direction shear loading

Fz = observed axial loading (+Fz = tension, -Fz = compression)

Fzcrit = critical intercept value for axial loading (different for tension/compression)

Mx = observed moment about the anatomical x axis (side bending)

Mxcrit = critical intercept value for side bending

My = observed moment about the anatomical y axis

(sagittal plane anterior/posterior bending, +My = flexion, -My = extension)

Mycrit = critical intercept value for sagittal plane moments (different for flexion/extension)

Mz = observed moment about the anatomical z axis (neck twisting)

Mzcrit = critical intercept value for neck twisting

(Parr et al., 2015)

The critical values (Fxcrit, Fycrit, Fzcrit, Mxcrit, Mycrit, Mzcrit) applied by Parr et al. are the same used by recent Department of Defense ejection seat testing (Parr, 2014:112; Parr et al., 2015; Nichols, 2006). However, two competing methods for dividing the critical values by subject mass, referred to as the 'eight-category critical values' and the 'three-category critical values', are offered in the current literature and are presented in Table 5 and Table 6, respectively (Parr, 2014). This research applied both the eight-category critical values, for direct comparison human/PMHS results presented by Parr et al., as well as the three-category critical values to evaluate the most appropriate approach when evaluating ATD responses (Parr et al., 2015). The categories applied to each type of ATD for this research is annotated within Table 5 and Table 6.

To determine human subject neck loads at the occipital condyles, angular accelerations measured on a bite bar are converted to neck loads using each subject's anthropometric factors (e.g. head circumference, neck size, etc). The same program used by Parr et al., Neckload4, was

used by the AFRL to make these conversions and maintain result comparability (Parr, 2014; Parr et al. 2015; Gallagher et al., 2007). Additional details about Neckload4 functionality and assumptions, as presented by Gallagher et al. (2007), are located in Appendix C.

Technological limitations at the time Study 199805 was conducted caused only two of the three head angular accelerations to be recorded on the bite bar (Parr, 2014; Parr et al. 2015). Rotational acceleration about the x axis, denoted 'Rx', was excluded. This exclusion forced the final computation of the equivalent human neck loads to be limited to five of the six primary loads, causing Mx to be excluded from MANIC calculations (Parr et al. 2015). The resulting equation defined by Parr et al. for calculating human MANIC responses to Gy accelerative input, denoted MANIC(Gy), is as shown in Equation 6 (Parr et al., 2015).

$$MANIC(Gy) = \sqrt{\left(\frac{Fx}{Fxcrit}\right)^2 + \left(\frac{Fy}{Fycrit}\right)^2 + \left(\frac{Fz}{Fzcrit}\right)^2 + \left(\frac{My}{Mycrit}\right)^2 + \left(\frac{Mz}{Mzcrit}\right)^2} \quad (6)$$

Due to known differences in ATD and human responses under Gy acceleration presented in the literature, this study independently calculated ATD responses using the MANIC(Gy) presented by Parr et al. and a modified version of the MANIC(Gy) that used all six primary neck loads, per the original MANIC structure presented by Perry et al. (Parr et al., 2015; Perry et al., 2003). The modified MANIC(Gy) is referred to as the Six-Factor(SF) MANIC(Gy) for the purposes of this study and is shown in Equation 7.

$$SF\ MANIC(Gy) = \sqrt{\left(\frac{Fx}{Fxcrit}\right)^2 + \left(\frac{Fy}{Fycrit}\right)^2 + \left(\frac{Fz}{Fzcrit}\right)^2 + \left(\frac{Mx}{Mxcrit}\right)^2 + \left(\frac{My}{Mycrit}\right)^2 + \left(\frac{Mz}{Mzcrit}\right)^2} \quad (7)$$

Table 5. Eight Category Upper Neck Critical Values Based Upon Body Mass (as edited from Parr et. al., 2015)

		Force			Moment		
Applicable ATD (Mass-lbs)	Human Mass (lbs)	Component	lb	N	Component	in-lb	N-m
LOIS (103)	<114	Fx/Fy	405	1802	Mx/-My(extens)/Mz	593	67
		-Fz (Comp)	872	3880	+My (flexion)	1372	155
		+Fz (Tens)	964	4287			
JPATS-S (116)	114-130.5	Fx/Fy	496	2206	Mx/-My(extens)/Mz	845	95
		-Fz (Comp)	1099	4889	+My (flexion)	1939	219
		+Fz (Tens)	1214	5400			
(136)	130.5-143	Fx/Fy	522	2322	Mx/-My(extens)/Mz	912	103
		-Fz (Comp)	1157	5147	+My (flexion)	2094	237
		+Fz (Tens)	1278	5685			0
ES-2 (160) AERO50 (161)	143-161	Fx/Fy	561	2495	Mx/-My(extens)/Mz	1016	115
		-Fz (Comp)	1243	5529	+My (flexion)	2333	264
		+Fz (Tens)	1373	6107			0
HB3-50 (170)	161-186	Fx/Fy	625	2780	Mx/-My(extens)/Mz	1195	135
		-Fz (Comp)	1385	6160	+My (flexion)	2744	310
		+Fz (Tens)	1530	6806			
(200)	186-210	Fx/Fy	683	3038	Mx/-My(extens)/Mz	1364	154
		-Fz (Comp)	1513	6730	+My (flexion)	3133	354
		+Fz (Tens)	1671	7433			
ADAM-L (218)	210-232.5	Fx/Fy	777	3456	Mx/-My(extens)/Mz	1584	179
		-Fz (Comp)	1673	7440	+My (flexion)	3673	415
		+Fz (Tens)	1847	8216			
JPATS-L (248)	232.5+	Fx/Fy	836	3719	Mx/-My(extens)/Mz	1850	209
		-Fz (Comp)	1853	8243	+My (flexion)	4248	480
		+Fz (Tens)	2047	9106			

Table 6. Three Category Upper Neck Critical Values Based Upon Body Mass (as edited from Nichols, 2006)

		Force			Moment		
Applicable ATD (Mass-lbs)	Mass (lbs)	Component	lb	N	Component	in-lb	N-m
LOIS (103)	<136	Fx/Fy	405	1802	Mx/-My(extens)/Mz	593	67
		-Fz (Comp)	872	3880	+My (flexion)	1372	155
JPATS-S (116)		+Fz (Tens)	964	4287			
ES-2 (160)	136-199	Fx/Fy	625	2780	Mx/-My(extens)/Mz	1195	135
AERO50 (161)		-Fz (Comp)	1385	6160	+My (flexion)	2744	310
HB3-50 (170)		+Fz (Tens)	1530	6806			
ADAM-L (218)	200+	Fx/Fy	777	3456	Mx/-My(extens)/Mz	1584	179
		-Fz (Comp)	1673	7440	+My (flexion)	3673	415
JPATS-L (247)		+Fz (Tens)	1847	8216			

Linear Regression

Linear regression was used to identify the relationships of the dependent variable (MANIC response) and its explanatory variables (Peak G, helmet weight, subject weight, etc). Both simple linear regression and multiple regression were employed to maintain comparability to previous research conducted by Zinck, but also to aid in developing statistically significant models of human and ATD MANIC(Gy) responses. All linear regression models were constructed using JMP Pro 12.0.1, SAS Institute Inc, statistical software package.

The following metrics, calculated in JMP, will be employed to evaluate null hypotheses (H_0) and appropriateness of each linear regression model: F-test to evaluate Analysis of Variance (ANOVA) for a regression relationship (H_0: there is not a regression relationship); F-test to evaluate lack of fit for the model (H_0: model fit is reasonable, i.e. no lack of fit); t-test for factor significance (H_0: the factor is not significant, i.e. the factors contribution to the model's slope or intercept is zero); studentized residuals to evaluate outliers in the model (studentized residual larger than three will be deemed an outlier and excluded from the model); and R^2 to evaluate

how much of the variance is explained by the model. All statistical tests will use the default JMP value of 0.05 for α.

Since it is intuitive that no injury should be obtained at 1G, RTO was utilized by Zinck to develop a MANIC(-Gx) regression models that met this assumption (Zinck, 2015). RTO forces the regression model to have an intercept at zero, which, with regard to MANIC responses, signifies a zero probability of injury if head accelerations are maintained at 1G. A similar approach will be investigated for MANIC(Gy) responses.

Transfer Function

In this application, the term "transfer function" is used to describe the relationship between the human and ATD linear regression models. The difference in human and ATD MANIC(Gy) or SF-MANIC(Gy) values at a particular acceleration is used to define the applicable transform between the two subject types. This application is consistent with the method employed by Zinck for definition of a MANIC(Gx) human to ATD transfer function (Zinck 2015).

Survival Analysis

Although the human risk curves developed by Parr et al. will remain as the Air Force standard for evaluating ejection system injury risk, per MIL-HDBK-516, the MANIC(Gy) transfer function is used to explore differences between the human and ATD risk curves.

To evaluate the probability of injury associated with an ATD, data points used to construct the MANIC(Gy) human risk curve presented by Parr et al. (2015) are converted to an equivalent ATD MANIC(Gy) response. Then, each ATD transformed point is associated with the AIS rating experienced by its corresponding human data point. Finally, survival analysis is

employed via Minitab version 17.1.0 (Minitab, Inc, State College, PA) to construct the respective ATD AIS 2+ and AIS 3+ neck injury risk curves.

To ensure comparability to results presented by Parr et al. (2015), all human MANIC responses were recomputed during this research. The recomputed points are then entered into Minitab to recreate the MANIC(Gy) human neck injury risk curve. Once an identical curve can be consistently created, the ATD transformed data is entered into Minitab. The human and ATD curves will be defined using Minitab parametric distribution analysis (arbitrary censoring), a maximum likelihood estimate, and an assumed logistic distribution.

During each evaluation, subjects are categorized as 'injury' or 'non-injury' with respect to their documented AIS rating (e.g. during evaluation of AIS 3+ risk, all subjects with an AIS rating of 2 or lower were placed in the 'non-injury' category). A logistic distribution is assumed when the response variable is binary (Montgomery, 2006). The cumulative distribution function of the logistic distribution is a monotonically increasing S-shaped function which is often used to characterize probability of injury and is shown in Equation 8 (Montgomery et al., 2006:429, Parr et al. 2015; Bass et al., 2006).

$$F(x;\mu,s) = \frac{1}{1+e^{-\frac{x-\mu}{s}}} \tag{8}$$

where:

x = observation under evaluation (MANIC response)

μ = midpoint of the curve (known as 'Location')

s = steepness of the curve (known as 'Scale')

The probability if injury at or above a specified AIS value with respect to the MANIC(Gy) response is expresses as Equation 9.

$$P(AIS \geq X) = \frac{1}{1 + e^{\frac{\mu - MANIC(Gy)}{s}}} \quad (9)$$

where:

X = 2+ or 3+ depending on the AIS level under evaluation

μ = midpoint of the curve (known as ‘Location’)

s = steepness of the curve (known as ‘Scale’)

IV. Results

MANIC Calculations

Calculated results for MANIC(Gy) and SF-MANIC(Gy) responses for the five studies under investigation (201610, 199101, 199805, 199801, and 199501) utilizing both eight-category and three-category critical values can be found in Appendix D. These calculations were performed at each time step of the recorded Gy data for each test run to identify the peak responses and are summarized in Figure 7 and Figure 8. Three tests from study 199901 and one test from study 199501 were noted to have significantly higher responses than other test with similar peak G vales.

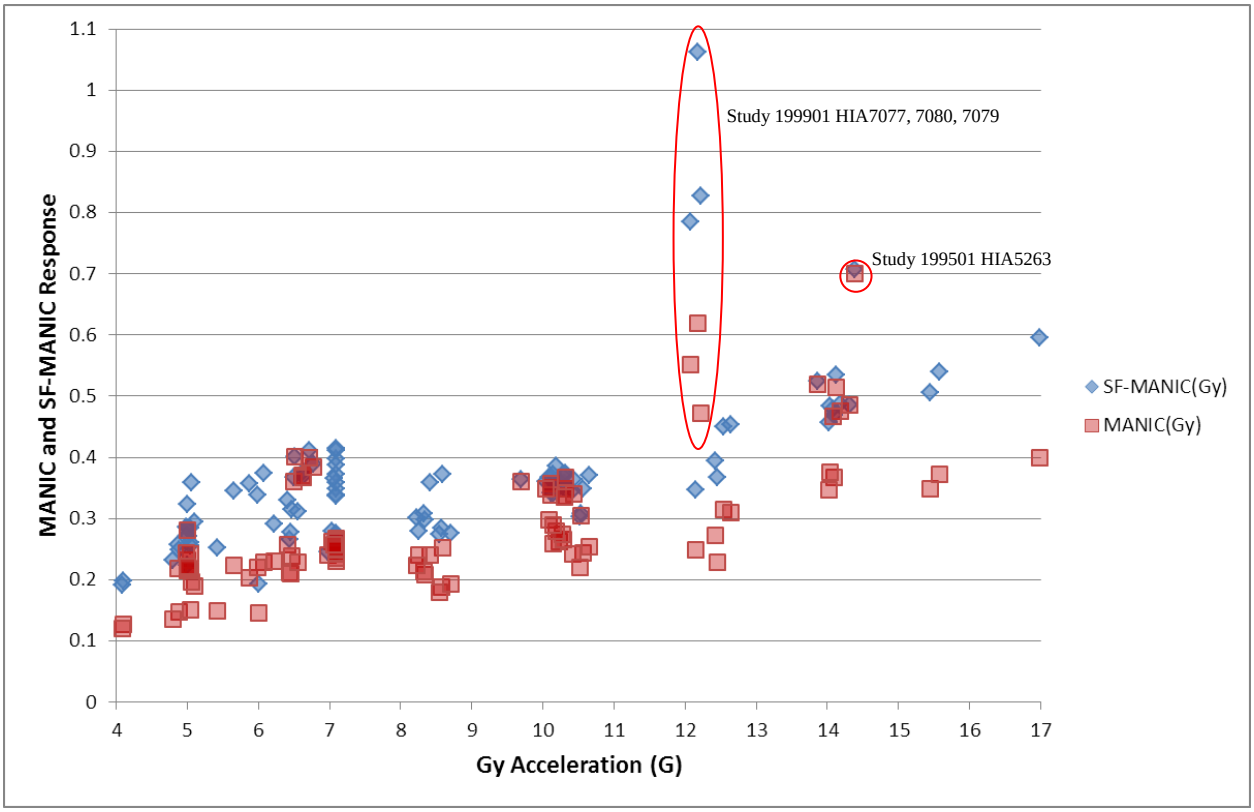

Figure 7. Peak ATD MANIC(Gy) and SF-MANIC(Gy) with 8-cat Critical Values

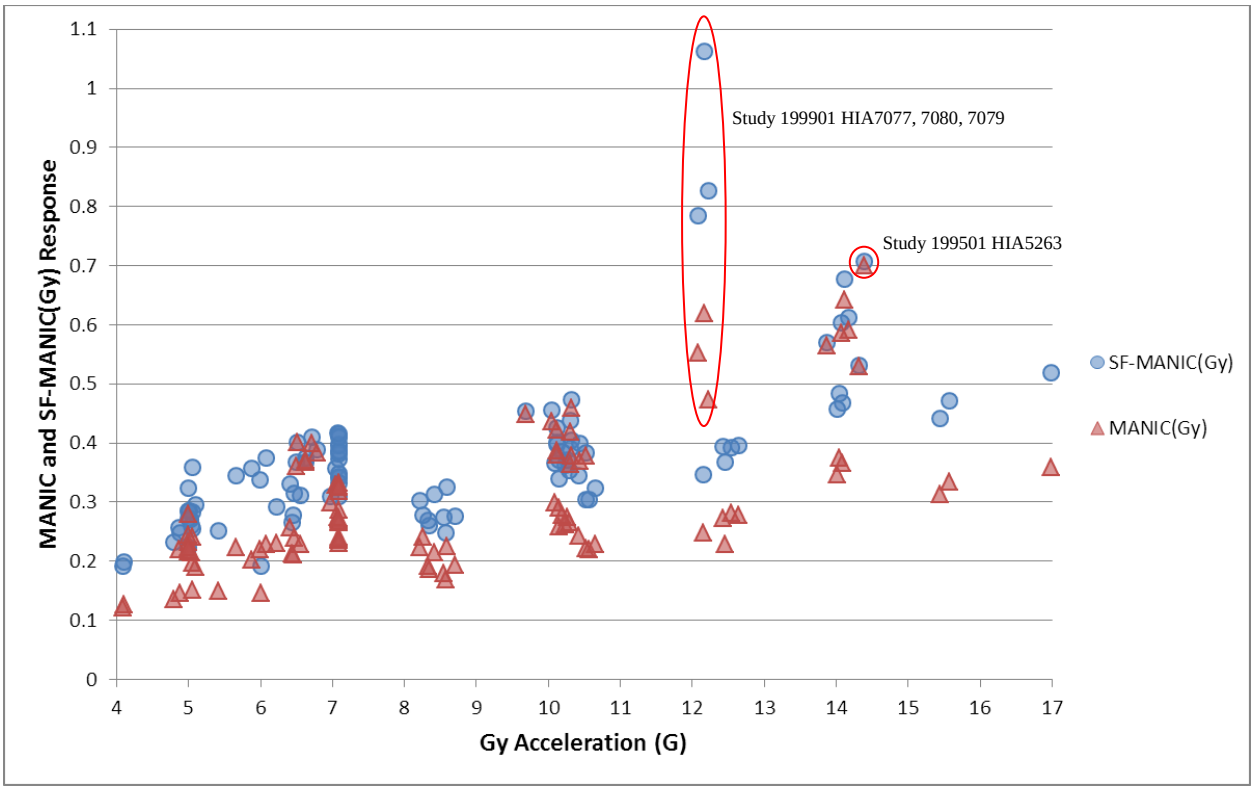

Figure 8. Peak ATD MANIC(Gy) and SF-MANIC(Gy) with 3-cat Critical Values

Neckload4 results for study 199805 used by Parr et al. were used to calculate the human MANIC(Gy) response at each time step of the recorded Gy data to identify peak response values for each test run (Parr et al., 2015; Parr, 2014). Similar to the ATD data, MANIC(Gy) calculations were performed using three- and eight-category critical values. The final human values are detailed in Appendix D and are summarized in Figure 9 and Figure 10. PMHS neck loads from the FAA study were used to calculate MANIC(Gy) peak responses.

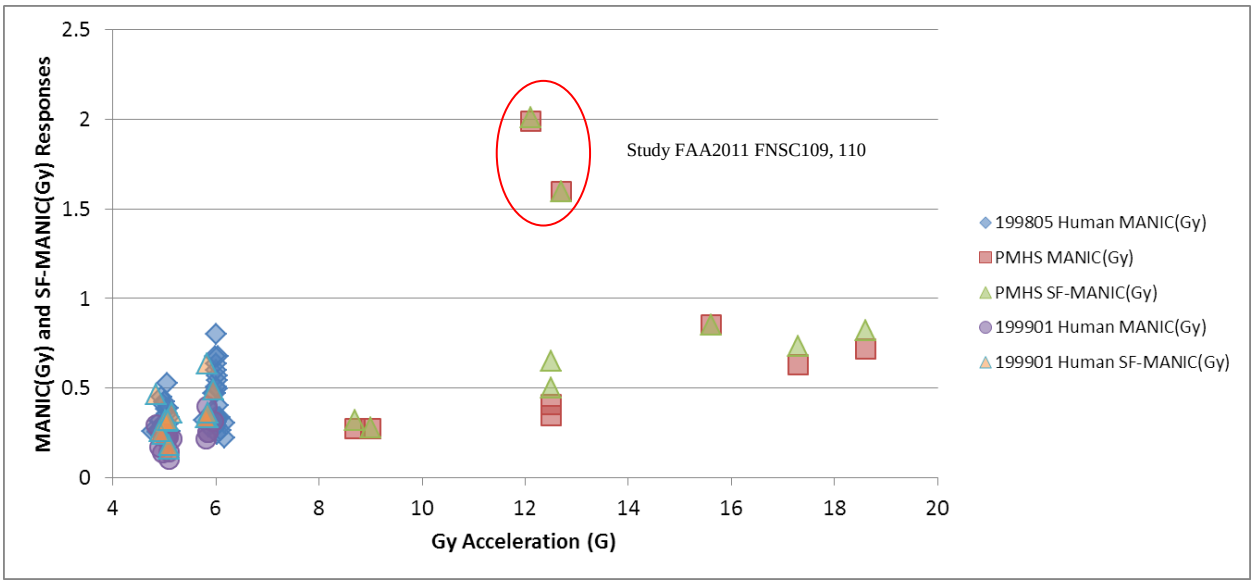

Figure 9. Peak Human MANIC(Gy) and SF-MANIC(Gy) with 8-cat Critical Values

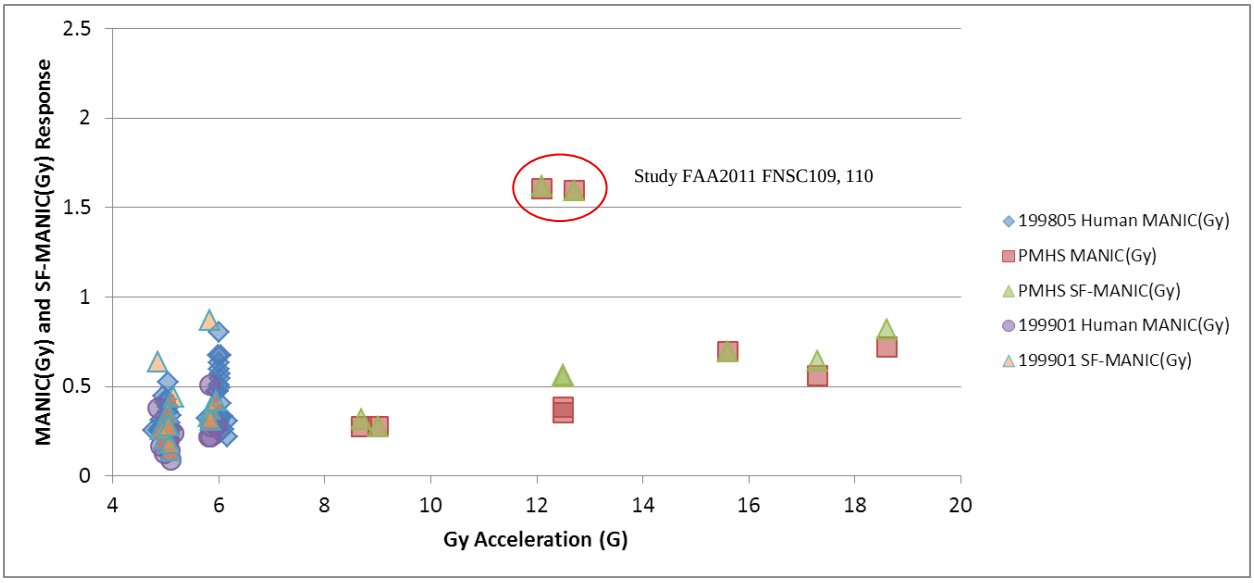

Figure 10. Peak Human MANIC(Gy) and SF-MANIC(Gy) with 3-cat Critical Values

Linear Regression Models

SF-MANIC(Gy) and Mx ANOVA

Due to technological limitations at the time of testing, the primary data used by Parr et al. to develop human risk curves did not record side bending (Mx) (Parr et al, 2015). It is known

that human and ATD neck responses are different under Gy loading, particularly with respect to My and its influence on Mx (Watkins, 1992). Therefore, ANOVA was employed to investigate if exclusion of Mx from the ATD response models, as was required by Parr et al during human MANIC(Gy) response calculation, is appropriate. Figure 11 shows the JMP output to identify ATD MANIC(Gy) response as influenced by Fx, Fy, Fz, Mx, My, Mz, subject weight, and peak G utilizing ATD data from all five studies under investigation. The t-test for Mx rejected the null hypothesis for both the three-category (Mx $p = 0.0189$) and eight-category (Mx $p < 0.0001$) calculations of the ATD SF-MANIC(Gy) response shown in Figure 11 (a) and Figure 11 (b) respectively, indicating that Mx is a significant factor when calculating ATD SF-MANIC(Gy).

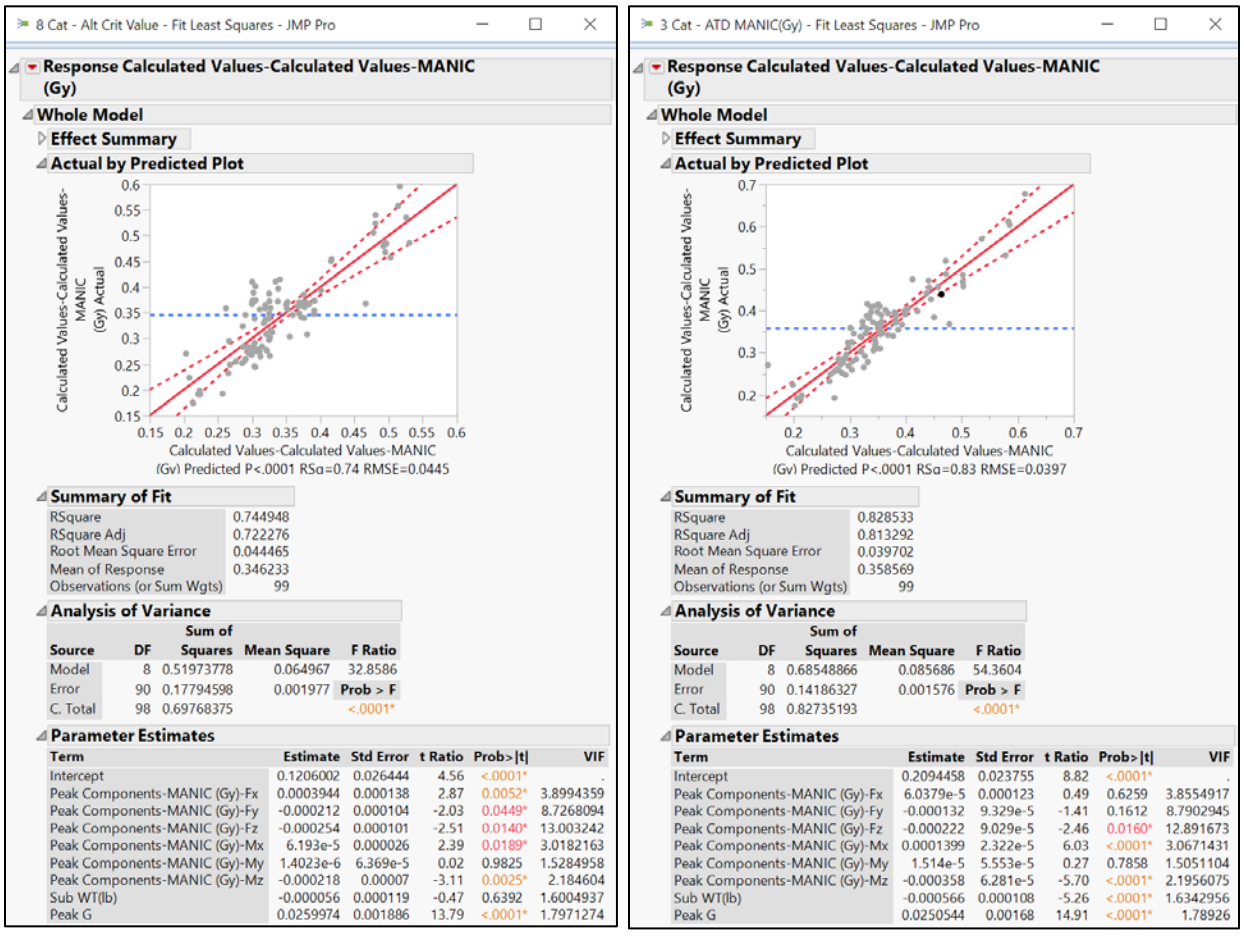

(a) (b)

Figure 11. JMP Model Results for ATD SF-MANIC(Gy) and Fx, Fy, Fz, Mx, My, Mz

During this research it was discovered that study 199901 recorded all three head accelerations during testing, enabling calculation of all six primary neck loads. This discovery supported construction of a comparative ANOVA to evaluate statistical significance of Mx in the human SF-MANIC(Gy) response. The JMP outputs to identify human SF-MANIC(Gy) responses as influenced by Fx, Fy, Fz, Mx, My, Mz, and Peak G utilizing human data from study 199901 with eight-category and three-category critical values are shown in Figure 12 (a) and Figure 12 (b), respectively. Although the t-test suggest rejecting the null hypothesis for Mx significance, a large Variance Inflation Factor (VIF) indicates multicollinearity among Fx, Fy, Mx, My, and Mz within the human SF-MANIC(Gy) response. The Pearson Product-Moment correlation coefficients calculated in JMP are shown in Table 7. The coefficients confirm strong linear correlations between Fx/My, Fy/Mx, Fy/Mz, and Mx/Mz; where a value close to 1 or -1 indicate a strong positive or negative linear correlation, respectively.

Table 7. Correlation Coefficients for Human SF-MANIC(Gy)

	Fx	**Fy**	**Fz**	**Mx**	**My**	**Mz**	**Peak G**
Fx	-						
Fy	0.6065	-					
Fz	-0.2789	-0.012	-				
Mx	0.3468	0.9267	0.1172	-			
My	-0.9859	-0.558	0.1851	-0.2801	-		
Mz	0.6267	0.9826	-0.0169	0.8758	-0.5807	-	
Peak G	-0.3558	-0.6493	0.4262	-0.581	0.2922	-0.6469	-
Sub WT(lb)	0.0252	0.2811	0.2853	0.2255	-0.0475	0.3462	0.0084

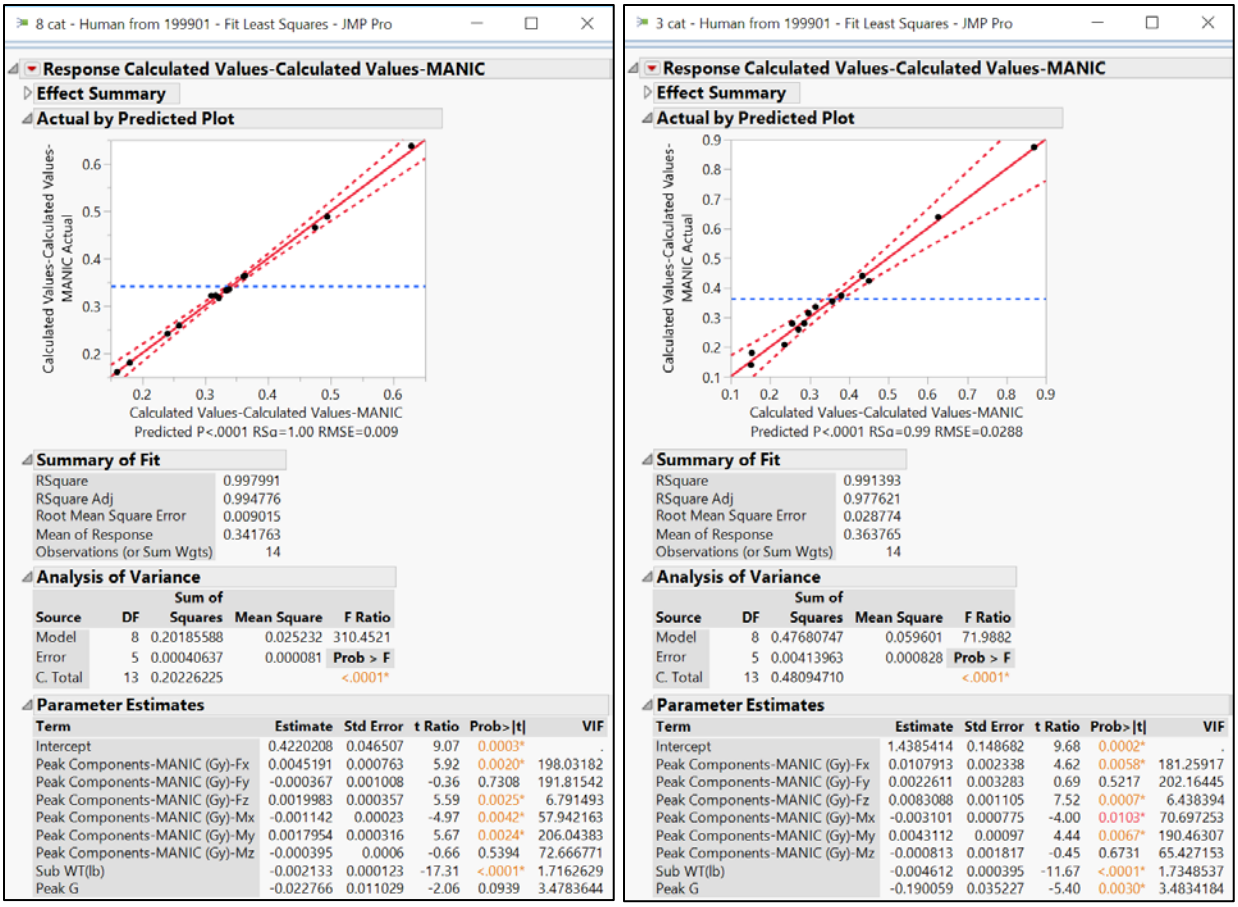

(a) (b)

Figure 12. JMP Model Results for Human SF-MANIC(Gy) and Fx, Fy, Fz, Mx, My, Mz

The SF-MANIC(Gy) statistical results are supported by qualitative physical evidence present during evaluation of the slow motion video from Gy testing of ATD and human subjects. Figure 13, Figure 14, and Figure 15 show typical ATD and human responses observed during testing at peak Gy, peak MANIC(Gy), and peak SF-MANIC(Gy). The dominant human Mz/My movement seen between test start and peak response in Figure 13 (a) and (b), respectively, is dramatically different than the dominant ATD Mx movement seen in Figure 14 and Figure 15. The ATD response is more easily observed in Figure 15 with an improved camera angle and updated video capture technology, while Figure 14 provides direct comparison to the human response at similar G, seat configuration, harness, helmet, and subject weight.

Start	Peak Gy	Peak MANIC(Gy)
0ms	73ms	135ms
(a)	(b)	(c)

Figure 13. Study 199805 HIA6761 Gy Response, Human-M (220 lbs), 6.02G

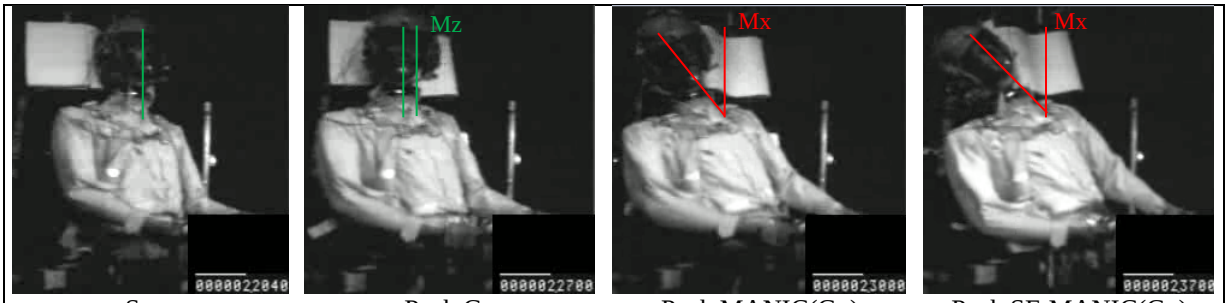

Start	Peak Gy	Peak MANIC(Gy)	Peak SF-MANIC(Gy)
0ms	70ms	100ms	171ms
(a)	(b)	(c)	(d)

Figure 14. Study 199805 HIA6679 Gy Response, ADAM-L (218 lbs), 6.08G

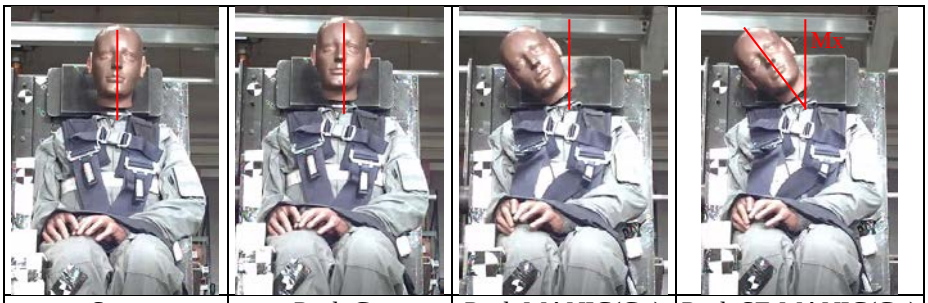

Start	Peak Gy	Peak MANIC(Gy)	Peak SF-MANIC(Gy)
0ms	36ms	98ms	105ms
(a)	(b)	(c)	(d)

Figure 15. Study 201610 HIA9210 Gy Response, AERO50 (161 lbs), 8.33G

Simple Linear Regression of MANIC(Gy)

First order simple linear regression models were created for MANIC(Gy) response and Peak G using the eight- and three-category critical values discussed in Chapter III. Figure 16 and Figure 17 show the JMP results for the eight- and three-category critical value SF-MANIC(Gy) regression respectively, where panel-a contains all available data points, panel-b is the final model after removing outliers based on their studentized residuals (res), and panel-c is the model from panel-b utilizing RTO. The regression model equations are shown in Equations 10-13. It should be noted that the RTO model depicted in Figure 16 panel-c, per the F-test, rejected the null hypothesis for lack of fit, indicating that the model is not a good fit of the data.

Use of the eight-category critical values provides better normalization of the SF-MANIC(Gy) responses, generating a more linear relationship between the SF-MANIC(Gy) response and peak G; thus making the eight-category results better suited for linear regression. This is evident in the improved R^2 and lack of fit for the eight-category model over the three-category model.

Figure 16 (b)	8-Cat SF-MANIC(Gy) =	$0.1624637 + 0.0214626 * \text{Peak G}$	(10)
Figure 16 (c)	(RTO) 8-Cat SF-MANIC(Gy) =	$0.0382382 * \text{Peak G}$	(11)
Figure 17 (b)	3-Cat SF-MANIC(Gy) =	$0.1858451 + 0.0197452 * \text{Peak G}$	(12)
Figure 17 (c)	(RTO) 3-Cat SF-MANIC(Gy) =	$0.0392248 * \text{Peak G}$	(13)

Figure 18 and Figure 19 show the JMP results for the eight- and three-category critical value MANIC(Gy) linear regression respectively, where panel-a contains all available data points, panel-b is the final model after removing outliers based on their studentized residuals (res), and panel-c is the model from panel-b utilizing RTO. Although a studentized residual of three is usually an indicator of an outlier, lower values were considered for this model in an attempt to improve the lack of fit. The regression model equations are shown in Equations 14-

17. It should be noted that all first order ATD MANIC(Gy) models, per the F-test (p = 0.0001), rejected the null hypothesis for lack of fit, indicating that the model is not a good fit for the data. Rejecting the null hypothesis for lack of fit is usually an indicator that the model is undefined; requiring the addition of other effects or higher order terms to better explain the data.

Figure 18 (b)	8-Cat MANIC(Gy) =	$0.1083121 + 0.0193896 * \text{Peak G}$	(14)
Figure 18 (c)	(RTO) 8-Cat MANIC(Gy) =	$0.030533 * \text{Peak G}$	(15)
Figure 19 (b)	3-Cat MANIC(Gy) =	$0.1056908 + 0.0212984 * \text{Peak G}$	(16)
Figure 19 (c)	(RTO) 3-Cat MANIC(Gy) =	$0.0321364 * \text{Peak G}$	(17)

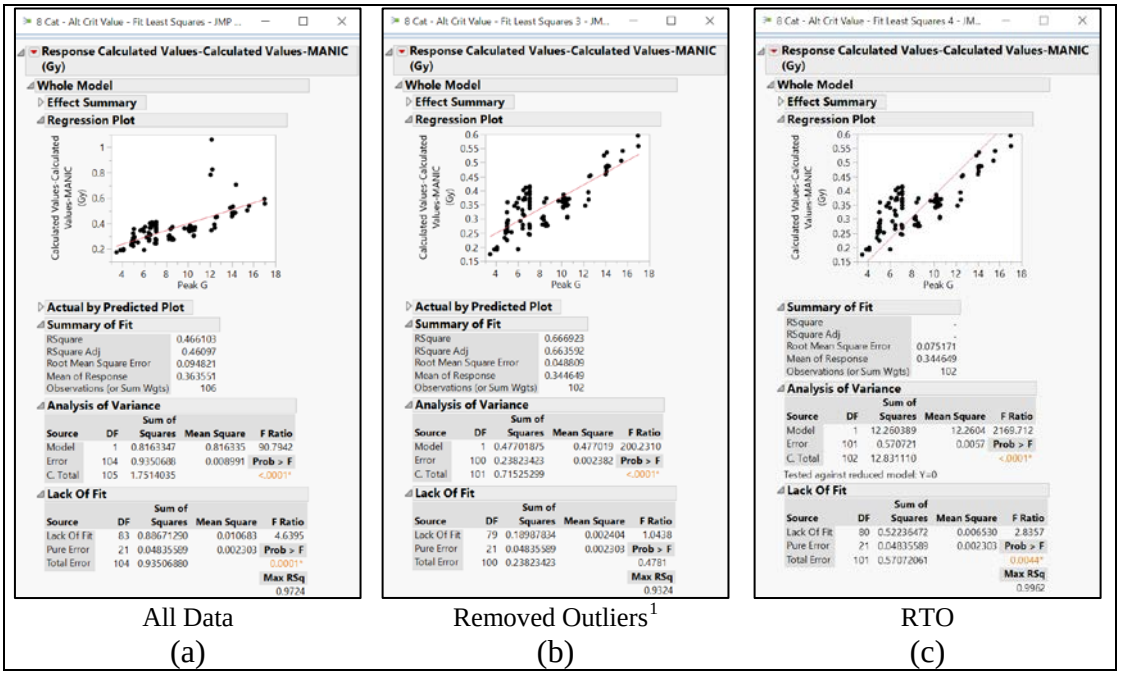

Figure 16. First Order Regression Models of 8-Cat ATD SF-MANIC(Gy)

[1] (HIA7080, 199901, 12G, res = 6.43, HIA7079, 199901, 12G, res = 3.91, HIA7077, 199901, 12G, res = 3.49); then HIA5263, 199501, 14G, res = 4.31

All Data (a) | Removed Outliers[2] (b) | RTO (c)

Figure 17. First Order Regression Models of 3-Cat ATD SF-MANIC(Gy)

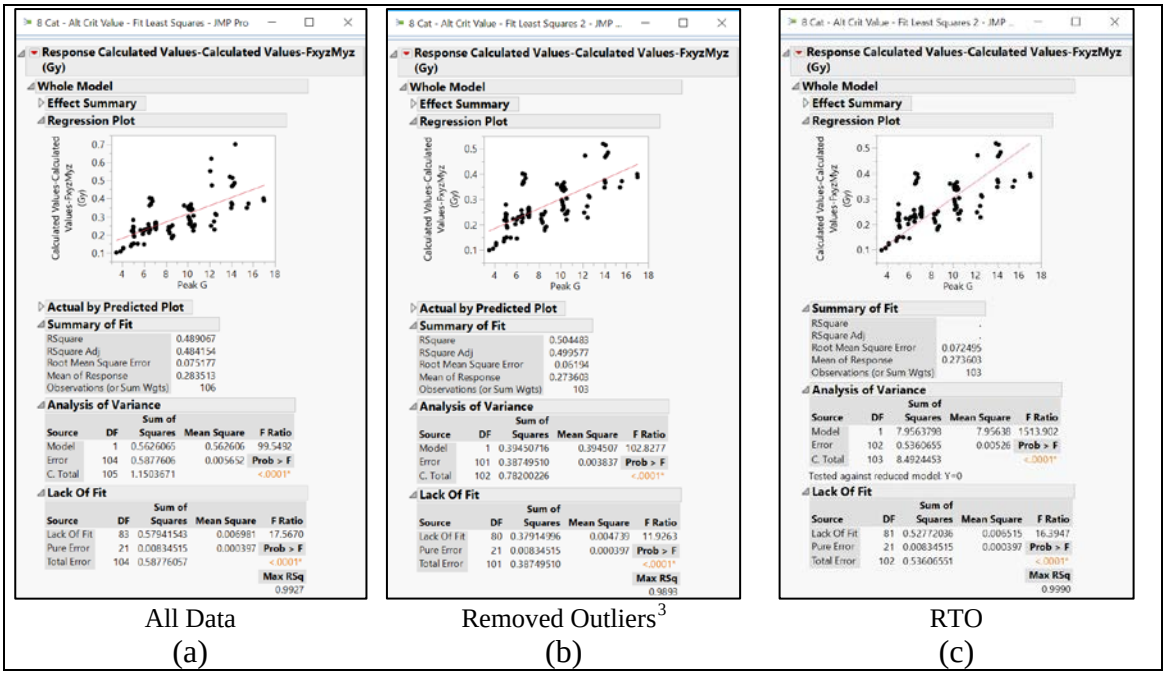

All Data (a) | Removed Outliers[3] (b) | RTO (c)

Figure 18. First Order Linear Regression Models of 8-Cat ATD MANIC(Gy)

[2] (HIA7080, 199901, 12G res = 6.01, HIA7079, 199901, 12G res = 3.61; HIA7077, 199901, 12G res = 3.21) then (HIA5263, 199501, 14G res = 3.41; HIA5257, 199501, 14G res = 3.01); then (HIA5263, 199501, 14G res = 3.79)

[3] (HIA5263, 199501, 14G, res = 3.89; HIA7080, 199901, 12G, res = 3.45); then (HIA7077, 199901, 12G res = 3.19)

All Data (a) | Removed Outliers[4] (b) | RTO (c)

Figure 19. First Order Regression Models of 3-Cat ATD MANIC(Gy)

A simple linear regression model was fit to the combined human/PMHS data set with MANIC(Gy) as a response of peak G. Figure 20 contains the JMP results for the eight-category critical value MANIC(Gy) regression, where panel-a contains all available data points, panel-b is the final model after removing outliers based on their studentized residuals (res), and panel-c is the model from panel-b utilizing RTO. Although removing the outliers did improve the lack of fit; both versions of the model have a very low R^2 value (R^2 = 0.29 and 0.16), indicating that the models do not explain much of the variance in the data. The regression model equations are shown in Equations 18-20.

Figure 20 (a)	8-Cat MANIC(Gy) =	$0.02613 + 0.06096 * \text{Peak G}$	(18)
Figure 20 (b)	8-Cat MANIC(Gy) =	$0.21742 + 0.02504 * \text{Peak G}$	(19)
Figure 20 (c)	(RTO) 8-Cat MANIC(Gy) =	$0.05557 * \text{Peak G}$	(20)

[4] (HIA5263, 199501, 14G, res = 2.99; HIA7080, 199901, 12G, res = 2.86)

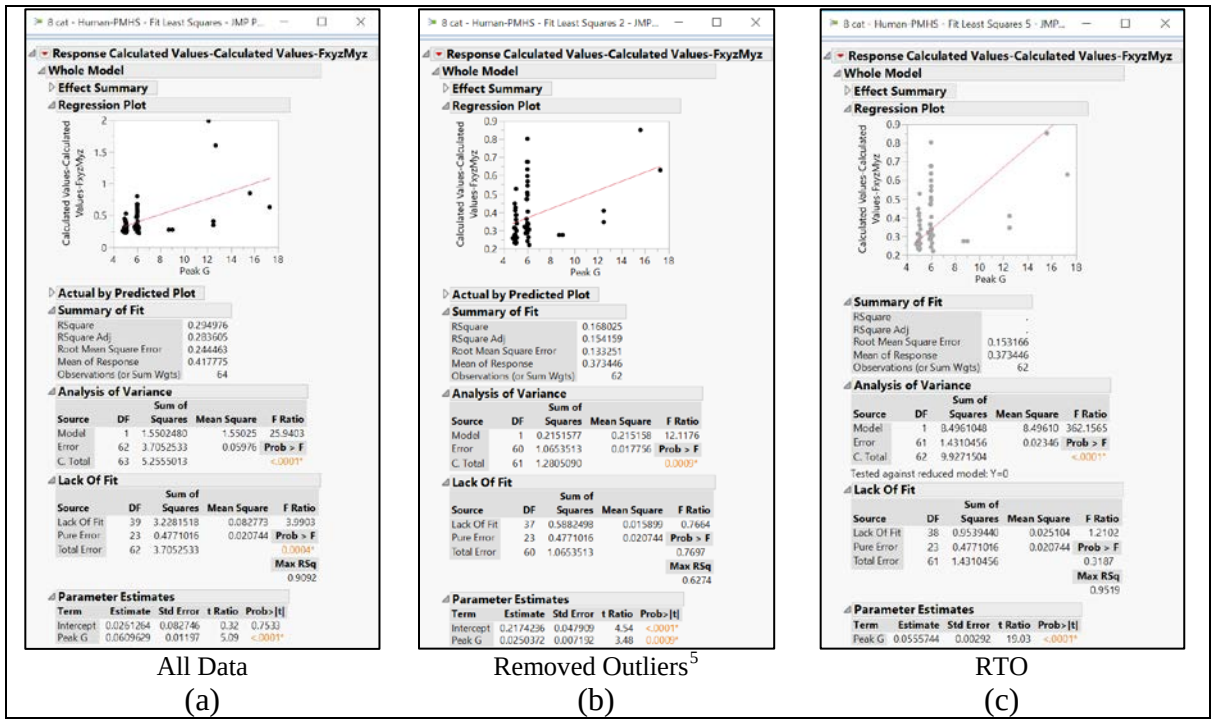

Figure 20. First Order Regression Models of 8-Cat Human MANIC(Gy)

Multiple Linear Regression for Human MANIC(Gy)

Departing from the methods used by Zinck (2015) to define the MANIC(-Gx) linear regression models, multiple regression (MR) techniques were employed to improve the human MANIC(Gy) model fit. Due to data limitations, statistical significance cannot be evaluated for MANIC(Gy) response between human male data and the available PMHS data since all PMHS were 50th percentile males. Similar to Parr et al. (2013, 2014, 2015), this analysis assumes that PMHS responses are representative of a human response to create a combined human/PMHS data set that spans the applicable Gy acceleration range, thus all PMHS were categorized as "HUMAN-M" when evaluating "Subject Type" effects in following analysis.

MR indicates that the human MANIC(Gy) response is better modeled by peak G, subject type, if the subject is wearing a helmet (Y/N), and subject weight; providing a much higher R^2

[5] (FNSC-109, FAA2011, 12.5G, res = 5.25); then (FNSC-110, FAA2011, 12.5G, res = 5.42)

(0.70 as opposed to the simple linear regression 0.17). Figure 21 contains the JMP results for the eight-category critical value MANIC(Gy) regression utilizing four explanatory variables, where panel-a contains all available data points and panel-b is the final model after removing outliers based on their studentized residuals (res), and panel-c is the model from panel-b utilizing RTO.

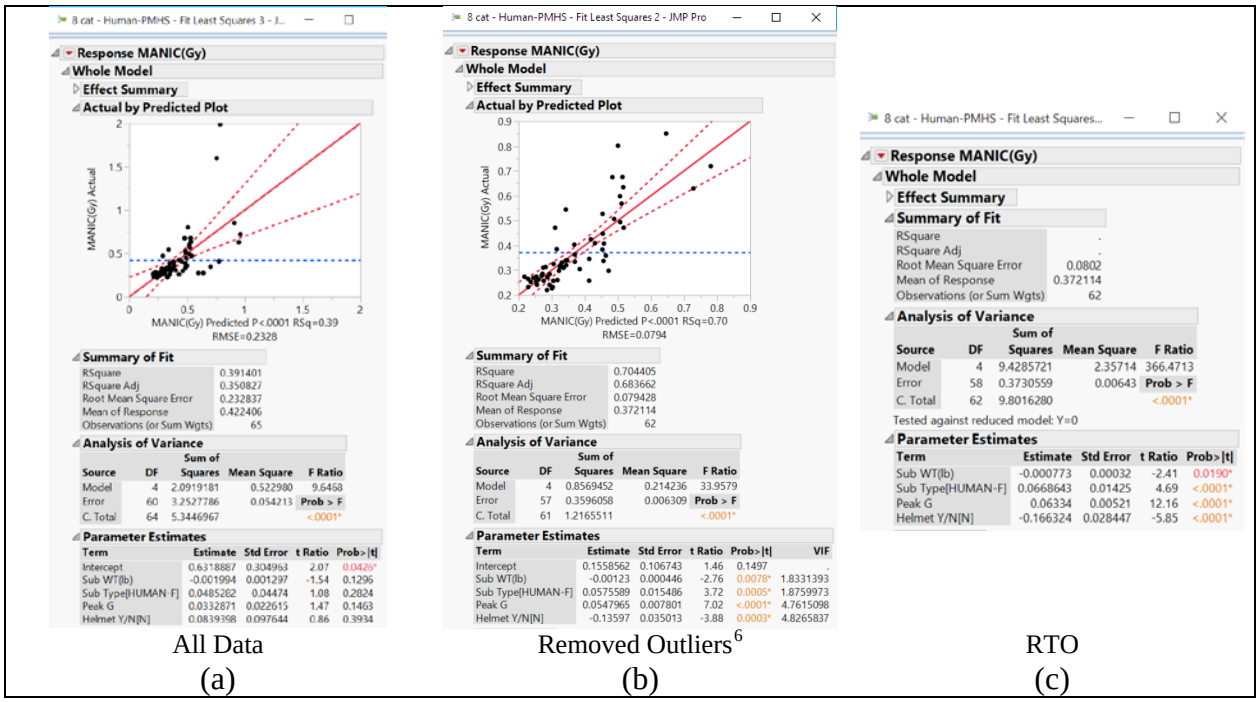

Figure 21. 8-Cat Human MANIC(Gy) MR Results

Residual analysis of the human MANIC(Gy) multiple regression model from Figure 21 b revealed an issue with non-constant variance in the model, violating the linear regression assumption for homoscedasticity (constant variance). The issue is detected by the increasing residuals associated with higher predicted MANIC(Gy) and is shown in Figure 22. This observation is confirmed numerically by using a median split of the predicted values and testing for unequal variance in the residuals between the upper and lower halves of the model. Figure

[6] (FAA 2011, FNSC-109, 12.1G, res = 5.55; FAA 2011, FNSC-110, 12.7G, res = 3.83; 199805, HIA6760, 6.01G, res = 3.16)

23 confirms the issue of heteroscedasticity with all tests for unequal variance rejecting the null hypotheses ($p < 0.05$) that the variances are equal.

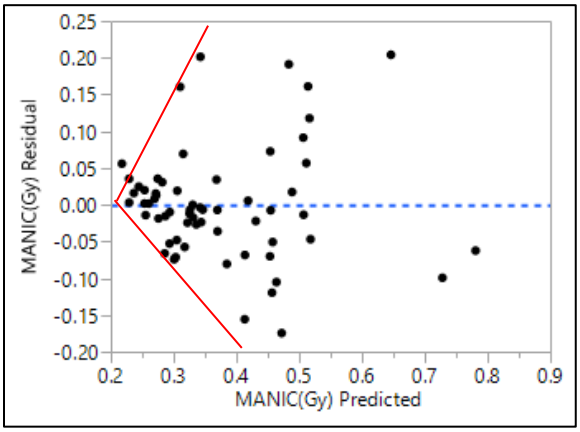

Figure 22. 8-Cat Human MANIC(Gy) MR Residuals

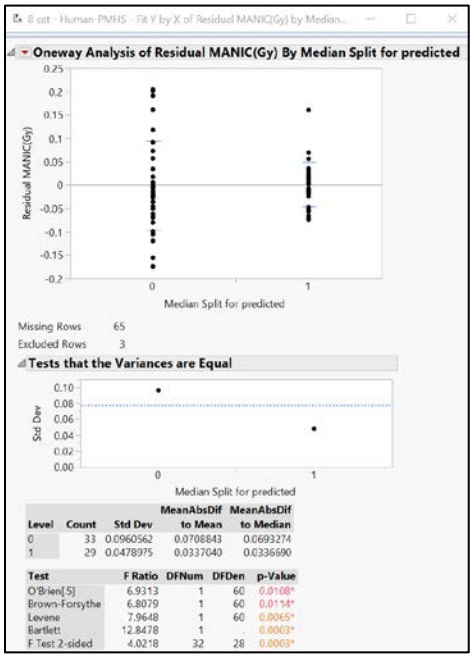

Figure 23. 8-Cat Human MANIC(Gy) MR Variance Testing

Known test differences between study 199805 and FAA 2011 were suspected as the cause of the model inaccuracy. Specifically, all 199805 testing used accelerations of 5-6Gs, some type of helmet, and a spread of subject weights and genders; while all FAA 2011 testing

consisted of accelerations of 8-17Gs, no helmets, and only 50th percentile male PMHS. The lack of gender, subject weight, and helmet variability at the higher accelerations is believed to be inducing the non-constant variance in the human multiple regression model. Review of the human/PMHS data, shown in Figure 24, reveals a notable difference in the male and female responses, as well as a larger variance in MANIC(Gy) responses within a specific G for the lower G levels (FNSC109, FNSC 110, and HIA6760 are consistently screened as outliers).

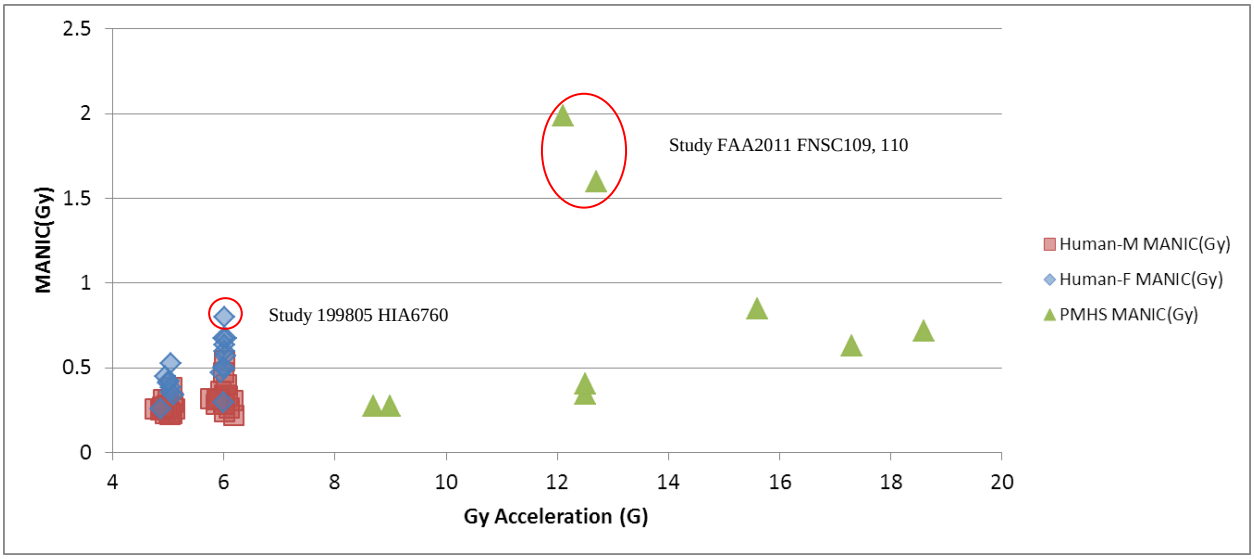

Figure 24. G vs Human/PMHS MANIC(Gy) by Subject Type

To compensate for the testing differences in the available data, multiple regression was performed using only 50th percentile males from study 199805 (137-199lbs) to define low G human MANIC(Gy) responses. Figure 25 contains the JMP results for the 50th percentile male MANIC(Gy) regression, where panel-a contains all available data points, panel-b is the final model after removing outliers based on their studentized residuals (res), and panel-c is the model from panel-b utilizing RTO. Lack of intercept significance ($p = 0.1914$) in panel-b indicates that RTO provides a better fit for this data set. Testing for unequal variance, shown in Figure 26, using a median split on the RTO model predicted values reveals a failure to reject the null

hypotheses (all $p > 0.70$), indicating that the assumption for homoscedasticity is met. These results illuminate two observations in the data: 1) subject type (male/female) induces variance in MANIC(Gy) results that is not normalized by the critical values, and 2) presence of a head supported mass (e.g. a helmet) causes a significant increase in human MANIC(Gy) response.

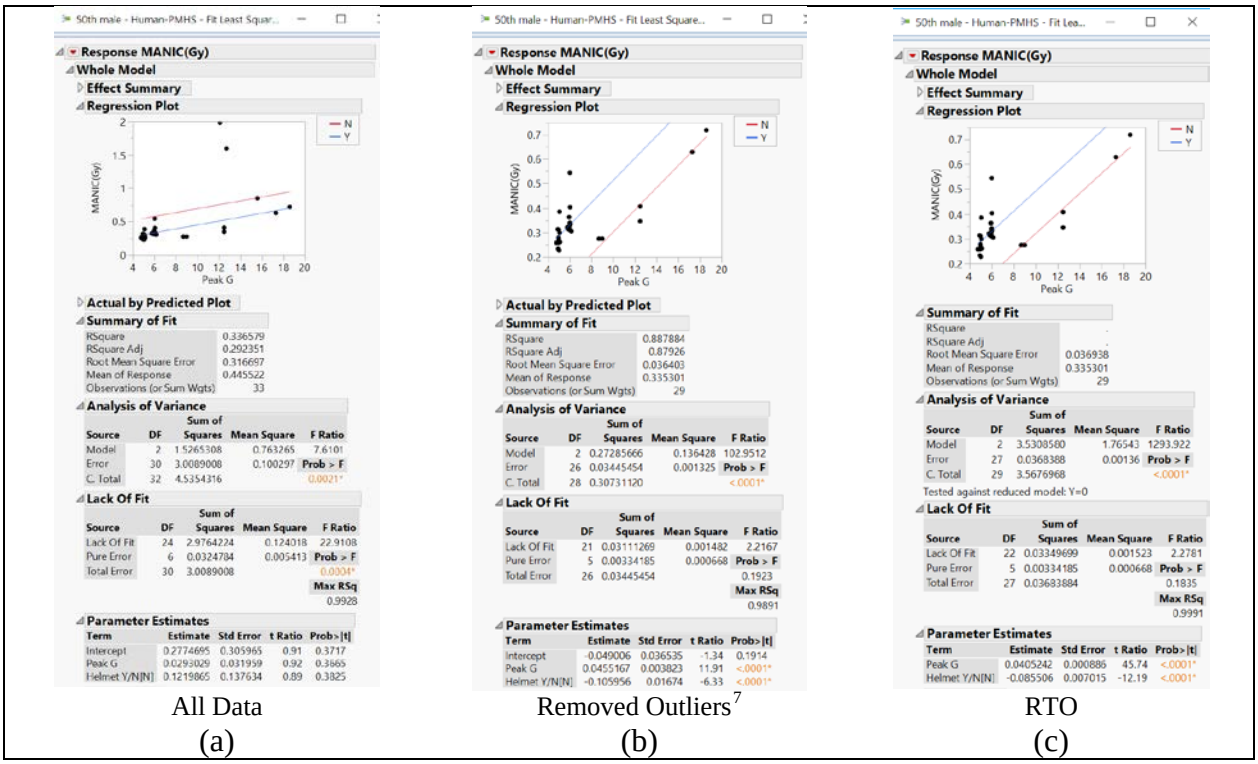

All Data (a) | Removed Outliers[7] (b) | RTO (c)

Figure 25. 8-Cat 50th Percentile Male MANIC(Gy) MR Results

[7] (FAA 2011, FNSC-109, 12.1G; FAA 2011, FNSC-110, 12.7G; FAA 2011, FNSC-118, 15.6G; 199805, HIA6772, 6.02G)

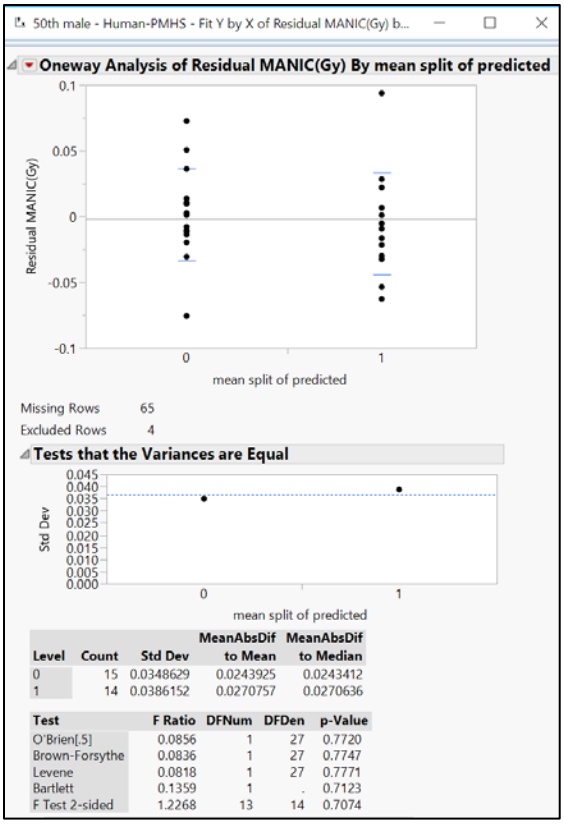

Figure 26. 50th Percentile Male MR Variance Testing

Data review suggests a significant difference between the male and female MANIC(Gy) response. MR techniques were applied in an attempt to quantify this difference. The JMP results are shown in Figure 27with the outliers removed. The only interest in this model is the delta between subject types (male/female) as the G range and other variables are insufficient for making any other determinations. This data suggests that the female MANIC(Gy) response is 0.18 higher than the male response. This indicates an inability for the eight-category critical values to normalize MANIC(Gy) response with respect to male and female anthropometric differences. Subject weight was investigated as a contributing factor, but did not appear significant in the available data set for this model or the 50th percentile male MR model.

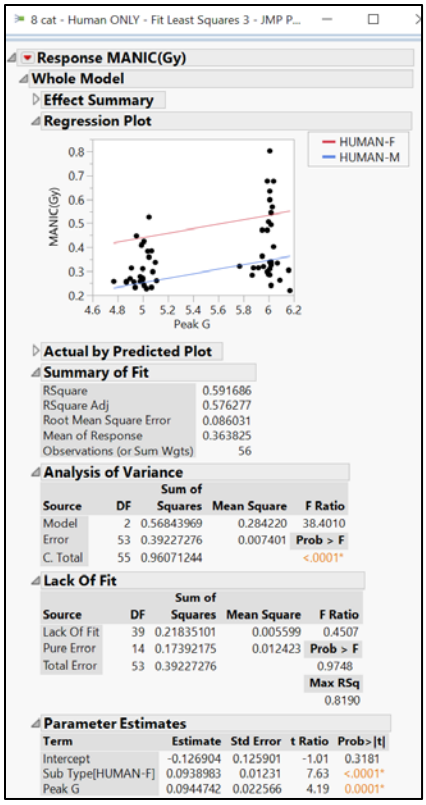

Figure 27. Male vs Female MANIC(Gy) Response MR

Multiple Linear Regression for ATD SF-MANIC(Gy)

Residual analysis of the simple linear regression ATD SF-MANIC(Gy) model indicates that either non-linear effects are present (as indicated by the 'U' shape in the residuals shown in Figure 28), or significant explanatory factors are missing from the model.

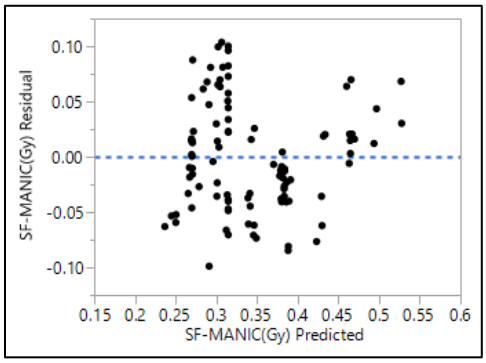

Figure 28. ATD SF-MANIC(Gy) Simple Linear Regression Residuals

MR techniques were employed to identify the explanatory variables missing from the ATD simple linear regression model. Figure 27 contains the JMP results for the ATD SF-MANIC(Gy) multiple regression, where panel-a contains all available data points and panel-b is the final model after removing outliers based on their studentized residuals (res). Use of a third order regression model for ATD neck response is supported by results from Spittle et al. (1992:45) where the hybrid III neck resistance to lateral loading was characterized by a third order regression model as shown in Figure 31. Residual analysis did not reveal any issues with the ATD MR assumptions; the residuals are shown in Figure 30.

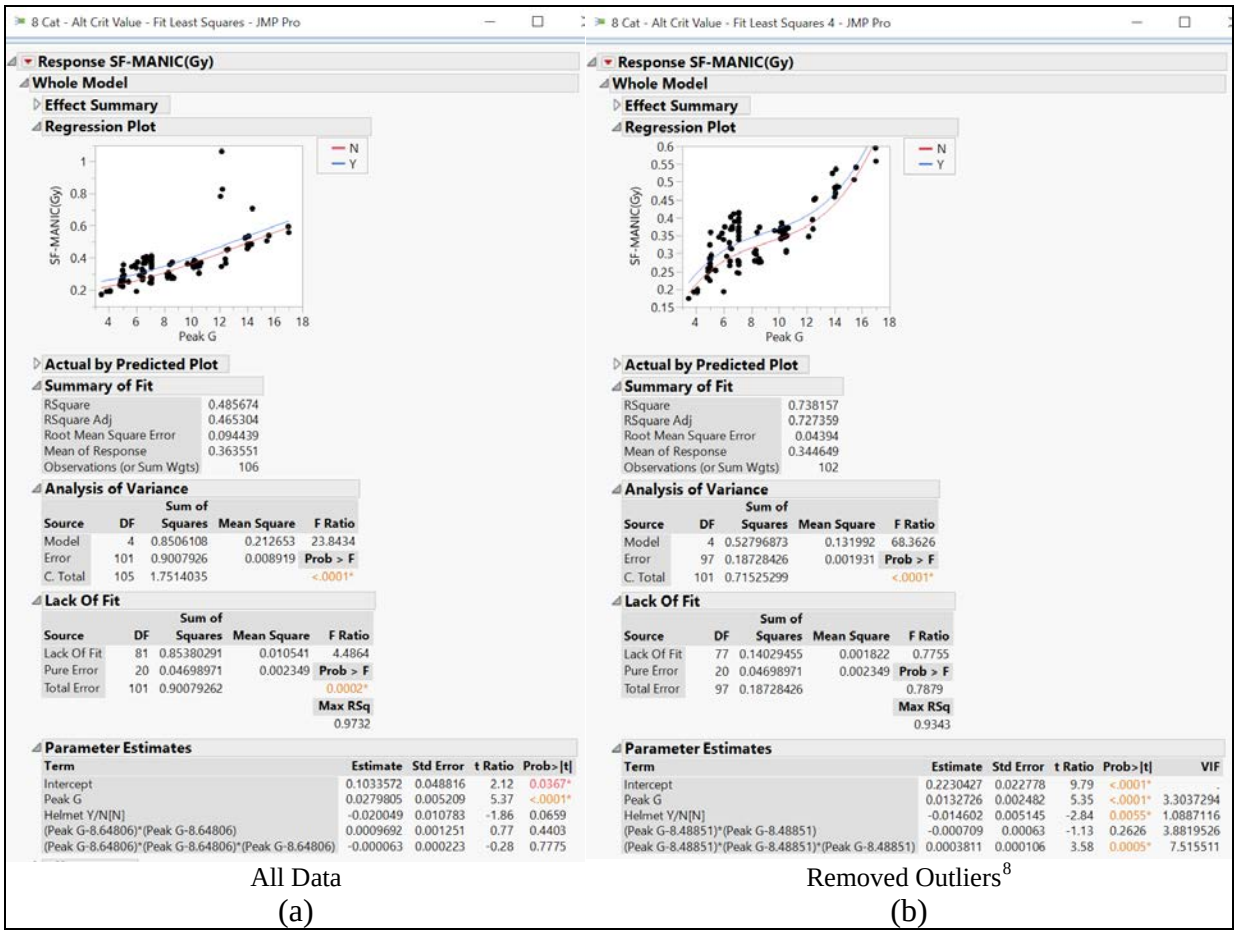

Figure 29. ATD SF-MANIC(Gy) MR Results

[8] 199901, HIA7077 12.1G, res = 3.80; 199901, HIA7080 12.2G, res = 6.35; 199901, HIA7079 12.2G, res = 3.80; 199501, HIA5263, 14.4G, res = 4.11

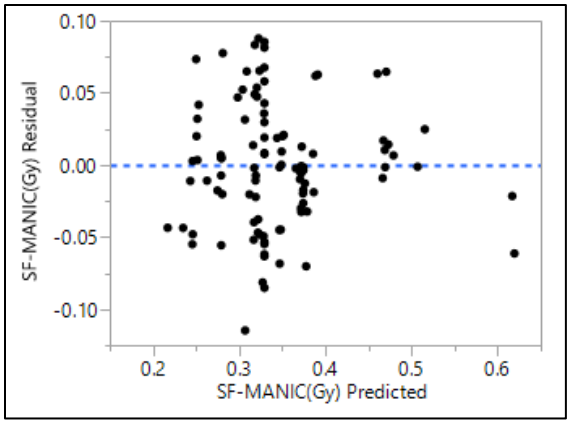

Figure 30. ATD SF-MANIC(Gy) MR Residuals

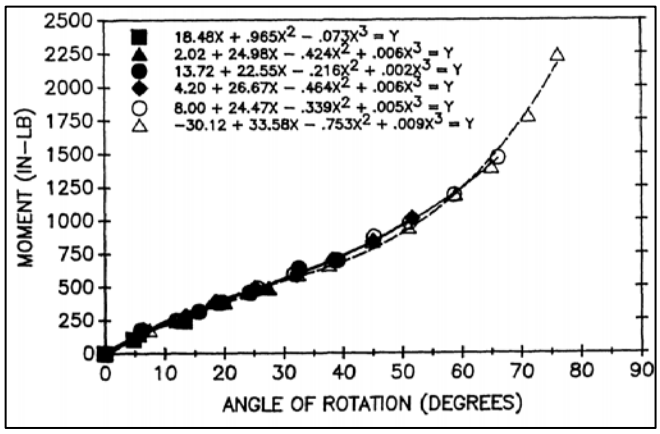

Figure 31. Static Lateral Test Hybrid III Third Order Regression (Spittle et al. 1992:45)

Model Selection for Transfer Function

Significance of Mx in the ATD response (p = 0.0189) necessitates use of the SF-MANIC(Gy) computation when evaluating ATD Gy neck responses. Linear correlation of Mx/Mz (coefficient of 0.8758) and Mx/Fy (coefficient of 0.9267) in the human SF-MANIC(Gy) supports use of the original human MANIC(Gy) computation for human responses presented by Parr et al. (2015). Slow motion video further supports the lack of Mx significance in the human MANIC(Gy) response. Thus, the ATD SF-MANIC(Gy) and human MANIC(Gy) calculations

were used to evaluate linear regression models of the ATD and human neck responses to Gy accelerative input.

First order linear regression model evaluations reveal that eight-category critical values provide better normalization of subject anthropometric factors for both humans and ATDs, generating a better linear relationship between neck responses and Gy acceleration. Thus, the eight-category critical value response is better suited for linear regression, and is selected for further evaluation.

Residual analysis of the simple linear regression models revealed issues of non-constant variance (as with the human model) and involvement of higher order terms (as with the ATD model). A revised human MANIC(Gy) MR model, using only 50^{th} percentile male subjects, resolved the issues with non-constant variance and identified significance of helmet (Y/N) and peak G variables. Lack of significance of the intercept supports use of RTO for the human model. A revised ATD SF-MANIC(Gy) MR model resolved the missing explanatory variables and identified significance of helmet (Y/N), peak G, and peak G^3 variables. Significance of the intercept does not support use of RTO for the ATD model. Further, use of a third order model for the ATD is supported by the hybrid III neck characterization performed by Spittle et al. (1992). Therefore the 50^{th} percentile male eight-category MANIC(Gy) MR model is chosen to represent the human response and the ATD eight-category SF-MANIC(Gy) MR is chosen to represent the ATD response for development of a transfer function. The regression estimates from the MR results for male and female MANIC(Gy) response differences will provide a means for evaluating female subjects in terms of a transfer function.

Transfer Function

Once the final regression models were selected, a comparison could be made between the ATD and human results. For purposes of this research a transfer function was only constructed for the best fit regression models: the 50th percentile male MANIC(Gy) MR and the ATD SF-MANIC(Gy) MR as represented in Equations 21 and 22. A simplified plot of the models is shown in Figure 32.

$$\text{MR 8-Cat ATD SF-MANIC(Gy)} \quad \begin{aligned} &0.223043 \\ &+ (Peak\ G * 0.013273) \\ &- ([Peak\ G - 8.48851]^2 * 0.000709) \\ &+ ([Peak\ G - 8.48851]^3 * 0.000381) \\ &+ \left(Match[Helmet\ Y/N] \begin{Bmatrix} N = & -0.014602 \\ Y = & 0.014602 \end{Bmatrix}\right) \end{aligned} \tag{21}$$

$$\text{MR (RTO) 8-Cat 50}^{\text{th}}\text{ Male MANIC(Gy)} \quad \begin{aligned} &(Peak\ G * 0.040524) \\ &+ \left(Match[Helmet\ 'Y/N'] \begin{Bmatrix} N = & -0.085506 \\ Y = & 0.085506 \end{Bmatrix}\right) \\ &+ \left(Match[Subject\ Type] \begin{Bmatrix} F = & 0.18 \\ M = & 0 \end{Bmatrix}\right) \end{aligned} \tag{22}$$

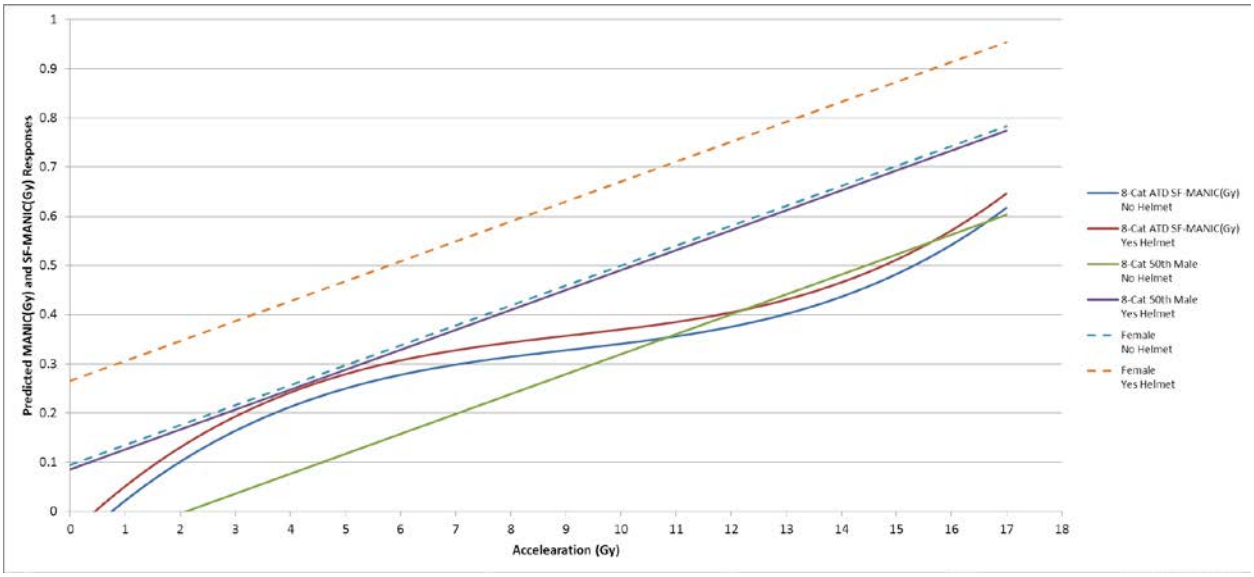

Figure 32. Selected Regression Models for Transfer Function

Human MANIC(Gy) values are transformed to equivalent ATD SF-MANIC(Gy) values using the following process:

1) Calculate the ATD MR Equivalent using the MR 8-Cat ATD SF-MANIC(Gy) regression model at the peak G and helmet category for each data point.
2) Calculate the Human MR Equivalent using the MR 50th Male MANIC(Gy) regression model at the Peak G, subject type, and helmet category for each data point.
3) Take the difference between the two response values
4) Add or subtract the response difference, depending on if the Human MR Equivalent value was lower or higher than the ATD regression value, respectively.

The resultant column, 'ATD Transform', of Table 8 displays MANIC(Gy) values that have undergone the human to ATD transform in accordance with the above process. The resultant transformed ATD SF-MANIC(Gy) points are associated with the AIS value from its corresponding human data point for evaluation of ATD injury risk probabilities. This process can be reversed for an ATD to human transform calculation as seen in Appendix E.

Table 8. Human to ATD Transfer Function

Recorded from Testing						Calculated		
Test No	Peak G	Subject Type (M/F)	Helmet ID (Y/N)	Human MANIC(Gy)	AIS	ATD MR Equivalent	Human MR Equivalent	ATD Transform
HIA6750	6.17	M	Yes	0.21973	0	0.31098	0.335539	0.1951671
HIA6751	6.16	M	Yes	0.30442	0	0.310752	0.335134	0.2800407
HIA6752	6.07	M	Yes	0.33405	0	0.308675	0.331487	0.311241
HIA6753	6	M	Yes	0.28702	0	0.307021	0.32865	0.2653908
HIA6755	6.01	M	Yes	0.30935	0	0.307259	0.329055	0.287551
HIA6757	5.96	M	Yes	0.31908	0	0.30606	0.327029	0.2981096
HIA6758	6.01	M	Yes	0.33851	0	0.307259	0.329055	0.316717
HIA6759	5.95	M	Yes	0.36265	0	0.305818	0.326624	0.3418419
HIA6760	6.01	F	Yes	0.80135	0	0.307259	0.509055	0.599552
HIA6761	6.02	M	Yes	0.24084	0	0.307497	0.32946	0.2188735
HIA6762	6.09	M	Yes	0.26219	0	0.309142	0.332297	0.2390301
HIA6769	6.02	M	Yes	0.33040	0	0.307497	0.32946	0.3084376
HIA6770	5.99	F	Yes	0.29767	0	0.306782	0.508245	0.0962032
HIA6771	5.87	M	Yes	0.28403	0	0.303856	0.323382	0.264508
HIA6772	6.02	M	Yes	0.54418	0	0.307497	0.32946	0.5222197
HIA6773	5.77	M	Yes	0.32024	0	0.301336	0.319329	0.3022419
HIA6774	6.02	M	Yes	0.32502	0	0.307497	0.32946	0.3030616
HIA6775	6.03	F	Yes	0.56817	0	0.307734	0.509866	0.3660426
HIA6781	6.02	M	Yes	0.33985	0	0.307497	0.32946	0.3178878
HIA6782	6.01	M	Yes	0.28536	0	0.307259	0.329055	0.2635686
HIA6783	6.01	F	Yes	0.59788	0	0.307259	0.509055	0.3960851
HIA6806	6.04	M	Yes	0.40275	0	0.307971	0.330271	0.380446
HIA6807	6.01	F	Yes	0.63415	0	0.307259	0.509055	0.4323558
HIA6809	6.04	F	Yes	0.67477	0	0.307971	0.510271	0.4724651
HIA6810	5.95	F	Yes	0.47123	0	0.305818	0.506624	0.2704237
HIA6819	5.99	M	Yes	0.47090	0	0.306782	0.328245	0.4494329
HIA6820	5.92	M	Yes	0.31365	0	0.305088	0.325408	0.2933273
HIA6821	5.88	M	Yes	0.31324	0	0.304104	0.323787	0.2935563
HIA6822	5.99	F	Yes	0.67515	0	0.306782	0.508245	0.4736878
HIA6833	6.02	F	Yes	0.49352	0	0.307497	0.50946	0.2915589
HIA6834	6	F	Yes	0.50622	0	0.307021	0.50865	0.304594
HIA6880	5	M	Yes	0.26454	0	0.279207	0.288126	0.25562
HIA6881	5.11	M	Yes	0.26008	0	0.282685	0.292584	0.2501805
HIA6882	5.05	F	Yes	0.35865	0	0.280801	0.470152	0.1693008
HIA6885	5	M	Yes	0.27158	0	0.279207	0.288126	0.2626648
HIA6892	4.94	M	Yes	0.23201	0	0.277262	0.285695	0.2235801
HIA6893	5.01	M	Yes	0.24143	0	0.279527	0.288531	0.2324222
HIA6894	5.07	M	Yes	0.23223	0	0.281433	0.290963	0.2226963
HIA6895	5.05	F	Yes	0.52667	0	0.280801	0.470152	0.3373207
HIA6899	4.95	F	Yes	0.44716	0	0.277588	0.4661	0.2586466

Test No	Peak G	Subject Type (M/F)	Helmet ID (Y/N)	Human MANIC(Gy)	AIS	ATD MR Equivalent	Human MR Equivalent	ATD Transform
HIA6900	5.08	M	Yes	0.29764	0	0.281747	0.291368	0.2880152
HIA6905	5	M	Yes	0.31010	0	0.279207	0.288126	0.3011808
HIA6906	5.04	F	Yes	0.38329	0	0.280484	0.469747	0.194029
HIA6907	5.07	M	Yes	0.38467	0	0.281433	0.290963	0.37514
HIA6909	5.03	M	Yes	0.22665	0	0.280166	0.289342	0.2174771
HIA6910	4.87	M	Yes	0.25267	0	0.27495	0.282858	0.2447653
HIA6913	5.1	F	Yes	0.33714	0	0.282373	0.472178	0.1473341
HIA6915	4.98	M	Yes	0.27792	0	0.278562	0.287316	0.2691646
HIA6916	4.93	M	Yes	0.25529	0	0.276934	0.285289	0.246935
HIA6917	4.98	M	Yes	0.25730	0	0.278562	0.287316	0.2485508
HIA6918	4.99	F	Yes	0.40889	0	0.278885	0.467721	0.2200587
HIA6919	4.77	M	Yes	0.25704	0	0.271564	0.278805	0.249796
HIA6926	4.91	M	Yes	0.31273	0	0.276277	0.284479	0.3045245
HIA6927	5.01	F	Yes	0.42419	0	0.279527	0.468531	0.2351893
HIA6929	4.9	M	Yes	0.26917	0	0.275946	0.284074	0.261044
HIA6972	4.87	F	Yes	0.25760	0	0.27495	0.462858	0.0696883
FAA26	18.6	M	No	0.71878	1	0.776715	0.66824	0.8272546
FNSC102	12.5	M	No	0.34532	1	0.387539	0.421044	0.311815
FNSC104	12.5	M	No	0.40725	1	0.387539	0.421044	0.373745
FNSC109	12.1	M	No	1.98735	5	0.377744	0.404834	1.9602592
FNSC110	12.7	M	No	1.59658	5	0.392893	0.429149	1.5603238
FNSC115	8.7	M	No	0.27364	3	0.323888	0.267053	0.3304752
FNSC116	9	M	No	0.27382	0	0.327763	0.27921	0.3223735
FNSC118	15.6	M	No	0.85038	2	0.516671	0.546668	0.8203821
FNSC126	17.3	M	No	0.62903	5	0.643675	0.615559	0.6571455

Survival Analysis

To ensure calculation accuracy and comparability to results presented by Parr et al (2015), a survival analysis was performed on the human and PMHS MANIC(Gy) responses from study 199805 and FAA 2011 using eight-category critical values. The human Gy risk curves generated in Minitab are shown in Figure 33. The governing equations for each curve are shown in Equations 23 and 24 and are identical to those presented by Parr et al (2015), though they are presented in unreduced form in this work to allow the location and scale to be easily identified.

$$P(Human\ AIS \geq 2) = \frac{1}{1 + e^{\frac{0.9024 - MANIC(Gy)}{0.1459}}} \quad (23)$$

$$P(Human\ AIS \geq 3) = \frac{1}{1 + e^{\frac{1.1492 - MANIC(Gy)}{0.2113}}} \quad (24)$$

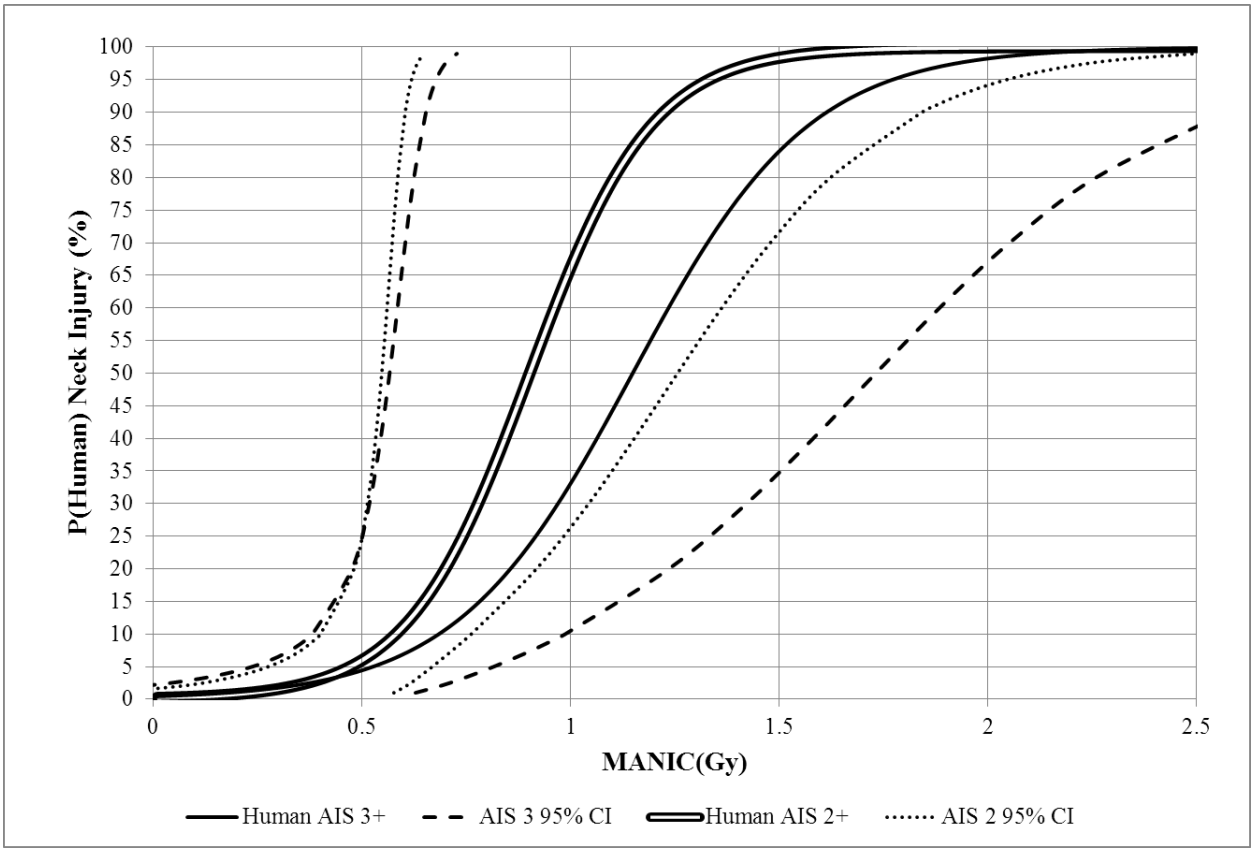

Figure 33. Human MANIC(Gy) AIS 2+ and AIS 3+ Risk Curves

Utilizing the transform results from Table 8 in the previous section, ATD AIS 2+ and 3+ risk curves were generated and are shown in Figure 34 and Figure 35, respectively. The governing equations for each curve are shown in Equations 25 and 26. It should be noted that of the injurious and non-injurious points used to calculate each curve, only one data point (FNSC118, AIS 2) changed injury categories between the two curves and is circled in both figures. The same observation was noted by Parr et al. (2015) during generation of the human risk curves. Predicted MANIC(Gy) values for human and ATD transformed risk curves are presented in Table 9. Both ATD curves are steeper (scale values [s] of 0.1132 for AIS 2+ and

0.1704 for AIS 3+) than their human risk curve counterparts (scale values of 0.1459 and 0.2113). Additionally, the ATD curves are both shifted to the left of the MANIC scale (location values [μ] of 0.7563 for AIS 2+ and 0.9691 for AIS 3+) when compared to their human risk curve counterparts (location values of 0.9024 and 1.1492).

Modified ATD AIS 2+ and 3+ curves were generated by excluding injury points from FAA 2011 test FAA-26 and FNSC116. Most testing from the FAA 2011 received AIS determinations from a pathologist and a surgeon. The two excluded tests were not evaluated by a surgeon due to issue with testing at multiple facilities. Both points had unusually low AIS values for their respective acceleration levels. However, the modified curves are within the 95% confidence intervals and do not yield a difference that is of significance. Thus, all data points are recommended to be included for direct comparison to results presented by Parr et al. (2015).

$$P(ATD\ AIS \geq 2) = \frac{1}{1 + e^{\frac{0.7563 - MANIC(Gy)}{0.1132}}} \quad (25)$$

$$P(ATD\ AIS \geq 3) = \frac{1}{1 + e^{\frac{0.9691 - MANIC(Gy)}{0.1704}}} \quad (26)$$

Table 9. Predicted MANIC(Gy) Values (95% CI) at Various Risk Percentages (as edited from Parr et al., 2015)

Risk Function	5%	10%	20%	50%
Human AIS 2+	0.473 (0.28, 0.67)	0.583 (0.40, 0.76)	0.700 (0.48, 0.92)	0.902 (0.55, 1.26)
ATD AIS 2+	0.423 (0.25, 0.359)	0.508 (0.35, 0.66)	0.600 (0.43, 0.77)	0.756 (0.52, 0.99)
Human AIS 3+	0.527 (0.24, 0.82)	0.685 (0.38, 0.99)	0.856 (0.48, 1.24)	1.149 (0.57, 1.73)
ATD AIS 3+	0.467 (0.22, 0.72)	0.594 (0.33, 0.86)	0.4733 (0.41, 1.06)	0.969 (0.47, 1.47)

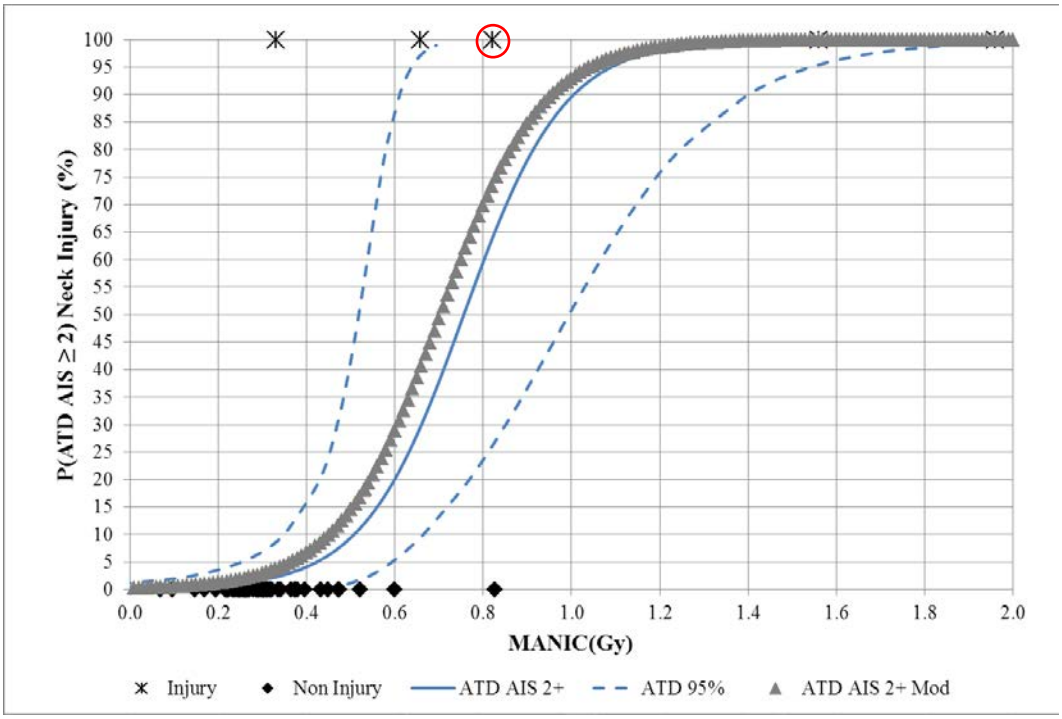

Figure 34. ATD MANIC(Gy) AIS 2+ Risk

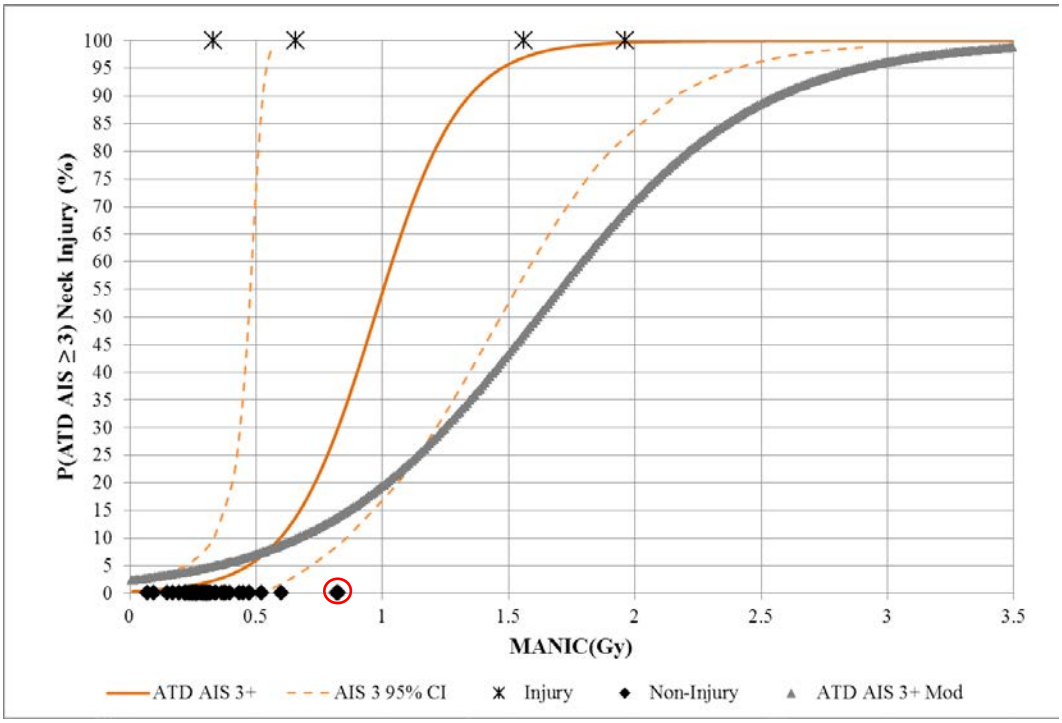

Figure 35**. ATD MANIC(Gy) AIS 3+ Risk**

V. Conclusions and Recommendations

Summary

Increased injury risk during ejection due to the increasing mass of modern HMDs drove Parr et al. to define new neck injury criteria that would reduce subjective interpretation of ejection system test results and provide early input to HMD and escape system design. As a direct result of the work done by Parr et al., the MANIC(Gx), MANIC(Gy), and MANIC(Gz) calculations and criteria were developed and adopted in MIL-HDBK-516 to define neck safety criteria for new and modified USAF aircraft ejection systems. The associated MANIC(Gx, Gy, Gz) human risk curves provide clear guidance for implementation of MANIC(Gx, Gy, Gz) responses with AFLCMC's requirement for ejection systems to maintain risk of AIS 2+ injury below 5%.

Extensive costs and safety limitations associated with human and PMHS testing drive most ejection system testing to use ATDs. Although biofidelity is sought with ATDs, differences remain in the human and ATD response, necessitating a transfer function between human and ATD MANIC responses to allow ATD testing to more precisely influence early system evaluation and comparison to AFLCMC risk requirements. Zinck (2015) furthered MANIC implementation by demonstrating proof of concept for an ATD to human transfer function of MANIC(-Gx) responses.

The next logical step to further the implementation of the MANIC was to develop a MANIC(Gy) transfer function. Through the use of linear regression and statistical analysis, MANIC(Gy) response models were developed and used to determine an appropriate ATD to human MANIC(Gy) transfer function. Risk functions generated using survival analysis provided

a practical review of ATD and human MANIC(Gy) responses and how they compare to current AFLCMC risk requirements.

Investigative Questions Answered

Is side bending (Mx) a significant neck loading mechanism when evaluating ATD and/or human MANIC(Gy) responses?

ANOVA conducted using 106 ATD test points evaluated the significance of inputs from each of the six primary neck loads on the ATD SF-MANIC(Gy) response. It was found that the t-test for Mx rejected the null hypothesis for both the 3-category (Mx $p = 0.0189$) and 8-category (Mx $p < 0.0001$) calculations of the ATD SF-MANIC(Gy); indicating that Mx is a significant response mechanism for the ATD SF-MANIC(Gy) response.

Human study 199901 was discovered to have recorded all three head accelerations (Rx, Ry, and Rz), enabling the calculation of the six primary neck loads using in-house software (Neckload4). This enabled a similar ANOVA to be conducted using 14 human test points to evaluate the significance of inputs from each of the six primary neck loads on the human SF-MANIC(Gy) response. Although the t-test suggest rejecting the null hypothesis, a large VIF indicates multicollinearity among Fx, Fy, Mx, My, and Mz within the human SF-MANIC(Gy) response. Thus, the effects of Mx in the human response can be explained through inclusion of Fx, Fy, Mx, My, and Mz; supporting Parr et al. in their determination, through nonparametric statistics, to exclude Mx from the human MANIC(Gy) calculation (Parr et al., 2015:12).

The literature and evaluation of test video from the ATD and human Gy acceleration testing confirmed the above analysis, with ATDs reacting with an observably dominant Mx response and humans reacting in an observably dominant combined Mz/My response.

Are human and ATD neck loading mechanisms sufficiently different to require an update to the MANIC(Gy) equation presented by Parr et al (2015)?

The significance of Mx in the ATD Gy response requires that ATD responses be calculated using the SF-MANIC(Gy) equation. Using the MANIC(Gy) equation presented by Parr et al (2015) to determine ATD responses artificially reduces ATD response results and drives an inaccurate transfer function.

What is the difference in expected MANIC(Gy) between human/PMHS and ATDs over the range of Gy accelerative input observed from previous laboratory experiments)?

Multiple regression techniques were used to develop models of expected ATD and human Gy responses. Both models revealed positive correlations of peak G and head supported mass (e.g. helmets) with MANIC(Gy) and SF-MANIC(Gy) responses. Additionally, linear regression indicated sensitivity to subject type (male/female), with female MANIC(Gy) responses being approximately 0.18 higher than males.

The difference in ATD and human MANIC(Gy) response over the range of Gy accelerative input changes since the ATD response is represented with a third order model (incorporating G^3) and the human response changes significantly with varying subject types and helmet use. Deltas in the ATD and human response at a specified G level can be calculated using the multiple regression models presented in this work.

Can the observed differences in peak MANIC(Gy) be used to create a transfer function to make Parr et al. human-based risk functions and associated neck injury criterion more appropriate for ejection system testing with ATDs?

The creation of multiple regression models in this research for both the human MANIC(Gy) response and ATD SF-MANIC(Gy) allow for corresponding responses to be

predicted with a known subject type (M/F), peak G, and helmet use (Y/N). A transfer function is then be defined as the difference between the two expected responses at a specified peak Gy input. This difference can then be utilized to convert between expected human and ATD responses. In general, to limit human neck injury risk to 5% of AIS 2 a human MANIC(Gy) response should be less than or equal to 0.473 (as presented by Parr et al. 2015) or the equivalent ATD SF-MANIC(Gy) response should be less than or equal to 0.423.

Recommendations for Future Work

Future work should further MANIC(Gx, Gy, Gz) implementation through the development of a MANIC(Gz) ATD to human transfer function. Additionally, the three transfer functions should be used to evaluate real-world rocket sled qualification testing that was performed with an ATD occupant. Potential exists to develop a combined ATD MANIC response evaluation that would evaluate the combined Gx, Gy, and Gz responses experienced during real-world testing.

Additional human and PMHS testing should be conducted, recording all six primary neck loads, to develop more robust injury/non-injury determinations for the development of more accurate human neck injury risk curves. Investigation into neck loading critical values that can normalize the effect of anthropometric factors of human neck loads under Gy accelerative inputs would support development of a simple linear regression model for human MANIC(Gy) responses; in turn simplifying the ATD to human transfer function.

Significance of Research

DoD budget constraints required the use of ATD testing to mitigate cost associated with escape system and HMD testing. While the human MANIC(Gx, Gy, Gz) developed by Parr et al. provides a reliable, quantitative assessment of neck injury for the purposes of evaluating

military escape systems, it does not inherently lend itself for evaluation with ATDs (Parr 2014, Parr et al., 2015). This research bridges the gap between the human response functions defined by Parr et al. and the practical use of ATDs for system evaluation. Merger of MANIC concepts with ATD testing will allow decision makers to identify potential escape system and/or HMD injury hazards earlier in development, where redesign costs can be minimized while meeting neck injury risk requirements.

Appendix A: Summary of Test Conditions

Table A-1. Test Conditions by Study

Study	Cell	Axis	NOM G	Subject ID	Subject Type	NEG-G	Cushion	Facility	Harness	H Rest	Helmet	Iner Reel	Lap Belt	Lap ADJ	Limb Rest	MISC	NVG/HMD	O-Mask	Pin	PLOAD	Seat Fix	SP/SB
201610	A	+Y	8.5	AERO50	ATD	NEG-G	NONE	HIA	5-pt Race	1"F	NONE	DOUBLE	Harness	In-line	W,A,H,K,UA,FF	Rigid Side Panels	NONE	NONE	4	30 ± 5	Generic	0/0
	A1	+Y	8.5	AERO50	ATD	NEG-G	NONE	HIA	5-pt Race	1"F	HGU-55/P	DOUBLE	Harness	In-line	W,A,H,K,UA,FF	Rigid Side Panels	NONE	NONE	4	30 ± 5	Generic	0/0
	B	+Y	10.5	AERO50	ATD	NEG-G	NONE	HIA	5-pt Race	1"F	NONE	DOUBLE	Harness	In-line	W,A,H,K,UA,FF	Rigid Side Panels	NONE	NONE	4	30 ± 5	Generic	0/0
	C	+Y	12.5	AERO50	ATD	NEG-G	NONE	HIA	5-pt Race	1"F	NONE	DOUBLE	Harness	In-line	W,A,H,K,UA,FF	Rigid Side Panels	NONE	NONE	4	30 ± 5	Generic	0/0
	D	+Y	15.5	AERO50	ATD	NEG-G	NONE	HIA	5-pt Race	1"F	NONE	DOUBLE	Harness	In-line	W,A,H,K,UA,FF	Rigid Side Panels	NONE	NONE	4	30 ± 5	Generic	0/0
	E	+Y	17	AERO50	ATD	NEG-G	NONE	HIA	5-pt Race	1"F	NONE	DOUBLE	Harness	In-line	W,A,H,K,UA,FF	Rigid Side Panels	NONE	NONE	4	30 ± 5	Generic	0/0
	F	+Y	8.5	AERO50	ATD	NONE	NONE	HIA	3-pt Auto	NONE	NONE	SINGLE	Harness	In-line	H,K,UA,FF	Foam Side Panels	NONE	NONE	4	30 ± 5	Generic	0/0
	G	+Y	10.5	AERO50	ATD	NONE	NONE	HIA	3-pt Auto	NONE	NONE	SINGLE	Harness	In-line	H,K,UA,FF	Foam Side Panels	NONE	NONE	4	30 ± 5	Generic	0/0
	H	+Y	12	AERO50	ATD	NONE	NONE	HIA	3-pt Auto	NONE	NONE	SINGLE	Harness	In-line	H,K,UA,FF	Foam Side Panels	NONE	NONE	4	30 ± 5	Generic	0/0

Study	Cell	Axis	NOM G	Subject ID	Subject Type	NEG-G	Cushion	Facility	Harness	H Rest	Helmet	Iner Reel	Lap Belt	Lap ADJ	Limb Rest	MISC	NVG/HMD	O-Mask	Pin	PLOAD	Seat Fix	SP/SB
199901	A1	+Y	5	Human	Human	NONE	NONE	HIA	PCU-15/P	0" C	NONE	DOUBLE	HBU-Std	E/W	W,T,A	NONE	NONE	NONE	11	20 ± 5	40G (F)	6/13
	B1	+Y	5	Human	Human	NONE	NONE	HIA	PCU-15/P	0" C	SIMPSON	DOUBLE	HBU-Std	E/W	W,T,A	NONE	NONE	NONE	11	20 ± 5	40G (F)	6/13
	C1	+Y	6	Human	Human	NONE	NONE	HIA	PCU-15/P	NONE	SIMPSON	DOUBLE	HBU-Std	E/W	W,T,A	NONE	NONE	NONE	11	20 ± 5	40G (F)	6/13
	D1	+Y	5	HB3-50	ATD	NONE	NONE	HIA	PCU-15/P	NONE	NONE	DOUBLE	HBU-Std	E/W	W,T,A	NONE	NONE	NONE	11	20 ± 5	40G (F)	6/13
	E1	+Y	5	HB3-50	ATD	NONE	NONE	HIA	PCU-15/P	0" C	SIMPSON	DOUBLE	HBU-Std	E/W	W,T,A	NONE	NONE	NONE	11	20 ± 5	40G (F)	6/13
	F1	+Y	12	HB3-50	ATD	NONE	NONE	HIA	PCU-15/P	0" C	NONE	DOUBLE	HBU-Std	E/W	W,T,A	NONE	NONE	NONE	11	20 ± 5	40G (F)	6/13
	G1	+Y	12	HB3-50	ATD	NONE	NONE	HIA	PCU-15/P	0" C	SIMPSON	DOUBLE	HBU-Std	E/W	W,T,A	NONE	NONE	NONE	11	20 ± 5	40G (F)	6/13
	H1	+Y	5	HB3-50	ATD	NONE	NONE	HIA	PCU-15/P	0" C	SIMPSON/S	DOUBLE	HBU-Std	E/W	W,T,A	NONE	NONE	NONE	11	20 ± 5	40G (F)	6/13
	I1	+Y	12	HB3-50	ATD	NONE	NONE	HIA	PCU-15/P	0" C	SIMPSON/S	DOUBLE	HBU-Std	E/W	W,T,A	NONE	NONE	NONE	11	20 ± 5	40G (F)	6/13
199805	A	+Y	4	ADAM-L	ATD	NONE	NONE	HIA	PCU-15/P	+0.5" F	VWI (B)	DOUBLE	HBU-Std	E/W	T,H,K,FP	NONE	NONE	NONE	11	20 ± 5	40G (F)	6/13
	B	+Y	5	ADAM-L	ATD	NONE	NONE	HIA	PCU-15/P	+0.5" F	VWI (B)	DOUBLE	HBU-Std	E/W	T,H,K,FP	NONE	NONE	NONE	11	20 ± 5	40G (F)	6/13
	C	+Y	6	ADAM-L Human	ATD Human	NONE	NONE	HIA	PCU-15/P	+0.5" F	VWI (B)	DOUBLE	HBU-Std	E/W	T,H,K,FP	NONE	NONE	NONE	11	20 ± 5	40G (F)	6/13
	D	+Y	5	ADAM-L	ATD	NONE	NONE	HIA	PCU-15/P	+0.5" F	NONE	DOUBLE	HBU-Std	E/W	T,H,K,FP	NONE	NONE	NONE	11	20 ± 5	40G (F)	6/13
	E	+Y	5	ADAM-L	ATD	NONE	NONE	HIA	PCU-15/P	+0.5" F	NONE	DOUBLE	HBU-Std	E/W	T,H,K,FP	NONE	NONE	NONE	11	20 ± 5	40G (F)	6/13
	F	+Y	5	ADAM-L Human	ATD Human	NONE	NONE	HIA	PCU-15/P	+0.5" F	VWI (C)	DOUBLE	HBU-Std	E/W	T,H,K,FP	NONE	NONE	NONE	11	20 ± 5	40G (F)	6/13

Study	Cell	Axis	NOM G	Subject ID	Subject Type	NEG-G	Cushion	Facility	Harness	H Rest	Helmet	Iner Reel	Lap Belt	Lap ADJ	Limb Rest	MISC	NVG/HMD	O-Mask	Pin	PLOAD	Seat Fix	SP/SB
199801	I	+Y	6	LOIS	ATD	NONE	APECS II	HIA	PCU-15/P	0"C	HGU-85/P	SIIIS	SIIIS/mod	TBD	W,T,C	NONE	NONE	MBU-12/P	19	20 ± 10	SIIIS/mod	6/13
	J	+Y	6	ADAM-L	ATD	NONE	APECS II	HIA	PCU-15/P	0"C	HGU-85/P	SIIIS	SIIIS/mod	TBD	W,T,C	NONE	NONE	MBU-12/P	19	20 ± 5	SIIIS/mod	6/13
	M	+Y	6	ADAM-L	ATD	NONE	APECS II	HIA	PCU-15/P	0"C	HGU-85/P	SIIIS	SIIIS/mod	TBD	W,T,C	NONE	NONE	MBU-12/P	19	20 ± 5	SIIIS/op	6/13
	N	+Y	6	LOIS	ATD	NONE	APECS II	HIA	PCU-15/P	0"C	HGU-85/P	SIIIS	SIIIS/mod	TBD	W,T,C	NONE	NONE	MBU-12/P	19	20 ± 10	SIIIS/op	6/13
199501	F	+Y	7	JPATS-S JPATS-L ADAM-L	ATD	NONE	NONE	HIA	PCU-15/P	0" C	HGU-55/P	DOUBLE	HBU-Std	E/W	W,T,K,H,FF	NONE	NONE	NONE	11	20 ± 5	40G (F)	6/13
	G	+Y	8	ADAM-L	ATD	NONE	NONE	HIA	PCU-15/P	0" C	HGU-55/P	SINGLE-V	HBU-Std	E/W	FF	NONE	NONE	MBU-12/P	11	20 ± 5	40G (C)	13/13
	G1	+Y	6	ADAM-L	ATD	NONE	NONE	HIA	PCU-15/P	0" C	HGU-55/P	SINGLE-V	HBU-Std	E/W	FF	NONE	NONE	MBU-12/P	11	20 ± 5	40G (C)	13/13
	H	+Y	10	JPATS-S JPATS-L ADAM-L	ATD	NONE	NONE	HIA	PCU-15/P	0" C	HGU-55/P	SINGLE-V	HBU-Std	E/W	K,H,FF	NONE	NONE	MBU-12/P	11	20 ± 5	40G (C)	13/13
	I	+Y	14	JPATS-S JPATS-L ADAM-L	ATD	NONE	NONE	HIA	PCU-15/P	0" C	HGU-55/P	SINGLE-V	HBU-Std	E/W	K,H,FF	NONE	NONE	MBU-12/P	11	20 ± 5	40G (C)	13/13

Study	Cell	Axis	NOMG	Subject ID	Subject Type	NEG-G	Cushion	Facility	Harness	H Rest	Helmet	Iner Reel	Lap Belt	Lap ADJ	Limb Rest	MISC	NVG/HMD	O-Mask	Pin	PLOAD	Seat Fix	SP/SB
FAA2011	-	+Y	9	ES-2 PMHS	ATD Human	NEG-G*	NONE	WSU	5-pt Race*	-	NONE	-	-	-	-	-	NONE	NONE	N/A	-	Rigid	-
	-	+Y	19	ES-2 PMHS	ATD Human	NEG-G*	NONE	WSU	5-pt Race	-	NONE	-	-	-	-	-	NONE	NONE	N/A	-	Rigid	-
	-	+Y	12.5	ES-2 PMHS	ATD Human	NEG-G*	NONE	MCW	5-pt Race*	-	NONE	-	-	-	-	-	NONE	NONE	N/A	-	Rigid	-
	-	+Y	12.5	ES-2 PMHS	ATD Human	NEG-G*	NONE	MCW	5-pt Race*	-	NONE	-	-	-	-	-	NONE	NONE	N/A	-	Rigid	-
	-	+Y	10.5	ES-2	ATD	NONE	-	MCW	3-pt Auto	-	NONE	-	-	-	-	-	NONE	NONE	N/A	-	Acft	-
	-	+Y	8.5	ES-2 PMHS	ATD Human	NONE	-	MCW	3-pt Auto	-	NONE	-	-	-	-	-	NONE	NONE	N/A	-	Acft	-
	-	+Y	15.5	PMHS	Human	NEG-G*	NONE	MCW	5-pt Race*	-	NONE	-	-	-	-	-	NONE	NONE	N/A	-	Rigid	-
	-	+Y	17	ES-2	ATD	NEG-G*	NONE	MCW	5-pt Race*	-	NONE	-	-	-	-	-	NONE	NONE	N/A	-	Rigid	-

Table A-2. Helmet Weights

Study	Subj	Helmet	Attachment	Weight (lbs)
199501	JPATS-S	HGU-55/P	none	2.30
	JPATS-L	HGU-55/P	none	2.47
	ADAM-L	HGU-55/P	none	2.47
	JPATS-S	HGU-55/P	MB-12/P and hose	3.30
	JPATS-L	HGU-55/P	MB-12/P and hose	3.47
	ADAM-L	HGU-55/P	MB-12/P and hose	3.47
199801	LOIS	HGU-68/P	MB-12/P	3.50
	ADAM-L	HGU-68/P	MBU-12/P	3.60
199901	HB3-50	SIMPSON	n/a	3.59
	HB3-50	SIMPSON/S	n/a	3.59
199805	ADAM-L	VWI (B)	custom	3.00
	ADAM-L	VWI (C)	custom	4.50

Table A-3. Test Condition Abbreviations

Category	Abbreviation	Description
Subj Type	HUMAN-F	Human female
	HUMAN-M	Human male
	MANIKIN-M	Manikin male
	MANIKIN-F	Manikin female
Neg-G	NEG-G	Negative-G or Crotch strap
	INV-V	Inverted Negative-G or Crotch strap
Cushion	APECS II	Confor Foam contoured seat cushion & back pad manufactured by Oregon Aero Inc.
Harness	PCU-15/P	Standard PCU-15/P double shoulder strap harness
	Race 5-pt	
	Auto 3-pt	Standard automotive 3-point harness
headrest	+0.5"C	Contoured headrest positioned 0.5" forward of seat back
	+2"C	Contoured headrest positioned 2" forward of seat back
	+2"F	Flat headrest positioned 2" forward of seat back
	+2.25"C	Contoured headrest positioned 2.25" forward of seat back
	-1"C	Contoured headrest positioned 1" aft of seat back
	0"C	Contoured headrest positioned in-line with seat back
	0"F	Flat headrest positioned in-line with seat back
	+0.5"F	Flat headrest positioned 0.5" forward of seat back
Helmet	HGU-55/P	Standard HGU-55/P flight helmet
	VWI(B)	Modified HGU-55/P helmet (side brackets added for mounting extra weight)
	VWI(C)	Modified HGU-55/P helmet with 1.5 lbs added weight

	HGU-85/P	Standard HGU-85/P flight helmet

Category	Abbreviation	Description
Inertia Reel	DOUBLE	Double inertia reel connection with each shoulder strap connected to its own load cell
	SINGLE-V	Single inertia reel connection with both shoulder straps connected to same point
	SIIIS	Operational inertia reel used on SIIIS ejection seat
Lap Belt	HBU-Std	Standard HBU lap belt with 1.75" wide nylon webbing
	SIIIS/mod	SIIIS lap belt modified with two inflatable inserts
Lap Belt Adjuster	E/W	East/West lap belt adjusters
Oxygen Mask	MBU-12/P	MBU-12/P oxygen mask
Seat Fixture	40G (C)	Contoured fiberglass seat pan & seat back mounted on aluminum fixture on HIA sled
	40G (F)	Flat wooden seat pan & seat back mounted on aluminum test fixture on HIA sled
	GENERIC	Generic seat fixture
	SIIIS/op	Operational SIIIS/AV8B ejection seat manufactured by UPCo, used in USMC vertical take-off aircraft
Seat Angle	0/0	Seat pan parallel to horizontal, seat back parallel to vertical
	6/13	Seat pan reclined aft of horizontal, seat back parallel to vertical
	13/13	Seat pan reclined aft of horizontal, seat back reclined aft of vertical

Category	Abbreviation	Description
Restraint	A	Ankle
	C	Chest
	FF	Feet flat on floor
	FP	Foot pedals
	HD	Head
	H	Hip
	K	Knee
	LA	Lower arm
	LL	Lower leg
	S	Shoulder
	T	Thigh
	UA	Upper arm
	W	Wrists

Appendix B: 201610 Test Plan

Measurement of Head/Neck Acceleration for during Lateral Impact Tests on the Horizontal Impulse Accelerator (+Gy MANIC)

Program/Study Number: 201610

Prepared by:

Mr. John Buhrman, 711th HPW/RHCPT
Mr. Chris Perry, 711th HPW/RHCPT

Oct 2016

APPROVED BY: _____ Date: _____
(711th HPW/RHCPT – PI)

APPROVED BY: _____ Date: _____
(711th HPW/RHCPT - Team Lead/PI)

APPROVED BY: _____ Date: _____
(711th HPW/RHCPT - Section Chief)

Aerospace Biodynamics and Performance Team
Applied Neuroscience Branch
Warfighter Interface Division
711th Human Performance Wing
Air Force Research Laboratory
Wright Patterson Air Force Base OH

1.0 INTRODUCTION

1.1 SCOPE OF PLAN

This plan describes the experimental design, methods, procedures, test equipment, data processing requirements, documentation requirements, and safety procedures for an experiment to conduct an evaluation of head/neck acceleration response under varying g-levels, restraint systems, and seat type.

1.2 SYNOPSIS OF EFFORT

The experimental effort will involve a series of +Y axis impact tests to be conducted on the Horizontal Impulse Accelerator (HIA). A Hybrid III Aerospace 50th instrumented manikin will be used in this test program to simulate human response. Data collection on the HIA will consist of sled velocity and acceleration, restraint loads, manikin neck and lumbar loads and moments, manikin head and chest accelerations, and high speed video. The data will be used to support the development of the Multi-Axial Neck Injury Criteria (MANIC) in collaboration with AFIT, as well as support the modeling work for development of a Finite Element (FE) Aerospace manikin model.

2.0 SPONSORS

This effort is an internal program funded by the USAF, Air Force Research Lab, 711th Human Performance Wing, Airman Systems Directorate.

3.0 BASIS FOR RESEARCH

3.1 BACKGROUND

The new Joint Strike Fighter (JSF) F-35 aircraft will employ a Martin-Baker Mk-US16E ejection seat, which is expected to accommodate the full range of aircrew (103-245 lbs). However, preliminary rocket sled qualification tests of this seat have shown that the neck forces and head rotations as measured in instrumented manikins may be unacceptably high for small human occupants. In addition, the current Neck Injury Criteria (Nichols 2007) contains neck injury limits that are based on automotive injury criteria that may not be appropriate for aircraft ejection.

The 711 HPW/RHCPT has been collaborating with USAFSAM to establish new neck injury criteria known as the Multi-Axial Neck Injury Criteria (MANIC) which consists of mathematical models being developed and validated with human, manikin, and PMHS tests. This effort has identified a gap in the full MANIC, where additional manikin lateral impact tests (-Gy) are needed to complete the development of a manikin transfer curve in this axis. The results of these tests will be analyzed and used in conjunction with human, PMHS and EuroSid 2 (ES2) manikin lateral impact data to establish the manikin and ultimately human transfer equations for the MANIC Gy injury criteria model.

3.2 PURPOSE

The primary purpose of this effort is to conduct instrumented manikin tests to collect manikin response data to fill a gap in angular head acceleration data for the 711 HPW/RHCPT MANIC. A secondary objective is to supply comparative data of the Aerospace manikins for our current FE human response model.

3.3 CRITICAL ISSUES

The critical issues to be addressed by the test program are:

a. Can linear and angular head/neck acceleration data from the Hybrid III Aerospace 50^{th} manikin be used to complete the gap in the Gy MANIC model?
b. How does the Hybrid III 50^{th} Aerospace manikin lateral response compare to that of the ES2 manikin?
c. Can Hybrid III 50^{th} Aerospace data collected under identical conditions be used to finalize the lateral response of the current Aerospace 50^{th} manikin FE model?

4.0 EXPERIMENTAL DESIGN

4.1 TEST MATRIX

A Hybrid III 50th Aerospace instrumented manikin will be used in this test program and shall be tested at the conditions shown in Table 2. The acceleration waveform for the HIA shall be an approximate square waveform with nominal acceleration levels of 8.5-17.0 G, rise-time of approximately 20 ms, duration of approximately 120 ms, and velocity change of approximately 28 ft/sec. The manikin shall be run twice under each test condition. The cell sequence may be randomized at the discretion of the PI. Pre-approval shall be obtained from the Test Conductor or PI prior to running the 17 G test.

Table 2. HIA Impact Test Matrix

Cell	Impact Level (G)	Restraint Configuration	Seat	Side Support	Helmet
A	8.5	5-point	Rigid	Rigid Plates	None
A1	8.5	5-point	Rigid	Rigid Plates	HGU-55/P
B	10.5	5-point	Rigid	Rigid Plates	None
C	12.5	5-point	Rigid	Rigid Plates	None
D	15.5	5-point	Rigid	Rigid Plates	None
E	17.0	5-point	Rigid	Rigid Plates	None
F	8.5	3-point	Padded	Full Padded	None
G	10.5	3-point	Padded	Full Padded	None
H	12.5	3-point	Padded	Full Padded	None

4.2 POST-TEST INSPECTION

The seat, restraint system, manikin, helmet system, and any additional flight equipment will be inspected by the Test Conductor, Principal Investigator, and/or Safety after each test. Infoscitex shall photograph any damaged areas. Damaged items will be assessed for their ability to continue use for testing before the next test is conducted.

5.0 EXPERIMENTAL METHODS

5.1 HORIZONTAL IMPULSE ACCELERATOR

The Horizontal Impulse Accelerator (HIA) shall be used for the Gy impact tests to evaluate manikin acceleration response, neck and spine loading, and restraint system loading during lateral acceleration. The HIA consists of a gas operated actuator, a test sled, and track rails. The acceleration pulse imparted to the sled depends on the pressure differential within the actuator (set pressure and load pressure), the volumes of the pressure chambers within the actuator (set length and load length), and the shape of the metering pin. Metering pin #4 shall be used for all tests. Emergency brakes are used at higher g-levels to stop the sled after the acceleration pulse is imparted to it.

5.2 SEAT FIXTURE

A generic seat shall be mounted on the multi-axial test buck located on the HIA sled. The seat shall be positioned such that the restrained manikin will face the light rack and instrumentation room, providing a +Gy impact. The seat shall be mounted with seat back 0° with respect to vertical and seat pan 0° with respect to horizontal. The headrest shall be mounted in-line with the seat back. A 1-inch thick high-density felt pad shall be attached to the headrest to reduce potential head-strike accelerations. This will cause the headrest to extend forward about 1" from the seatback. Padding shall also be affixed to the edge of the headrest and vertical brace in case of slam-back. The feet and lower legs shall be restrained during the tests by straps connected to brackets at the underside of the seat fixture. The sled, seat pan, and restraint belts shall be instrumented with load cells and/or accelerometers to collect dynamic response data during the impact. Load cells shall be mounted at the lap belt and shoulder belt termination points to simulate the restraint attachment points.

For cells A-E (rigid seat), upper arm/shoulder and hip extensions with hard felt padding shall be mounted on the side support of the seat. For cells F-H (padded seat) the full side support panel shall be securely mounted to the seat fixture on the manikin's right side with both seat pan and shoulder support fully padded.

5.3 RESTRAINT

The manikins shall be restrained with either a 5-point racing harness including crotch strap, or a 3-point harness consisting of lap belt and single diagonal strap. The manikin shall be centered in the seat prior to attaching the straps.

The lap and shoulder belts of the 5-point harness shall be affixed to separate load cells mounted on each side of the seat pan and above/behind the seat back respectively. The crotch strap shall be affixed to an anchor point mounted underneath the front of the seat pan. The shoulder straps, lap belt, and crotch straps shall be tightened securely at the anchor points with pre-tension levels of a minimum of 30 ± 5 lbs. An additional lap belt configuration shall be added as a safety strap to loosely secure the upper torso to the seat back (un-instrumented). Additional straps/belts shall be used to secure the lower legs and feet to the seat structure.

The 3-point harness shall be tightened to pre-tension levels of 20 ± 5 lbs at each of the two lap belt anchor points and the single shoulder belt anchor point. The single shoulder belt shall be positioned over the shoulder away from the HIA thrust piston.

5.4 SUBJECTS

A Hybrid III 50th Aerospace manikin with Large ADAM head will be used in this test program. The manikin shall be dressed in a USAF flight suit with no helmet except HGU-55/P helmet in cell A1. The manikin shall be instrumented with accelerometers and load cells to collect data for all channels specified in Attachment 4.

5.5 DATA ACQUISTION REQUIREMENTS

5.5.1 ELECTRONIC DATA.

The electronic data channel assignments are specified in Attachment 4. The "right-handed" coordinate system shown in Attachment 1 shall be used. Transducer excitation, signal amplification, filtering, digitizing, and transmission shall be provided by the on-board portion of two (2) TDAS G5s.

5.5.2 TRANSDUCER CALIBRATION.

Infoscitex shall be responsible to ensure the calibration of all accelerometers, restraint system load cells, and manikin load cells.

5.5.3 ACCELEROMETER AND LOAD CELL MOUNTING (MANIKIN)

Three single-axis accelerometers or a tri-axial accelerometer shall be mounted in the manikin head. Angular rate sensors shall be mounted in the manikin head that are capable of providing measurements in Rx, Ry, and Rz. Six-axis force and moment load cells shall be mounted at the upper neck and lower neck in the manikin. Three single-axis accelerometers or a tri-axial accelerometer will be mounted in the chest and pelvis of each manikin. A force and moment load cell shall also be mounted at the junction of the lumbar spine and pelvis in the manikin. See the Electronic Data Requirements (Attachment #4).

5.5.4 FACILITY INSTRUMENTATION

Three single-axis or a tri-axial accelerometers shall be mounted on the HIA sled and seat pan to measure the impact acceleration. The sled velocity shall be computed by integration. Lap belt and shoulder strap termination points on the test fixture shall be instrumented with three-axis load cells to measure restraint forces and pre-loads.

5.5.5 VIDEO COVERAGE.

Two high-speed video cameras shall be mounted on-board the HIA to provide test documentation. The camera systems have immediate playback capability. Infoscitex shall convert the video coverage to *.mp4 format at the completion of the testing.

5.5.6 STILL PHOTOGRAPHY.

The pre-impact position of the manikin, helmet system, and restraint configuration set-up will be documented by still photographs. The photographs shall include a placard listing the designation (test cell) of the test, the test number and date, and the manikin's ID. "Candid" shots

of test preparations shall also be taken at the discretion of the Test Conductor. Any structural failures or other items of interest shall also be photographed.

5.5.7 MOTION ANALYSIS

Motion analysis will not be performed for this series of tests.

5.6 TEST PROCEDURES

a. Zeros shall be taken for channel calibration.

b. The manikin shall be properly dressed and configured with the correct mask, helmet, and restraint configuration; mechanical checks shall then be performed and the manikin will be centered in the seat. The lap belt and shoulder harness will then be attached and preloaded.

c. Final checks will be conducted by the operator to ensure proper restraint fit and proper positioning have been completed.

d. The manikin's upper arms shall be positioned parallel to the seat back. The manikin's hands shall be placed in its lap and secured with Velcro straps wrapped around the thighs and attached to the underside of the seat pan. The manikin's ankles shall be secured loosely to foot pedals.

e. The Test Conductor will give final approval and then photographs shall be taken from the side and frontal views.

f. The test area around the HIA will then be evacuated and the Safety Officer will check all safety systems and assure that the test area is secured.

g. The HIA load chamber shall be pressurized to the prescribed PSI.

h. If all safety systems continue to be satisfactory, the Test Conductor will instruct the operator to start the automatic countdown and activate the facility.

5.7 TEST SCHEDULING

The impact tests are scheduled for Nov 2016 and should take approximately 1-2 weeks.

5.8 TEST EVALUATION CRITERIA

The collected data will be used to evaluate the adequacy of each test prior to further tests. This evaluation will be accomplished on the basis of a set of "quick-look" data or, if available, a complete set of data. Quick look data will consist of all measurements given in Section 6.2.

5.8.1 SUCCESSFUL TEST.

A successful test is a test in which:

a. All electronic data channels were present and continuous.

b. All other data were successfully collected.

c. Desired impact level was achieved within +/- 2% of peak G.

5.8.2 NO TEST.

A no-test is a test that does not meet the requirements of the test plan and must be repeated. A no-test will be declared if failure occurs in either the data collection system resulting in insufficient data to permit adequate and satisfactory analysis of the test, or if the required G-level is not achieved. A no-test will also be declared if any of 711 HPW/RHCPT

test personnel stop the test. A no-test will also be declared if the manikin has an improper body position prior to the initiation of the test.

5.8.3 NOT FULLY SUCCESSFUL TEST.

A test that fails to meet the requirements of a "successful test", yet is not classified as a "no-test", will be called a "not-fully-successful test". This classification of test will be made by the decision of the Principal Investigator or Associate Investigator on the basis that sufficient useful data have been collected. It may not be necessary to repeat a not-fully-successful test.

6.0 DATA PROCESSING REQUIREMENTS

6.1 ELECTRONIC DATA HANDLING

The transducer signals on the HIA will be handled by two (2) on-board TDAS G5 Data Acquisition System (DAS). All data will be collected at 1,000 samples/sec, and filtered at 120 Hz. Signal conditioning; filtering, amplification, and digitizing will take place on-board the test fixture. Following each test, the data will be prepped for additional processing and permanent storage. All test data will be entered into the Collaborative Biomechanics Data Network (CBDN) upon completion of the test program.

6.2 QUICK LOOK DATA PLOTS

After each test, the filtered data will be graphically plotted in a portrait format of 4-6 plots per page, and grouped with similar channels. This spreadsheet should also contain pertinent maxima, minima, and respective times of each occurrence. For all data, time = 0 should be at initial HIA sled motion. The plots to be arranged in this fashion include:

a. Sled acceleration (x)
b. Sled velocity (x) (computed)
c. Seat pan acceleration (x, y, and z)
d. Head linear acceleration (x, y, and z)
e. Head angular rate (Rx, Ry, and Rz)
f. Head angular acceleration (Rx, Ry, Rz) (computed)
g. Upper Neck loads (x, y, and z)
h. Upper Neck moments (Mx, My, and Mz)
i. Lower Neck loads (x, y, and z)
j. Lower Neck moments (Mx, My, and Mz)
k. Chest linear acceleration (x, y, and z)
l. Chest angular acceleration (Rx)
m. Pelvis linear accelerations (x, y, and z)
n. Lumbar loads (x, y, and z)
o. Lumbar moments (Mx, My, and Mz)
p. Lap, shoulder, and crotch strap loads (x, y, and z)
q. Nij (see Section 7.1)

6.3 MOTION ANALYSIS DATA

After each test, the high-speed video data will be reviewed to determine quality of the video, and also to determine if there were any large or abnormal displacements of the test subject during impact. Any noted discrepancies will be reported to the Principal Investigator or the Facility Contract Monitor as soon as possible, and prior to the next test. 3D Motion analysis will not be performed for this series of tests.

6.4 PHOTOGRAPHIC AND VIDEO DATA

All photographic and *.mp4 format video data shall be stored on a RHCP network drive for future use. Photo and video data shall be provided to program sponsors on CD if requested.

7.0 DATA ANALYSIS REQUIREMENTS

7.1 TEST EVALUATION CRITERIA

Immediately following each test, the "quick look" data will be evaluated to determine the adequacy of the test. These data will consist of all measurements in Appendix A. No further tests will be performed until the quick-look data from the previous test has been printed out and given to the Test Conductor for review.

Analysis of head accelerations, neck loads & moments, and restraint harness effects on an injury risk assessment will be conducted by the PI at the conclusion of the test program.

The combined cervical-force-and-moment limit, expressed as Neck Injury Criteria (Nij), shall be calculated after each test and included in the Quick Look plots. The peak Nij limit for aerospace applications is 0.5. The Nij value shall be calculated throughout the time history of the impact test according to the following formula:

$$Nij = F/F_{int} + M/M_{int}$$

where:

F is the measured manikin axial neck tension/compression or shear in pounds

F_{int} is the critical intercept load

M is the measured manikin flexion/extension bending moment in in-lbs

M_{int} is the critical intercept moment

The Nij criteria do not apply to loading in pure tension or compression. Nij values are computed for each of the following combined loading cases:

N_{te} = Tension - Extension

N_{tf} = Tension - Flexion

N_{ce} = Compression - Extension

N_{cf} = Compression - Flexion

8.0 TEST DOCUMENTATION REQUIREMENTS

8.1 HORIZONTAL IMPULSE ACCELERATOR (HIA) FACILITY

Documentation of the HIA is located at the operator's stations. These documents contain the following information:

8.1.1 TEST LOG.

The test log documents the machine operating parameters and conditions for each test. The logs are stored in the Impact Information Center and are maintained by the operations and maintenance contractor.

8.1.2 CHECKLISTS.

Operator checklists are provided for each station and are used by the station operators during each test.

8.1.3 OPERATING PROCEDURES.

This document provides detailed procedures for operating the various stations are available at each station with references to specific subsystem information. The operating procedures include an abort sequence to be used in cases of aborted tests.

8.1.4 MAINTENANCE INSTRUCTIONS.

This document provides detailed maintenance information and the inspection interval are documented here. Last inspection date is also documented.

8.1.5 MAINTENANCE LOG.

This document provides details on facility failures, dates of failures, corrective actions and date. It also provides history of accomplished maintenance.

8.1.6 TEST CONDUCTOR'S CHECKLIST.

The Test Conductor will note on the checklist (Attachment #3) any deviations from the test plan or special problems encountered during the experimentation or the data processing.

8.1.7 SAFETY CHECKLIST.

This checklist contains a list of all safety-related items that are required to be checked by the Safety Officer prior to initiation of each test.

8.2 ELECTRONIC DATA

The following documentation of the electronic data systems and procedures will be maintained:

8.2.1 INSTRUMENTATION PROGRAM REQUIREMENTS.

This document identifies the transducer and associated electronics for each data channel in addition to the sensitivities, gains, calibration values, and filters used. This document will be filed in the Impact Information Center.

8.2.2 TRANSDUCER CALIBRATION.

Each transducer maintained by Infoscitex are calibrated to check sensitivity, frequency response, and resonant frequency in accordance with the standard practice instructions of calibration procedures for each transducer type. Calibration records of individual transducers as well as the standard practice instructions are maintained in the Impact Information Center. For this test program, a record will be made identifying the data channel, transducer manufacturer, model number, serial number, date and sensitivity of calibration. Calibration information is maintained with the program data.

8.2.3 COMPUTER LOG.

This log is maintained to identify data channels and processing parameters. These records are redundant, but provide backup and data verification.

8.2.4 PLOTS AND PRINTOUTS.

The data plots and printouts are provided to the Test Conductor or Principal Investigator for review and analysis. The records will be permanently stored within the Branch.

8.3 REPORTING

The following reporting requirements will be met:

8.3.1 POST-TEST DOCUMENTATION.

Immediately after each test the Test Conductor will document any deviations from the test plan, unanticipated test results, or problems encountered in carrying the test procedures. This information will be provided to the principal investigator, or if unavailable, to the associate investigators as soon as possible and before the next test if the finding could influence the outcome of the next test.

8.3.2 TEST METHODS.

The Operations and Maintenance Contractor will document all aspects of the test methods prior to completion of testing. The documentation will include the geometry of the seat and restraint systems, location of the seat with respect to the sled, the harness materials, and the location of the instrumentation transducers. Infoscitex will also accomplish thorough documentation of the electronic and data processing techniques. This documentation will be suitable for publication in an 711th HPW/RHCPT technical report and shall be provided to the investigators for review.

8.3.3 INCIDENT AND MISHAP REPORTING.

See AFI 40-402 for injuries and DODI 5000-2AFSUP1 for equipment damage reporting requirements.

8.3.4 TECHNICAL REPORT.

Infoscitex test conductor personnel assigned to this test program are responsible for the documentation of the experimental results within a test/data report.

8.4 DISPOSITION OF TEST PLAN

The original copy of this test plan will be provided to contractor and RHCPT test personnel and filed in the R&D workunit case file. A copy will also be provided for storage within the CBDN.

9.0 TEST PERSONNEL ASSIGNMENTS

9.1 LABORATORY PERSONNEL

a. Principal Investigators: John Buhrman, Chris Perry
b. Associate Investigator: Chris Burneka
c. Test Conductors: Chris Perry, John Buhrman, Joseph Strzelecki, Chris Burneka
d. Facility Engineer: Joseph Strzelecki
e. Facility Operating Official: Joseph Strzelecki
f. Safety Officer: The safety officer for the HIA will be appointed by the Test Conductor from the list of qualified personnel specified in the Branch file entitled "Installations Management."

9.2 CONTRACTOR PERSONNEL

a. Horizontal Impulse Accelerator Operator - Qualified operators are designated in the "Installations Management" file in the Branch office.

b. Operations and Maintenance Functions - Infoscitex will provide operation and maintenance of the facilities under contract FA8650-14-D-6500 with 711th HPW/RHC. The Engineering Supervisor for Infoscitex is Ms. Annette Rizer. The Impact Testing Support is technically monitored by Capt. Robert Latta, and requests for support will be managed by him.

9.3 QUALITY ASSURANCE INSPECTIONS

Infoscitex will perform quality assurance inspections to assure the accuracy and reliability of the electronic instrumentation and data processing operations. Mr. Joe Strzelecki (or designated alternate) will perform Air Force inspection of instrumentation calibration and data processing systems operations to assure the accuracy of the electronic data and adherence to operational procedures.

9.4 TECHNICAL PHOTOGRAPHIC SERVICES

Still photographic coverage will be provided by Infoscitex. The Test Conductor will be responsible for quality assurance inspection of the photographic prints.

10.0 SAFETY AND EMERGENCY PROCEDURES

10.1 BRIEFING OF TEST PERSONNEL

All Branch and contractor personnel will be briefed on safety and emergency procedures by their supervisors.

10.2 TEST AREA ACCESS

The Safety Officer is responsible for securing the test area and restricting visitors. Only visitors approved by the Principle Investigator or the Test Conductor will be permitted in the test area. No unauthorized photography will be permitted.

10.3 HAZARDS TO OPERATORS AND TEST PERSONNEL

Hazards to operators and other test personnel will be minimized by ensuring that no personnel are to be within the designated yellow lines or down track from the leading edge of the sled before pressurization of the Impulse Accelerator is initiated. Safety inter-locks and latches will be used in accordance with established facility operating procedures and checklists referenced elsewhere in this test plan.

10.4 RISK CATEGORY

The risk category for this program is IIIc, which is defined by MIL-STD-882C to be undesirable and requiring management approval. This is due to the potential risk of equipment damage or test personnel injury.

10.5 DAMAGE TO TEST EQUIPMENT AND FACILITY

Damage to the test equipment, manikins, and minor damage to the facility is expected to occur only if catastrophic failure of the restraint harness should occur. This has not occurred at the acceleration levels that will be used during this program. The risk of catastrophic failure has been reduced by using a restraint harness that has been designed to carry loads approximately ten times higher than expected and by conducting dynamic proof-load tests of the equipment at one and one-half times the highest load levels expected during the test program. Furthermore the restraint loads will be evaluated after each test and compared to the strength of the restraint materials.

10.6 SAFETY PERMIT

The facilities and the test fixtures are approved to operate under safety permit #2016-01RHCP (exp. 12 Feb 2017). A hazard analysis was performed as part of the Safety Permit Request.

10.7 EMERGENCY PROCEDURES

Emergency procedures are defined in the attached fire evacuation plan (see Attachment #2).

11.0 REFERENCES

1. Nichols J.P. (2006). Overview of Ejection Neck Injury Criteria. 44th Annual SAFE Symposium, Reno, NV.
2. Parr J.C. (2014). A Method to Develop Neck Injury Criteria to Aid Design and Test of Escape Systems Incorporating Helmet Mounted Displays, AFIT Dissertation AFIT-ENV-DS-14-S-22, Wright-Patterson AFB OH.
3. Perry C.E., Buhrman J.R., Doczy E.J., and Mosher S.E. (2004). Evaluation of the Effects of Variable Helmet Weight on Human Response during Lateral +Gy Impact. Air Force Technical Report AFRL-HE-WP-TR-2004-0013, Wright-Patterson AFB, OH.
4. Shaffer J.T. (1976). The Impulse Accelerator: An Impact Sled Facility for Human Research and Safety Systems Testing. Aerospace Medical Research Laboratory Technical Report AMRL-TR-76-8, Wright-Patterson AFB, OH.
5. Strzelecki J.P. (2005). Characterization of Horizontal Impulse Accelerator Pin Profiles. Air Force Research Laboratory Technical Report AFRL-HE-WP-SR-2006-0057, Wright-Patterson AFB, OH.

Appendix C: In-House Neckload Program (Gallagher, 2007)

An in-house software program, “Neckload4”, was designed to calculate neck forces and moments using measured head linear and angular accelerations and inertial properties of the helmet, head, and neck. The user would have the choice to calculate the force and moment at four different junctions of the cervical neck. These junctions include the occipital condyles (OC or head-neck junction), C1/C2 junction, C4/C5 junction, and C7/T1 junction. The calculated forces and moments describe the force and moment (Figure C-1) on the surface of C1, C2, C5, and T1. These calculated forces and moments are based on the equations of motion for rigid bodies or systems. This program separates the head, neck, and helmet into two systems: the head and neck are combined as the first system and the helmet is the second system.

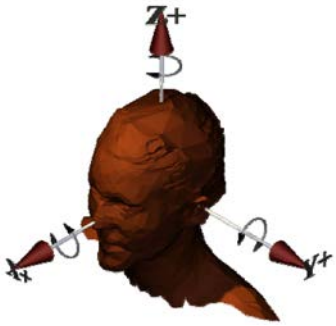

Figure C-1: Anatomical Axis System of the Human Head and Neck.

Neck Mass/Center of Mass.

Total and partial neck lengths of the subjects are calculated to obtain dimensions needed for estimating the center of mass of the selected neck segments. The total neck length is calculated using the subject’s anthropometric measurements, by taking the difference between the height of the nuchale (the lowest point in the mid-sagittal plane of the occiput that can be palpated among the nuchal muscles[8]) and the height of the cervicale (the superior tip of the spine

of the seventh cervical vertebra[8]) (Figure C-2). This gives the effective distance between the superior surface of C1 and the inferior surface of C7.

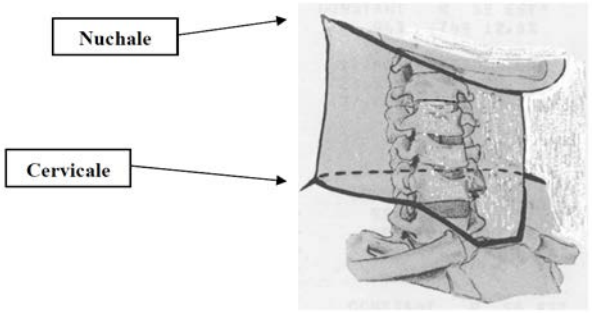

Figure C-2. Human Head and Neck

Partial neck lengths as a proportion of total neck length were calculated using cadaveric data from a study by Williams and Belytschko[10], who determined the average vertical heights of the vertebral slices (including intervertebral discs) of the human neck (Table C-1). Slices above the C2 and C5 surfaces (Figure C-3) were then summed and divided by the total neck length to obtain the percentages for these two partial neck lengths. The percentages are multiplied by the measured total neck length of individual subjects (above) to find their specified neck segment lengths.

Table C-1. Height of Vertebral Slices[10]

Vertebral Slice	Vertical Height (cm)
C1	0.8
C2	1.8
C3	1.1
C4	1.2
C5	0.9
C6	1.1
C7	1.3

- Total Average Vertical Height = 8.2 cm
- Superior Surface of C2 and Above = 0.80 / 8.2 = 10 % of Total Neck Length
- Superior Surface of C5 and Above = 4.90 / 8.2 = 60 % of Total Neck Length

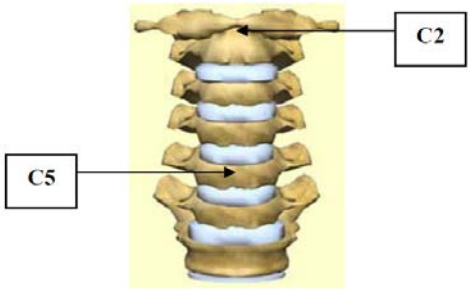

To find the total neck mass of the subject, first an estimated neck volume is obtained and multiplied by the neck density. Separate regression equations for male[7, 8] and female[11] neck volumes are used. Each regression equation uses the subject's measured anthropometry to determine the neck volume in cubic centimeters.

Male Subject:

Neck Volume = 36.89 * Neck Circumference + 1.83 * Body Weight – 659.40[7,8]

Female Subject:

Neck Volume = 10.25 * Stature + 19.10 * Neck Circumference – 1543.33[11]

Total neck mass of the subject is then obtained by multiplying the calculated neck volume by a homogeneous density of 0.00112287 slugs per cubic inch5. This density was estimated from studies by Dempster[7], McConville[8], and Young[11].

Partial neck masses were determined by a neck segmented into vertebral slices, where the total neck mass was distributed to each slice according to the volume of the slice[10] (Table C-2).

Percentages of total neck mass for the C2 and C5 surfaces and above are calculated from these data. These percentages are then multiplied by the subject's total neck mass (above) to obtain estimates of these two neck segments for individual subjects.

Table C-2. Mass of Vertebral Slices[10]

Vertebral Slice	Mass (g)
C1	815
C2	815
C3	815
C4	815
C5	815
C6	900
* A portion of C7 slice	900

*Estimated by AFRL/HEPA

• Total Average Mass = 5875 g

• Superior Surface of C2 and Above = 815 / 5875 = 14 % of Total Neck Mass

• Superior Surface of C5 and Above = 3260 / 5875 = 55 % of Total Neck Mass

Only a portion of the C7 vertebral slice was included in this program in order for it to correspond with the lower neck segmentation from the thorax performed and described by Dempster[7]. The head was segmented from the neck through the right and left gonial points and nuchale. The neck was segmented from the thorax with two connecting planes. The first plane originates at the cervicale and passes anteriorly parallel with the standing surface. The second plane originates at the lower of the two clavicale landmarks, rises 45 degrees from the horizontal and then passes diagonally superiorly-posteriorly until it intersects with the first plane (Figure C-4) [7].

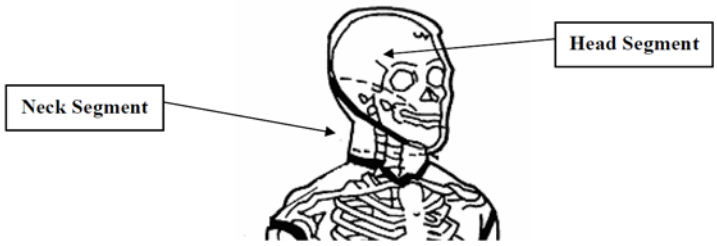

Figure C-4. Head and Neck Segmentation

The mass of the neck can be calculated for four different junctions. The mass is calculated for the neck segment down to the C1/C2 junction, the neck segment from the C1/C2 junction down to the C4/C5 junction, and the neck segment for the C4/C5 junction down to the C7/T1 junction. The mass was distributed evenly for the C1-C5 vertebral slices[11], as seen from Table C-2; therefore the center of mass is located in the center of each neck segment. The center of mass for the C7/T1 junction however is not located in the center of the neck. An average distance was calculated from nuchale to the center of mass of small, mid-size, and large male aviators[2]. The distance from nuchale to the center of mass was estimated to be 82% of the total neck length for the C7/T1 junction. Depending on the neck junction selected by the program user, the masses of the three neck segments and the centers of mass of the segments are combined in order to calculate the mass and center of mass of the segment of neck that is above the selected neck junction.

The user chooses the neck junction with a drop down menu (Figure C-5). When the user chooses to calculate the force at the OC, the properties of the neck are not included. The force on the surface of T1 would include the total neck length and total neck mass. For C2, 10% of the total neck length will be incorporated along with 14% of the total neck mass. For C5, 60% of the total neck length will be included along with 55% of the total neck mass.

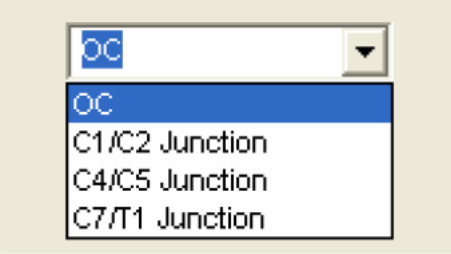

Figure C-5. Drop Down Menu for Neck Junction Selection

Head Mass/Center of Mass.

The following regression equation is used to determine the subject's head mass. Clauser et al.[6] predicted the head mass in kilograms by using the subject's measured head circumference and body weight.

Head Mass = 0.104 * Head Circumference + 0.015 * Body Weight – 2.189[6]

The center of mass of the head is assumed to be at the average location for the head center of gravity determined by Beier[3]. The mean and standard deviation for the head center of gravity was calculated from twenty-one fresh cadavers. The three-dimensional location of the center of gravity of the head was related to the anatomically based coordinate reference system (Table C-3).

Table C-3. Head Center of Gravity[3]

Coordinates of Head Center of Gravity	Mean and Standard Deviation (cm)
X	0.83 +/- 0.25
Y	-0.05 +/- 0.13
Z	3.12 +/- 0.56

Total Neck Supported Mass/Center of Mass.

Biodynamic response data are collected by an on-board data acquisition system during testing on the Vertical Deceleration Tower (VDT) at Wright-Patterson AFB, Ohio. The subject is instrumented with accelerometers. Head linear and angular accelerations are measured by a triaxial accelerometer and an angular accelerometer array mounted on a bite bar. The head acceleration is normalized to eliminate the variations in carriage acceleration.

The inertial properties of the helmet were previously measured by General Dynamics using the methods described in a report by Albery, et al.[1] and within the accuracies stated in AL-TR-1992-0137[9].

Force and Moment Calculation.

The bite bar acceleration and the bite bar angular acceleration are used to compute the acceleration at the center of mass of the combined helmet, head and neck system. A 1G vector in the vertical direction was added to the measured bite bar acceleration when the head is in its initial position. As the bite bar accelerometer rotated, the bite bar acceleration always contained 1G in the vertical direction due to the force of gravity. The 1G vector is carried over to the computed acceleration at the center of mass. The 1G vector represents the weight of the combined system in the calculation. The force is computed based on the total mass and the acceleration at the center of mass. The torque is calculated based on the total mass, inertial tensor, acceleration at the center of mass, position relative to the center of mass, angular acceleration, and angular velocity.

The acceleration at the center of mass is[12]: $\vec{a}_{cm} = \vec{a} + \dot{\vec{\omega}} \times \vec{r} + \vec{\omega} \times (\vec{\omega} \times \vec{r})$, where a is the actual acceleration at the bite bar, ω is the angular velocity, ώ is the angular acceleration, and r is a vector from the bite bar accelerometer location to the center of mass. The angular velocity can be calculated by integrating the angular acceleration. However, the piezoresistive accelerometers measure a combination of the actual acceleration and the force of gravity:$\vec{a} = \vec{a}_M - \vec{g}_0 + \vec{g}$, where a_M is the measured acceleration at the bite bar as measured by the piezoresistive accelerometers, a is the actual acceleration at the bite bar and g_0 is the initial acceleration of gravity vector at the time before the impact when the accelerometer is zeroed. The input bite bar acceleration that is read in by the Neckload4 program is assumed to be $\vec{a}_M - \vec{g}_0$, a value that is normally stored in the Biodynamic Data Bank[4]. Combining the two equations, $\vec{a}_{cm} - \vec{g} = \vec{a}_M - \vec{g}_0 + \dot{\vec{\omega}} \times \vec{r} + \vec{\omega} \times (\vec{\omega} \times \vec{r})$.

Force Calculation.

The force is then calculated using[13] $\vec{F} = m(\vec{a}_{cm} - \vec{g})$; where F is the force, m is the total mass of the combined helmet, head and neck, acm is the acceleration at the center of mass, and g is a vector in the direction of the acceleration of gravity.

Moment Calculation.

The moment (or torque) is calculated using[13]: $\vec{\tau} = \vec{R} \times m(\vec{a}_{cm} - \vec{g}) + I \cdot \dot{\vec{\omega}} + \vec{\omega} \times (I \cdot \vec{\omega})$. Where τ is the torque, R is a vector from the point at which the torque is calculated to the center of mass and I is the inertial tensor for the moments of inertia in the head anatomical coordinate system. The torque represents the torque as it would be measured at the corresponding location in the neck.

The total mass and the location of the center of mass of the combined helmet, head, and neck system are calculated based on the masses and center of masses of the helmet, head and neck. The inertial tensor of the combined system is calculated from the principal moments of inertia of the helmet, head and neck by finding the inertial tensors of the individual components using: $I = AI_{\ P}A^T$ where A is the direction cosine matrix, I is the inertial tensor in the anatomical coordinate system and I_p is the inertial tensor in the principle axis coordinate system. The inertial tensors of the individual components are then combined using the parallel-axis theorem.

Time histories and summary information about the calculated neck forces and moments are output and stored in an Excel workbook. The sign conventions use SAE J211 sign convention for the output which has the z-axis positive downward.

A source of error for the program is the use of regression equations. These equations do take into account some of the subject's true measurements, but the segment weights and inertial properties are still estimations. Also, the program calculates the acceleration at the center of mass

based on the measured head linear and angular accelerations. Unfortunately, the angular accelerations are often noisy. The program gives the user the option to filter the angular acceleration, but the noise on the angular acceleration could cause the calculated acceleration at the center of mass to be higher than it should be.

A limitation of the Neckload4 program is that the program assumes that the linear and angular accelerations of the head are caused entirely by the neck forces. The forces due to the neck were assumed to be the only external force acting on the system. If external forces other than the neck (such as due to a headrest) were acting on the head, they would need to be subtracted out of the total force that is calculated by the program in order to find the neck force and moment. Consequently, the results from the program only accurately represent the neck force and moment for each axis direction during the time period when no other external forces are acting on the head in that direction.

Appendix C REFERENCES

1) Albery, C.B., Kaleps, I. (1997) A Procedure to Measure the Mass Properties of Helmet Systems. NDIA Design and Integration of Helmet Systems Symposium Proceedings. Framingham, MA.
2) Anthropometry and Mass Distribution for Human Analogues. Volume 1: Military Male Aviators. (1988) Harry G. Armstrong Aerospace Medical Research Laboratory, WPAFB, OH. AAMRL-TR-88-010.
3) Beier, G., Schuller, E., Schuck, M., Ewing, C.L., Becker, E.D., Thomas, D.J. (1980) Center of Gravity and Moments of Inertia of Human Heads. Scientific Report No. 1:218-228. Institute for Forensic Medicine, University of Munich. Naval Biodynamics Laboratory, New Orleans, LA.
4) Buhrman, J.R., Plaga, J.A., Cheng, H., Mosher, S.E. (2001) The AFRL Biodynamics Data Bank on the web: A repository of human impact acceleration response data. Proceedings of the 39th Annual SAFE Symposium.
5) Cheng, H., Obergefell, L., Rizer, A. (1994) Generator of Body Data (GEBOD) Manual. Armstrong Laboratory, Crew Systems Directorate. WPAFB, OH. AL/CF-TR-1994-0051.
6) Clauser, C.E., McConville, J.T., Young, JW. (1969) Weight, Volume, and Center of Mass of Segments of the Human Body. AMRL-TR-69-70.
7) Dempster, W.T. (1955) Space Requirements of the Seated Operator. Geometrical, Kinematic, and Mechanical Aspects of the Body with Special Reference to the Limbs. Human Mechanics: 215-328. AMRL-TDR-63-123.
8) McConville, J.T., Churchill, T.D., Kaleps, I., Clauser, C.E., Cuzzi, J. (1980) Anthropometric Relationships of Body and Body Segment Moments of Inertia. Air Force Aerospace Medical Research Laboratory, WPAFB, OH. AFAMRL-TR-80-119.
9) Self, B.P., Spittle, E.K., Kaleps, I., Albery, C.B. (1992) Accuracy and Repeatability of the Standard Automated Mass Properties Measurement System. AL-TR-1992-0137.
10) 10)Williams, J., Belytschko, T. (1981) A Dynamic Model of the Cervical Spine and Head. Air Force Aerospace Medical Research Laboratory, WPAFB, OH. AFAMRL-TR-81-5.
11) Young, J.W., Chandler, R.F., Snow, C.C., Robinette, K.M., Zehner, G.F., Lofberg, M.S. (1983) Anthropometric and Mass Distribution Characteristics of the Adult Female. FAAAM-83-16.
12) Wells, D.A., (1967) Lagrangian Dynamics, Schaum's Outline Series, McGraw-Hill, p. 180.
13) Symon, K.R. (1960) Mechanics, Addison-Wesley, p. 451.

Appendix D: ATD and Human MANIC(Gy) and SF-MANIC(Gy) Values

Table D-1. ATD SF-MANIC(Gy) and MANIC(Gy) Using Eight-Category Critical Values

Test No	Sty No	Cell	Peak G	Sub ID	Sub Type	Sub WT (lb)	Helmet ID	Subj Age	**SF-MANIC (Gy) Time (ms)**	**SF-MANIC (Gy)**	**MANIC (Gy) Time (ms)**	**MANIC (Gy)**
HIA9209	201610	A	8.35	AERO50	MANIKIN-M	161	NONE	N/A	104	0.29704449	94	0.2084928
HIA9210	201610	A	8.33	AERO50	MANIKIN-M	161	NONE	N/A	105	0.30817957	98	0.21298777
HIA9211	201610	A1	8.59	AERO50	MANIKIN-M	161	HGU-55/P	N/A	108	0.37252731	104	0.25154709
HIA9212	201610	A1	8.41	AERO50	MANIKIN-M	161	HGU-55/P	N/A	109	0.35862833	102	0.24017183
HIA9213	201610	B	10.57	AERO50	MANIKIN-M	161	NONE	N/A	104	0.34926243	101	0.2442982
HIA9214	201610	B	10.66	AERO50	MANIKIN-M	161	NONE	N/A	105	0.3704791	104	0.25387915
HIA9215	201610	C	12.54	AERO50	MANIKIN-M	161	NONE	N/A	102	0.4503433	96	0.3145235
HIA9216	201610	C	12.64	AERO50	MANIKIN-M	161	NONE	N/A	102	0.45395094	96	0.30986332
HIA9217	201610	D	15.44	AERO50	MANIKIN-M	161	NONE	N/A	99	0.50593242	96	0.34800499
HIA9218	201610	D	15.58	AERO50	MANIKIN-M	161	NONE	N/A	99	0.54029508	94	0.37187417
HIA9219	201610	E	17.02	AERO50	MANIKIN-M	161	NONE	N/A	99	0.55802651	93	0.38815922
HIA9220	201610	E	16.99	AERO50	MANIKIN-M	161	NONE	N/A	100	0.59531926	96	0.3996817
HIA9221	201610	F	8.57	AERO50	MANIKIN-M	161	NONE	N/A	149	0.28452164	141	0.18756988
HIA9222	201610	F	8.54	AERO50	MANIKIN-M	161	NONE	N/A	129	0.27486709	127	0.17923821
HIA9223	201610	F	8.7	AERO50	MANIKIN-M	161	NONE	N/A	146	0.27565357	150	0.19329203
HIA9224	201610	G	10.23	AERO50	MANIKIN-M	161	NONE	N/A	157	0.3628314	150	0.26229505
HIA9225	201610	G	10.42	AERO50	MANIKIN-M	161	NONE	N/A	165	0.34529395	162	0.24213141
HIA9226	201610	G	10.52	AERO50	MANIKIN-M	161	NONE	N/A	146	0.30352725	144	0.22085735
HIA9227	201610	H	12.15	AERO50	MANIKIN-M	161	NONE	N/A	141	0.34664541	140	0.24876368
HIA9228	201610	H	12.43	AERO50	MANIKIN-M	161	NONE	N/A	141	0.3935074	135	0.27280451

HIA9229	201610	H	12.46	AERO50	MANIKIN-M	161	NONE	N/A	74	0.36766368	93	0.22810207
HIA7075	199901	D1	5.10	HB3-50	MANIKIN-M	170	NONE	N/A	167	0.29483233	168	0.18916523
HIA7073	199901	E1	5.06	HB3-50	MANIKIN-M	170	SIMPSON	N/A	179	0.35864125	164	0.19639936
HIA7077	199901	F1	12.08	HB3-50	MANIKIN-M	170	NONE	N/A	124	0.78406087	124	0.55175808
HIA7080	199901	G1	12.17	HB3-50	MANIKIN-M	170	SIMPSON	N/A	139	1.06296183	138	0.61982269
HIA7074	199901	H1	5.00	HB3-50	MANIKIN-M	170	SIMPSON/S	N/A	155	0.22363946	155	0.21549892
HIA7079	199901	I1	12.22	HB3-50	MANIKIN-M	170	SIMPSON/S	N/A	136	0.82752528	137	0.47269083
HIA6660	199805	A	3.46	ADAM-L	MANIKIN-M	218	VWI (B)	N/A	174	0.17365335	162	0.09959863
HIA6661	199805	A	3.84	ADAM-L	MANIKIN-M	218	VWI (B)	N/A	173	0.19139188	241	0.10648157
HIA6662	199805	A	4.1	ADAM-L	MANIKIN-M	218	VWI (B)	N/A	177	0.19814246	107	0.12723404
HIA6663	199805	A	4.09	ADAM-L	MANIKIN-M	218	VWI (B)	N/A	176	0.19085171	106	0.12105033
HIA6671	199805	B	4.87	ADAM-L	MANIKIN-M	218	VWI (B)	N/A	100	0.25728368	95	0.21914794
HIA6672	199805	B	5	ADAM-L	MANIKIN-M	218	VWI (B)	N/A	105	0.28422224	97	0.23215344
HIA6673	199805	B	5.04	ADAM-L	MANIKIN-M	218	VWI (B)	N/A	106	0.2602969	99	0.2147416
HIA6677	199805	C	5.66	ADAM-L	MANIKIN-M	218	VWI (B)	N/A	172	0.34533325	97	0.22354544
HIA6678	199805	C	5.88	ADAM-L	MANIKIN-M	218	VWI (B)	N/A	170	0.35640854	103	0.20244901
HIA6679	199805	C	6.08	ADAM-L	MANIKIN-M	218	VWI (B)	N/A	171	0.37384336	100	0.22828967
HIA6680	199805	C	5.99	ADAM-L	MANIKIN-M	218	VWI (B)	N/A	168	0.33826519	97	0.22038756
HIA6664	199805	D	5.42	ADAM-L	MANIKIN-M	218	NONE	N/A	148	0.25181833	142	0.14959375
HIA6665	199805	D	4.88	ADAM-L	MANIKIN-M	218	NONE	N/A	158	0.24882174	153	0.14680797
HIA6666	199805	D	4.8	ADAM-L	MANIKIN-M	218	NONE	N/A	152	0.23229725	150	0.13547001
HIA6667	199805	D	5.05	ADAM-L	MANIKIN-M	218	NONE	N/A	156	0.25504346	148	0.15098394
HIA6668	199805	E	5.02	ADAM-L	MANIKIN-M	218	NONE	N/A	236	0.27061345	92	0.21633275
HIA6669	199805	E	5.05	ADAM-L	MANIKIN-M	218	NONE	N/A	99	0.28359937	92	0.24136712
HIA6670	199805	E	5	ADAM-L	MANIKIN-M	218	NONE	N/A	103	0.3233465	101	0.28015015
HIA6674	199805	F	5.01	ADAM-L	MANIKIN-M	218	VWI (C)	N/A	177	0.28415994	104	0.2185053
HIA6675	199805	F	4.99	ADAM-L	MANIKIN-M	218	VWI (C)	N/A	113	0.28573271	111	0.2436344

HIA6676	199805	F	5	ADAM-L	MANIKIN-M	218	VWI (C)	N/A	108	0.27193297	104	0.22251274
HIA6556	199801	I	6.51	LOIS	MANIKIN-F	103	HGU-85/P	N/A	176	0.40168336	176	0.4014249
HIA6557	199801	I	6.62	LOIS	MANIKIN-F	103	HGU-85/P	N/A	172	0.37422727	174	0.37133115
HIA6558	199801	I	6.5	LOIS	MANIKIN-F	103	HGU-85/P	N/A	173	0.36716851	169	0.3600086
HIA6559	199801	J	6.44	ADAM-L	MANIKIN-M	218	HGU-85/P	N/A	205	0.26503891	199	0.2122442
HIA6560	199801	J	6.22	ADAM-L	MANIKIN-M	218	HGU-85/P	N/A	199	0.29172251	192	0.23048308
HIA6561	199801	J	6.41	ADAM-L	MANIKIN-M	218	HGU-85/P	N/A	198	0.32991264	191	0.25687354
HIA6529	199801	M	6.46	ADAM-L	MANIKIN-M	218	HGU-85/P	N/A	202	0.27763417	195	0.21053308
HIA6530	199801	M	6.47	ADAM-L	MANIKIN-M	218	HGU-85/P	N/A	196	0.31549185	190	0.23944435
HIA6531	199801	M	6.56	ADAM-L	MANIKIN-M	218	HGU-85/P	N/A	199	0.31204222	193	0.2278988
HIA6534	199801	N	6.63	LOIS	MANIKIN-F	103	HGU-85/P	N/A	176	0.36813586	176	0.36713201
HIA6535	199801	N	6.78	LOIS	MANIKIN-F	103	HGU-85/P	N/A	183	0.38903887	183	0.38417368
HIA6536	199801	N	6.72	LOIS	MANIKIN-F	103	HGU-85/P	N/A	185	0.41031724	183	0.39868697
HIA5220	199501	F	7.04	JPAT-S	MANIKIN-F	116	HGU-55/P	N/A	163	0.27911614	152	0.26300451
HIA5221	199501	F	7.09	JPAT-S	MANIKIN-F	116	HGU-55/P	N/A	128	0.26603351	135	0.25315586
HIA5222	199501	F	6.98	JPAT-S	MANIKIN-F	116	HGU-55/P	N/A	159	0.24597833	156	0.23958176
HIA5224	199501	F	7.09	JPAT-S	MANIKIN-F	116	HGU-55/P	N/A	154	0.27447211	155	0.2676627
HIA5225	199501	F	7.09	JPAT-S	MANIKIN-F	116	HGU-55/P	N/A	152	0.27594056	152	0.2631556
HIA5226	199501	F	7.09	JPAT-S	MANIKIN-F	116	HGU-55/P	N/A	151	0.26743833	152	0.26277368
HIA5227	199501	F	7.09	JPAT-S	MANIKIN-F	116	HGU-55/P	N/A	145	0.24414859	142	0.23046748
HIA5228	199501	F	7.09	ADAM-L	MANIKIN-M	218	HGU-55/P	N/A	138	0.372142	124	0.24121886
HIA5229	199501	F	7.09	ADAM-L	MANIKIN-M	218	HGU-55/P	N/A	157	0.3969295	145	0.24331199
HIA5230	199501	F	7.09	ADAM-L	MANIKIN-M	218	HGU-55/P	N/A	149	0.38737392	139	0.23591978
HIA5231	199501	F	7.09	ADAM-L	MANIKIN-M	218	HGU-55/P	N/A	148	0.41074259	135	0.24283704
HIA5232	199501	F	7.09	ADAM-L	MANIKIN-M	218	HGU-55/P	N/A	145	0.41475068	132	0.24291603
HIA5233	199501	F	7.09	JPAT-L	MANIKIN-M	247	HGU-55/P	N/A	157	0.33696955	138	0.25571973
HIA5234	199501	F	7.09	JPAT-L	MANIKIN-M	247	HGU-55/P	N/A	164	0.34838233	143	0.25428984
HIA5235	199501	F	7.09	JPAT-L	MANIKIN-M	247	HGU-55/P	N/A	148	0.33767389	129	0.24930334

HIA5236	199501	F	7.09	JPAT-L	MANIKIN-M	247	HGU-55/P	N/A	163	0.35894183	142	0.25115392
HIA5238	199501	F	7.07	JPAT-L	MANIKIN-M	247	HGU-55/P	N/A	164	0.3647226	144	0.25791202
HIA5267	199501	G	8.25	ADAM-L	MANIKIN-M	218	HGU-55/P	N/A	130	0.27869471	130	0.24070556
HIA5268	199501	G	8.22	ADAM-L	MANIKIN-M	218	HGU-55/P	N/A	141	0.30167409	133	0.2236272
HIA5266	199501	G1	6	ADAM-L	MANIKIN-M	218	HGU-55/P	N/A	130	0.19227514	143	0.14614735
HIA5239	199501	H	10.09	ADAM-L	MANIKIN-M	218	HGU-55/P	N/A	127	0.36672054	127	0.29815602
HIA5240	199501	H	10.12	JPAT-L	MANIKIN-M	247	HGU-55/P	N/A	141	0.36716289	140	0.35075061
HIA5241	199501	H	10.12	JPAT-L	MANIKIN-M	247	HGU-55/P	N/A	141	0.36593734	140	0.35718923
HIA5242	199501	H	10.3	JPAT-L	MANIKIN-M	247	HGU-55/P	N/A	142	0.35694218	140	0.33712285
HIA5243	199501	H	10.32	JPAT-L	MANIKIN-M	247	HGU-55/P	N/A	144	0.37108035	144	0.34901461
HIA5244	199501	H	10.44	JPAT-L	MANIKIN-M	247	HGU-55/P	N/A	145	0.36360224	143	0.33991388
HIA5245	199501	H	10.15	ADAM-L	MANIKIN-M	218	HGU-55/P	N/A	139	0.33962103	135	0.25815562
HIA5246	199501	H	10.29	ADAM-L	MANIKIN-M	218	HGU-55/P	N/A	125	0.35436763	125	0.2661922
HIA5247	199501	H	10.27	ADAM-L	MANIKIN-M	218	HGU-55/P	N/A	123	0.37063953	121	0.27440762
HIA5248	199501	H	10.19	ADAM-L	MANIKIN-M	218	HGU-55/P	N/A	134	0.38545899	123	0.27850662
HIA5249	199501	H	10.15	ADAM-L	MANIKIN-M	218	HGU-55/P	N/A	134	0.37141129	124	0.28983911
HIA5250	199501	H	10.53	JPAT-S	MANIKIN-F	116	HGU-55/P	N/A	136	0.307465	135	0.30374312
HIA5251	199501	H	10.12	JPAT-S	MANIKIN-F	116	HGU-55/P	N/A	139	0.34167539	138	0.33877531
HIA5252	199501	H	10.04	JPAT-S	MANIKIN-F	116	HGU-55/P	N/A	139	0.36073965	139	0.34896552
HIA5253	199501	H	10.32	JPAT-S	MANIKIN-F	116	HGU-55/P	N/A	138	0.37306444	137	0.36716426
HIA5254	199501	H	9.69	JPAT-S	MANIKIN-F	116	HGU-55/P	N/A	138	0.36352042	138	0.35998028
HIA5255	199501	H	10.3	JPAT-S	MANIKIN-F	116	HGU-55/P	N/A	136	0.34784469	135	0.33536303
HIA5257	199501	I	14.12	JPAT-S	MANIKIN-F	116	HGU-55/P	N/A	127	0.53528748	126	0.51424943
HIA5258	199501	I	14.18	JPAT-S	MANIKIN-F	116	HGU-55/P	N/A	126	0.48736496	126	0.47453454
HIA5259	199501	I	14.08	JPAT-S	MANIKIN-F	116	HGU-55/P	N/A	125	0.47939816	124	0.46775904
HIA5260	199501	I	14.09	ADAM-L	MANIKIN-M	218	HGU-55/P	N/A	125	0.46786864	121	0.36664415
HIA5261	199501	I	14.04	ADAM-L	MANIKIN-M	218	HGU-55/P	N/A	120	0.48432588	111	0.37549676
HIA5262	199501	I	14.02	ADAM-L	MANIKIN-M	218	HGU-55/P	N/A	123	0.45746371	120	0.34716272

HIA5263	199501	I	14.39	JPAT-L	MANIKIN-M	218	HGU-55/P	N/A	134	0.7076891	134	0.699674
HIA5264	199501	I	13.87	JPAT-L	MANIKIN-M	247	HGU-55/P	N/A	135	0.52394072	134	0.51926115
HIA5265	199501	I	14.32	JPAT-L	MANIKIN-M	247	HGU-55/P	N/A	130	0.48580633	130	0.48494599

Table D-2. Human/PMHS SF-MANIC(Gy) and MANIC(Gy) Using Eight-Category Critical Values

Test No	Sty No	Cell	Peak G	Sub ID	Sub Type	Helmet ID	Sub WT (lb)	Subj Age	AIS	**SF-MANIC (Gy) Time (ms)**	**SF-MANIC (Gy)**	**MANIC(Gy) Time (ms)**	**MANIC(Gy)**
HIA6750	199805	C	6.17	B-11	HUMAN-M	VWI (B)	233	37	0	N/A	N/A	130	0.21973
HIA6751	199805	C	6.16	M-21b	HUMAN-M	VWI (B)	152	39	0	N/A	N/A	146	0.30442
HIA6752	199805	C	6.07	H-13	HUMAN-M	VWI (B)	160	35	0	N/A	N/A	137	0.33405
HIA6753	199805	C	6	D-11	HUMAN-M	VWI (B)	237	32	0	N/A	N/A	122	0.28702
HIA6755	199805	C	6.01	B-23	HUMAN-M	VWI (B)	185	37	0	N/A	N/A	120	0.30935
HIA6757	199805	C	5.96	B-24	HUMAN-M	VWI (B)	191	32	0	N/A	N/A	150	0.31908
HIA6758	199805	C	6.01	W-12	HUMAN-M	VWI (B)	180	43	0	N/A	N/A	147	0.33851
HIA6759	199805	C	5.95	B-26	HUMAN-M	VWI (B)	155	21	0	N/A	N/A	136	0.36265
HIA6760	199805	C	6.01	B-25	HUMAN-F	VWI (B)	145	20	0	N/A	N/A	146	0.80135
HIA6761	199805	C	6.02	E-4	HUMAN-M	VWI (B)	220	37	0	N/A	N/A	135	0.24084
HIA6762	199805	C	6.09	H-18	HUMAN-M	VWI (B)	250	27	0	N/A	N/A	129	0.26219
HIA6769	199805	C	6.02	D-12	HUMAN-M	VWI (B)	190	30	0	N/A	N/A	136	0.3304
HIA6770	199805	C	5.99	S-23	HUMAN-F	VWI (B)	167	25	0	N/A	N/A	137	0.29767
HIA6771	199805	C	5.87	D-13	HUMAN-M	VWI (B)	213	34	0	N/A	N/A	136	0.28403
HIA6772	199805	C	6.02	H-16	HUMAN-M	VWI (B)	180	42	0	N/A	N/A	161	0.54418
HIA6773	199805	C	5.77	B-9	HUMAN-M	VWI (B)	168	30	0	N/A	N/A	136	0.32024
HIA6774	199805	C	6.02	H-19	HUMAN-M	VWI (B)	210	20	0	N/A	N/A	138	0.32502
HIA6775	199805	C	6.03	B-22	HUMAN-F	VWI (B)	137	28	0	N/A	N/A	173	0.56817
HIA6781	199805	C	6.02	C-17b	HUMAN-M	VWI (B)	177	31	0	N/A	N/A	137	0.33985
HIA6782	199805	C	6.01	R-21	HUMAN-M	VWI (B)	237	38	0	N/A	N/A	151	0.28536
HIA6783	199805	C	6.01	E-5	HUMAN-F	VWI (B)	140	25	0	N/A	N/A	133	0.59788
HIA6806	199805	C	6.04	J-7	HUMAN-M	VWI (B)	160	30	0	N/A	N/A	140	0.40275

HIA6807	199805	C	6.01	L-11	HUMAN-F	VWI (B)	132	32	0	N/A	N/A	150	0.63415
HIA6809	199805	C	6.04	P-12	HUMAN-F	VWI (B)	160	30	0	N/A	N/A	146	0.67477
HIA6810	199805	C	5.95	M-32	HUMAN-F	VWI (B)	128	23	0	N/A	N/A	148	0.47123
HIA6819	199805	C	5.99	S-11b	HUMAN-M	VWI (B)	205	34	0	N/A	N/A	32	0.4709
HIA6820	199805	C	5.92	C-12a	HUMAN-M	VWI (B)	185	37	0	N/A	N/A	124	0.31365
HIA6821	199805	C	5.88	Y-4	HUMAN-M	VWI (B)	188	28	0	N/A	N/A	123	0.31324
HIA6822	199805	C	5.99	B-16a	HUMAN-F	VWI (B)	133	33	0	N/A	N/A	142	0.67515
HIA6833	199805	C	6.02	W-11	HUMAN-F	VWI (B)	140	22	0	N/A	N/A	148	0.49352
HIA6834	199805	C	6	C-19	HUMAN-F	VWI (B)	154	27	0	N/A	N/A	150	0.50622
HIA6880	199805	F	5	B-11	HUMAN-M	VWI (C)	227	37	0	N/A	N/A	154	0.26454
HIA6881	199805	F	5.11	J-7	HUMAN-M	VWI (C)	160	30	0	N/A	N/A	131	0.26008
HIA6882	199805	F	5.05	B-16a	HUMAN-F	VWI (C)	132	33	0	N/A	N/A	157	0.35865
HIA6885	199805	F	5	H-16	HUMAN-M	VWI (C)	180	42	0	N/A	N/A	44	0.27158
HIA6892	199805	F	4.94	B-9	HUMAN-M	VWI (C)	164	30	0	N/A	N/A	156	0.23201
HIA6893	199805	F	5.01	D-11	HUMAN-M	VWI (C)	206	32	0	N/A	N/A	134	0.24143
HIA6894	199805	F	5.07	E-4	HUMAN-M	VWI (C)	230	37	0	N/A	N/A	149	0.23223
HIA6895	199805	F	5.05	E-5	HUMAN-F	VWI (C)	140	25	0	N/A	N/A	138	0.52667
HIA6899	199805	F	4.95	B-25	HUMAN-F	VWI (C)	135	20	0	N/A	N/A	145	0.44716
HIA6900	199805	F	5.08	B-26	HUMAN-M	VWI (C)	155	21	0	N/A	N/A	149	0.29764
HIA6905	199805	F	5	D-12	HUMAN-M	VWI (C)	190	30	0	N/A	N/A	153	0.3101
HIA6906	199805	F	5.04	B-22	HUMAN-F	VWI (C)	140	28	0	N/A	N/A	161	0.38329
HIA6907	199805	F	5.07	H-13	HUMAN-M	VWI (C)	160	35	0	N/A	N/A	153	0.38467
HIA6909	199805	F	5.03	C-17b	HUMAN-M	VWI (C)	170	31	0	N/A	N/A	146	0.22665
HIA6910	199805	F	4.87	D-13	HUMAN-M	VWI (C)	215	34	0	N/A	N/A	139	0.25267
HIA6913	199805	F	5.1	W-11	HUMAN-F	VWI (C)	140	22	0	N/A	N/A	164	0.33714
HIA6915	199805	F	4.98	B-24	HUMAN-M	VWI (C)	193	32	0	N/A	N/A	148	0.27792
HIA6916	199805	F	4.93	S-11b	HUMAN-M	VWI (C)	204	34	0	N/A	N/A	159	0.25529

HIA6917	199805	F	4.98	Y-4	HUMAN-M	VWI (C)	188	28	0	N/A	N/A	165	0.2573
HIA6918	199805	F	4.99	C-19	HUMAN-F	VWI (C)	156	27	0	N/A	N/A	152	0.40889
HIA6919	199805	F	4.77	M-21b	HUMAN-M	VWI (C)	155	39	0	N/A	N/A	155	0.25704
HIA6926	199805	F	4.91	W-12	HUMAN-M	VWI (C)	180	43	0	N/A	N/A	161	0.31273
HIA6927	199805	F	5.01	S-23	HUMAN-F	VWI (C)	167	25	0	N/A	N/A	151	0.42419
HIA6929	199805	F	4.9	H-19	HUMAN-M	VWI (C)	210	20	0	N/A	N/A	143	0.26917
HIA6972	199805	F	4.87	P-12	HUMAN-F	VWI (C)	165	30	0	N/A	N/A	146	0.2576
FAA26	FAA2011	WSU	18.6	FAA26	PMHS	NONE	163	57	1	81.6	0.8210319	81.3	0.71878
FNSC102	FAA2011	MCW	12.5	FNSC102	PMHS	NONE	190	55	1	61.28	0.5019899	54.32	0.34532
FNSC104	FAA2011	MCW	12.5	FNSC104	PMHS	NONE	154	49	1	59.92	0.6491434	58.88	0.40725
FNSC109	FAA2011	MCW	12.1	FNSC109	PMHS	NONE	142	59	5	86.16	2.008566	86.16	1.98735
FNSC110	FAA2011	MCW	12.7	FNSC110	PMHS	NONE	167	55	5	97.2	1.5966004	97.2	1.59658
FNSC115	FAA2011	MCW	8.7	FNSC115	PMHS	NONE	180	57	3	111.52	0.3177232	96.8	0.27364
FNSC116	FAA2011	MCW	9	FNSC116	PMHS	NONE	164	47	0	99.44	0.2765215	99.44	0.27382
FNSC118	FAA2011	MCW	15.6	FNSC118	PMHS	NONE	139	63	2	33.6	0.8529132	33.6	0.85038
FNSC126	FAA2011	MCW	17.3	FNSC126	PMHS	NONE	148	61	5	44.32	0.7354568	43.92	0.62903
HIA7090	199901	A1	5.09788	H-19	HUMAN-M	210	NONE	21	0	185	0.160578663	184	0.100422444
HIA7092	199901	A1	4.97044	H-13	HUMAN-M	160	NONE	36	0	153	0.241107314	153	0.140405185
HIA7095	199901	A1	5.08756	W-12	HUMAN-M	183	NONE	44	0	181	0.180254911	166	0.143750313
HIA7096	199901	A1	5.14553	G-14a	HUMAN-M	190	NONE	35	0	191	0.363597466	200	0.218743276
HIA7100	199901	B1	5.04979	G-14a	HUMAN-M	190	SIMPSON	35	0	141	0.316516467	141	0.239203484
HIA7103	199901	B1	5.01961	H-13	HUMAN-M	160	SIMPSON	36	0	144	0.321485904	144	0.221587047
HIA7104	199901	B1	4.9042	W-12	HUMAN-M	184	SIMPSON	44	0	144	0.258529047	144	0.168580458
HIA7106	199901	B1	5.06828	H-19	HUMAN-M	210	SIMPSON	21	0	139	0.322216644	139	0.225988839
HIA7108	199901	C1	5.85152	G-14a	HUMAN-M	190	SIMPSON	35	0	134	0.332898177	134	0.250194885
HIA7109	199901	C1	5.81365	W-12	HUMAN-M	185	SIMPSON	44	0	129	0.335233048	129	0.218819048
HIA7110	199901	C1	5.82305	M-33	HUMAN-F	130	SIMPSON	30	0	136	0.636906121	136	0.39614856
HIA7111	199901	C1	5.84095	H-19	HUMAN-M	210	SIMPSON	21	0	130	0.361683423	130	0.251773114

HIA7113	199901	C1	5.94887	H-13	HUMAN-M	160	SIMPSON	36	0	136	0.488319689	135	0.314951048

Appendix E: Transfer Function Procedures

ATD SF-MANIC(Gy) and human MANIC(Gy) responses can each be independently evaluated on the AIS risk functions presented in this work, or each can be transformed to be evaluated with a specific risk function. The following process describes the steps required to conduct the ATD to human transform.

1) Perform Gy testing on the HIA, or equivalent test fixture, with desired harness, seat fixture, ATD, head mounted mass (helmet, mask, goggles, etc), and G level.
2) During testing record time history data for neck moments and loads (Fx, Fy, Fz, Mx, My, Mz) at the ATD representative occipital condyle location.
3) Using the SF-MANIC(Gy) equation shown in Equation E1 and the eight-category critical values for the associated ATD weight, calculate the ATD MANIC(Gy) response for each time step of the neck load data.
4) Identify the peak MANIC(Gy) response and peak Gy acceleration (typically the peak response will occur 50-100ms after the peak acceleration)
5) Apply the ATD test conditions for peak G and helmet to the ATD multiple regression model shown in Equation E2 to calculate a predicted ATD Gy response.
6) Apply the ATD test conditions for peak G and helmet to the human multiple regression model shown in Equation E3 to calculate a predicted human Gy response. NOTE: when conducting an ATD to human transform, the subject should always be considered “Female” to provide the most conservative risk evaluation that applies to the entire pilot population.
7) Take the absolute value of the difference between the predicted ATD and human Gy responses calculated in steps 5 and 6.

8) Depending on the predicted response values, follow one of the below steps
    a. If the predicted ATD response is larger than the predicted human response, subtract the delta from step 7 from the peak MANIC(Gy) found in step 4.
    b. Else, add the delta from step 7 to the peak MANIC(Gy) found in step 4

The resultant value calculated in step 8 is the human MANIC(Gy) response equivalent for the conducted ATD test. This value can then be evaluated using the human neck injury risk curve equation shown in Equations E4 and E5 to identify the probability of human AIS 2 or AIS 3 injury associated with the conducted ATD test. Alternatively, the original ATD result could be evaluated against the ATD risk curves shown in Equations E6 and E7.

ATD SF-MANIC(Gy)

$$\sqrt{\left(\frac{Fx}{Fxcrit}\right)^2+\left(\frac{Fy}{Fycrit}\right)^2+\left(\frac{Fz}{Fzcrit}\right)^2+\left(\frac{Mx}{Mxcrit}\right)^2+\left(\frac{My}{Mycrit}\right)^2+\left(\frac{Mz}{Mzcrit}\right)^2} \quad \text{(E1)}$$

Multiple Regression Model
8-Cat ATD SF-MANIC(Gy)

$$\begin{aligned}&0.223043\\&+(Peak\ G*0.013273)\\&-([Peak\ G-8.48851]^2*0.000709)\\&+([Peak\ G-8.48851]^3*0.000381)\\&+\left(Match[Helmet\ Y/N]\begin{Bmatrix}N=&-0.014602\\Y=&0.014602\end{Bmatrix}\right)\end{aligned} \quad \text{(E2)}$$

Multiple Regression Model
(RTO) 8-Cat 50th Male MANIC(Gy)

$$\begin{aligned}&(Peak\ G*0.040524)\\&+\left(Match[Helmet\ 'Y/N']\begin{Bmatrix}N=&-0.085506\\Y=&0.085506\end{Bmatrix}\right)\\&+\left(Match[Subject\ Type]\begin{Bmatrix}F=&0.18\\M=&0\end{Bmatrix}\right)\end{aligned} \quad \text{(E3)}$$

$$P(Human\ AIS\geq 2)\qquad \frac{1}{1+e^{\frac{0.9024-MANIC(Gy)}{0.1459}}} \quad \text{(E4)}$$

$$P(Human\ AIS\geq 3)\qquad \frac{1}{1+e^{\frac{1.1492-MANIC(Gy)}{0.2113}}} \quad \text{(E5)}$$

$$P(ATD\ AIS\geq 2)\qquad \frac{1}{1+e^{\frac{0.7563-MANIC(Gy)}{0.1132}}} \quad \text{(E6)}$$

$$P(ATD\ AIS\geq 3)\qquad \frac{1}{1+e^{\frac{0.9691-MANIC(Gy)}{0.1704}}} \quad \text{(E7)}$$

Example ATD to Human Transform:

- If testing with the ADAM-L(218lbs) on the HIA reveals a peak SF-MANIC(Gy) of 0.500 and a peak G of 7.2 while wearing a helmet with an advanced HMD attached
- The predicted ATD response is 0.331
- The predicted human (female) response is 0.557
- The delta between the predicted responses is 0.226
- Since the predicted human response is higher than the predicted ATD response, the delta in the previous step is added to the measured ATD response, giving an equivalent human MANIC(Gy) response of 0.726 for the particular test in question.
- Evaluating this response using the human AIS 2 risk curve, it is revealed that there is a 23.5% risk of AIS 2 or higher injury for the associated test conditions.
- Evaluating the original ATD response (0.5) against the ATD risk curve would provide a 9.4% risk of AIS2 or higher injury.
- Using the less conservative ATD to human transform (not assuming the ATD to be female) would yield a predicted human (male) MANIC(Gy) of 0.377, equivalent human MANIC(Gy) of 0.546 and human AIS 2+ risk of 8.2%
- These results indicate that this fictional setup should take mitigating steps to reduce the peak MANIC(Gy) response and its associated risk for neck injury.

Bibliography

Association for the Advancement of Automotive Medicine (AAM). (2017) *Abbreviated Injury Scale Overview*. Retrieved from https://www.aaam.org/abbreviated-injury-scale-ais/

Bass, C., Donnellan, L., Salzar, R., Lucas, S., Folk, B., Davis, M., Rafaels, K., Planchak, C., Meyerhoff, K., Ziemba, A., Alem, N. (2006). "A New Neck Injury Criterion in Combined Vertical/Frontal Crashes with Head Supported Mass." 2006 International IRCOBI Conference on the Biomechanics of Impact. Madrid, Spain.

Bevan, M., Ward, E., & Luong, Q. (2010). Neck Torque Study Induced by Head-Borne Visual Augmentation Systems in Ground-Based Applications. John Hopkins University Applied Physics Laboratory, MD. Report No. NSTD-09-1057.

Brohi, K. (2007). *Abbreviated Injury Scale (AIS) Score*. Retrieved from http://www.trauma.org/index.php/main/article/510

Buhrman, J.R. and Perry, C.E. (1994). "Human and Manikin Head/Neck Response to +Gz Acceleration When Encumbered by Helmets of Various Weights." Aviation, Space, and Environmental Medicine: 1086-1090.

Chancey, C.V., Ottaviano, D., Myers, B.S., & Nightingale, R.W. (2007). "A Kinematic and Anthropometric Study of the Upper Cervical Spine and the Occipital Condyles." Journal of Biomechanics: 40: 1953-1959.

Doczy, E., Mosher, S., & Buhrman, J. (2004). "The Effects of Variable Helmet Weight and Subject Bracing on Neck Loading During Frontal -Gx Impact." Proceedings of the 42nd Annual SAFE Symposium, 186-192.

Eveland, E., Esken, B., Shouse, N., Goodyear, C., & Kane, M. (2008). Neck Muscle Fatigue Resulting from Prolonged Wear of Weighted Helmets under High G Acceleration. Wright-Patterson AFB, OH: Air Force Research Laboratory. Report No. AFRL-RH-WP-TR-2008-0085

Federal Aviation Administration (FAA). (2011). Neck injury criteria for side-facing aircraft seats. Washington, DC: Federal Aviation Administration.

Gallagher, H. Buhrman, J. Perry, C. (2007). An Analysis of Vertebral Stress and BMD During +Gz Impact Accelerations. Wright-Patterson AFB, OH: Air Force Research Laboratory. Report No. AFRL-HE-WP-TR-2007-0085.

Gallagher, H. & Caldwell, E. (2008). Neck muscle fatigue resulting from prolonged wear of weighted helmets. Wright-Patterson AFB, OH: Air Force Research Laboratory. Report No. AFRL-RH-WP-TR-2008-0096.

Herbst, B., Forrest, S., Chng, D., & Sances, A. (1998). Fidelity of Anthropometric Test Dummy Necks in Rollover Accidents. National Highway Traffic Safety Administration. Paper No. 98-S9-W-20. Retrieved from https://www-nrd.nhtsa.dot.gov/pdf/Esv/esv16/98S9W20.PDF

Manoogian, S., Kennedy, E., Wilson, K., Alem, N., & Duma, S. (2005). Predicting Neck Injuries Due to Head Supported Mass. Virginia Tech- Wake Forest, Center for Injury Biomechanics, Blacksburg, VA

Montgomery, D, Peck, E., & Vining, G. (2006). Introduction to Linear Regression Analysis. Hoboken, NJ: John Wiley & Sons, Inc.

Nichols, J. (2006). “Overview of Ejection Neck Injury Criteria.” Proceedings of the 44th Annual SAFE Symposium, 159-171.

Parr, J. (2014). "A Method To Develop Neck Injury Criteria To Aid Design And Test Of Escape Systems Incorporating Helmet Mounted Displays." Doctoral Dissertation, Air Force Institute of Technology. Dayton, OH

Parr, J. C., Miller, M. E., Pellettiere, J. A., & Erich, R. A. (2013). Neck injury criteria formulation and injury risk curves for the ejection environment: A pilot study. Aviation, Space, and Environmental Medicine, 84(12), 1240–1248.

Parr, J. C., Miller, M. E., Schubert Kabban, C. M., Pellettiere, J. A., & Perry, C. E. (2014). Development of an updated tensile neck injury criterion. Aviation, Space, and Environmental Medicine, 85(10), 1026–1032.

Parr, J., Miller, M., Colombi, J., Shubert Kabban, C., & Pellettiere, J. (2015). "Development of a Side-Impact (Gy) Neck Injury Criterion for Use in Aircraft and Vehicle Safety Evaluation." IIE Transactions on Occupational Ergonomics and Human Factors: 3 (4), 151–164.

Perry, C. (1998). “The Effect of Helmet Inertial Properties on Male and Female Head Response During +Gz Impact Accelerations.” SAFE Journal: 28(1): 32-38.

Perry CE, & Carter L. (2003). Criteria and Experimental Measurement Difficulties in Assessing Head and Neck Injuries during Crashes and Ejections. Proceedings of the joint RTO AVT/HFM Specialists’ Meeting on Equipment for Personal Protection and Personal Protection: Bio-Mechanical Issues and Associated Physio Pathological Risks, 2003, Koblenz, Germany

Rash, C., Mozo, B., McLean, W., McEntire, B., Joseph, H., Joseph L., Licina, J., & Richardson, L. (1996). Assessment methodology for integrated helmet and display systems in rotary-wing aircraft. Fort Rucker, AL: U.S. Army Aeromedical Research Laboratory. Report No. 961.

Seemann, M., Muzzy, W., & Lustick, L. (1986). Comparison of Human and Hybrid III Head and Neck Dynamic Response. SAE Technical Paper No. 861892, 1986. doi: 10.4271/861892

Spittle, E., Shipley, B., & Kaleps, I. (1992). Hybrid II and Hybrid III Dummy Neck Properties for Computer Modeling. Wright-Patterson AFB, OH: Armstrong Laboratory. Report No. AL-TR-1992-0049.

Watkins, T. and Guccione, S. (1992). Scaling Hybrid III and Human Head Kinematic Response to -Gx, +Gy and +Gz Impact Acceleration, SAE Technical Paper 922512, doi:10.4271/922512.

Zinck, C. (2015). "Neck injury criteria development for use in system level ejection testing; characterization of atd to human response correlation under –Gx accelerative input." Masters Thesis, Air Force Institute of Technology. Dayton, OH

REPORT DOCUMENTATION PAGE

Form Approved
OMB No. 0704-0188

1. REPORT DATE (DD–MM–YYYY)	2. REPORT TYPE	3. DATES COVERED *(From — To)*
23-03-2017	Master's Thesis	Aug 2015 – March 2017

4. TITLE AND SUBTITLE
Neck Injury Criteria Development for Use in System Level Ejection Testing; Characterization of ATD to Human Response Correlation under Gy Accelerative Input

5a. CONTRACT NUMBER
5b. GRANT NUMBER
5c. PROGRAM ELEMENT NUMBER

6. AUTHOR(S)
Satava, Stephen, J. II, Captain, USAF

5d. PROJECT NUMBER
5e. TASK NUMBER
5f. WORK UNIT NUMBER

7. PERFORMING ORGANIZATION NAME(S) AND ADDRESS(ES)
Air Force Institute of Technology
Graduate School of Engineering and Management (AFIT/EN)
2950 Hobson Way
WPAFB OH 45433-7765

8. PERFORMING ORGANIZATION REPORT NUMBER
AFIT-ENV-MS-17-M-221

9. SPONSORING / MONITORING AGENCY NAME(S) AND ADDRESS(ES)
Mr. John Buhrman and Mr. Chris Perry
2800 Q Street, Blg 824, Rm 142
Wright-Patterson AFB OH 45433-7947

10. SPONSOR/MONITOR'S ACRONYM(S)
711th HPW/RHCPT

11. SPONSOR/MONITOR'S REPORT NUMBER(S)

12. DISTRIBUTION / AVAILABILITY STATEMENT
DISTRIBUTION STATEMENT A. APPROVED FOR PUBLIC RELEASE; DISTRIBUTION UNLIMITED

13. SUPPLEMENTARY NOTES

14. ABSTRACT
Increased neck injury risk during ejection due to the increasing mass of modern Helmet Mounted Displays (HMDs) drove Parr et al. (2013, 2014, 2015) to define new neck injury criteria to reduce subjective interpretation of ejection system test results and provide early input to HMD and escape system design. The latest revision of MIL-HDBK-516 includes Multi-Axis Neck Injury Criteria (MANIC) interpretation, as described by Parr et al., to guide HMD and escape system evaluation. This research developed a MANIC(Gy) transfer function to make MIL-HDBK-516 criteria applicable to cost effective Anthropometric Test Device (ATD) escape system testing in the Gy acceleration axis. Statistical analysis of the six primary neck loads for ATDs revealed Mx (side bending) significance, necessitated adjustment to the human MANIC(Gy) calculation developed by Parr et al. before applying it to ATDs. Multiple regression produced models of ATD Six Factor (SF) MANIC(Gy) and human MANIC(Gy) to quantify response differences across the applicable Gy acceleration range. The resulting deltas between the regression models at instantaneous peak-G values defined the transfer function between ATD and human responses. Parametric survival analysis of transformed ATD SF MANIC(Gy) responses produced ATD injury risk curves, indicating 5% risk of AIS 2 injury during Gy accelerations corresponds to a MANIC(Gy) of 0.473 for humans and 0.423 for ATDs.

15. SUBJECT TERMS
Helmet Mounted Display, Neck Injury, Ejection, Testing, MANIC

16. SECURITY CLASSIFICATION OF:			17. LIMITATION OF ABSTRACT	18. NUMBER OF PAGES	19a. NAME OF RESPONSIBLE PERSON
a. REPORT	b. ABSTRACT	c. THIS PAGE			Lt Col Jeffrey C. Parr, PhD, AFIT/ENV
U	U	U	UU	108	19b. TELEPHONE NUMBER (Include Area Code) (937) 255-3636 x4709

THIS PAGE INTENTIONALLY LEFT BLANK